INSTITUTO SUPERIOR DE ENGENHARIA DE LISBOA

Área Departamental de Engenharia de Electrónica e Telecomunicações e de Computadores

Design of textile antennas for cardiopulmonary applications

Tiago Alexandre de Oliveira e Cunha

(Licenciado)

Dissertação para obtenção do Grau de Mestre
em Engenharia Eletrónica e Telecomunicações

Orientadores : Prof. Doutor Carlos Mendes
Prof. Doutor Pedro Pinho

Júri:
Presidente: Drª Paula Garcia Louro
Vogais: Dr Henrique Faria Salgado

May, 2023

INSTITUTO SUPERIOR DE ENGENHARIA DE LISBOA

Área Departamental de Engenharia de Electrónica e Telecomunicações e de Computadores

Design of textile antennas for cardiopulmonary applications

Tiago Alexandre de Oliveira e Cunha

(Licenciado)

Dissertação para obtenção do Grau de Mestre
em Engenharia Eletrónica e Telecomunicações

Orientadores : Prof. Doutor Carlos Mendes
Prof. Doutor Pedro Pinho

Júri:

Presidente: [Grau e Nome do presidente do juri]

Vogais: [Grau e Nome do primeiro vogal]
[Grau e Nome do segundo vogal]

May, 2023

Acknowledgments

Firstly, I want to express my gratitude towards my family, who gave me unlimited support and conditions for my academic career. Especially to my mom and sister, my academic and personal growth were all due to them.

A major thank to my supervisor Dr. Pedro Pinho, his knowledge and guidance were important for the development of this dissertation. I want to thank Dr. Caroline Loss for the help on manufacturing the antennas to make the final results possible, as well as the support through the project. I would also like to thank to Eng. Carolina Gouveia and Dr. Daniel Albuqerque for the enormous patience, for the advices given and the help gave using CST and MATLAB. The knowledge and constant help from these four persons were crucial for the whole work to be possible.

I would like to thank Instituto Superior de Engenharia de Lisboa for having me in these last years and for giving me the knowledge to being able to accomplish this work. Thanks to The Instituto de Telecomunicações - Aveiro as well, as they provided the equipment for the measurements.

Lastly, I want to thank my friends and colleagues who have been with me since the beginning. They gave me the motivation, support and great memories throughout the years.

Abstract

Vital signs monitoring is a crucial medical application to obtain information about the heath status of a subject. The existing methods existing consist on intrusive and rigid devices, such as the Holter monitors, which are less comfortable for the subject. In order to be able to provide a less intrusive and more comfortable experience for the subject, textile antenna are a suitable solution for this case. Furthermore, textile antennas can be incorporated in clothes, as they use flexible and light materials. Previous works have been made with textile antennas close to a human body, but mostly radiate in the opposite direction of it.

This dissertation presents a study on textile antennas and the possibility to detect vital signs. The process of the textile antenna design will be explained, including the designs picked and tested to obtain the final textile antenna capable to be in a vicinity of human body and capture vital signs. As well as how the antenna was optimized close to a human body and the method used. The final design was a patch antenna with slots with a resonance frequency of 433.93 MHz and with a superstrate to optimize the antenna performance close to a human body. The antenna was able to obtain vital signs using a method based on the reflection coefficient phase variation as the respiration and heart cycle occurred.

Resumo

O monitorazação de sinais vitais é uma aplicação médica crucial para obter informações sobre o estado de saúde de um sujeito. Os métodos existentes consistem em métodos intrusivos e em dispositivos rígidos, como os monitores Holter, que são menos confortáveis para o sujeito. Para poder proporcionar uma experiência menos intrusiva e mais confortável para o sujeito, as antenas têxteis são uma solução adequada para este caso. Além disso, as antenas têxties podem ser incorporadas em peças de roupa, pois utilizam materiais flexíveis e leves. Existem trabalhos anteriormente feitos com antenas têxteis colocadas na proximidade de um corpo humano, no entanto elas irradiam na direção oposta.

Esta dissertação apresenta um estudo sobre antenas têxteis e a possibilidade de detectar sinais vitais. O processo do design da antena têxtil será explicado tal como os designs escolhidos e testados para obter a antena têxtil final capaz de estar na proximidade de um corpo humano e captar sinais vitais. Incluindo também a forma de como a antena foi otimizada para ser utilizada perto de um corpo humano e o método utilizado. O design final foi uma antena patch com slots usando uma frequência de ressonância de 433,93 MHz e com um superstrato para otimizar o desempenho da antena perto de um corpo humano. A antena foi capaz de obter sinais vitais, como a respiração, usando o método baseado na variação da fase do coeficiente de reflexão.

Contents

Acknowledgments **v**

Abstract **vii**

Resumo **ix**

List of Figures **xv**

List of Tables **xxi**

1 Introduction **1**

1.1 Motivation 3

1.2 Objectives 4

1.3 Contribution of this work 4

2 Vital signs acquired by textile antennas **5**

2.1 Human vital signs 6

2.1.1 Respiration rate 6

2.1.2 Cardiac pulse 7

2.2 Textile Antennas 8

2.2.1 Textile materials 9

2.2.1.1 Dielectric constant and thickness 10

2.2.1.2 Surface resistivity and conductivity 10
2.2.1.3 Absorption of Moisture 11
2.2.1.4 Deformations of the dielectric 11
2.2.2 Types of textile antennas 12
2.2.2.1 Induction antennas 12
2.2.2.2 Conventional antennas 14
2.3 Impact of human body in the antenna performance 19
2.3.1 Considered body models 20
2.4 State of the Art Conclusions 23

3 On-body textile antenna design 25
3.1 Study of a simple microstrip patch antenna 25
3.1.1 Dimensions of the patch 25
3.1.2 Feeding of the patch 27
3.1.3 Design of the simple patch antenna 28
3.1.4 Width of the patch 30
3.1.5 Length of the patch 31
3.1.6 Feeding point of the patch 31
3.2 The impact of the body on the antenna 32
3.3 Textile patch antenna 33
3.3.1 Textile antenna in vicinity of the human body 35
3.3.1.1 Optimizing the textile antenna without a superstrate . . 36
3.3.1.2 Optimizing the textile antenna with a superstrate 38
3.4 Textile triangle patch antenna 40
3.4.1 Optimizing the antenna in vicinity of the human body 42

4 Textile patch antenna with slots 49
4.1 Studying of the slots in the antenna 50
4.1.1 Variation of the slots on the patch 51
4.1.2 Variation of the slots on the ground plane 53

4.1.3 Parametric study about the variables of the antenna 55
4.2 Optimizing the antenna in proximity of a body 58
4.3 Simulating Deformations in the antenna 63
4.4 Simulating vital signs 65
4.4.1 Variation of the lungs in Z axis 67
4.4.2 Variation of the lungs in X axis 70
4.4.3 Variation of the lungs in Y axis 73
4.4.4 Total variation of the lungs 76
4.4.5 Variation of the heart 78

5 Experimental Results **81**
5.1 Experimental Setup 82
5.2 Textile antenna with slots calibration 83
5.3 Acquisition of vital signs 85

6 Conclusions and future work **89**
6.1 Conclusions 89
6.2 Future work 90

References **93**

List of Figures

1.1 Example of wearables [1]. 1

1.2 Example of a textile antenna embedded in clothes [2]. 2

1.3 Example of vital signs monitoring [5]. 3

2.1 Chest wall motion resultant due to the contraction and relaxation of diaphragm. [10]. 6

2.2 Example of the position of the heart in relation to the rib cage [13]. . . . 7

2.3 Diagram of synthetic and natural fibers [15]. 9

2.4 Example of Fabric area network [25]. 12

2.5 Textile coils for ECG monitoring suits: sewn coils of stainless steel yarn for inductive links [23]. 13

2.6 Examples of dipoles: a) Log-periodic folded dipole array [28]; b) Bow-tie antenna [29]; c) embroidered conductive yarn spiral [29]. 14

2.7 Examples of each type of Patch antennas: a) Microstrip Patch antenna [32], b) Microstip patch antenna array [33] 15

2.8 Antenna used in [34]: (a) Top view of patch, (b) Bottom view with slots on the ground plane, (c) Side view of the antenna. 17

2.9 S_{11} parameter of the antenna presented in [34]. 17

2.10 Example of a UWB antenna [35] 18

2.11 Dual-band coplanar antenna on EBG plane [21]. 18

2.12 a) A cylindrical model; b) A stacked model. 19

2.13 Microstrip patch antenna design with superstrate. 20
2.14 Simple three layer model of a human body. 21
2.15 Human body model containing front side of rib cage, the lungs and the heart. 21
2.16 Body models: a) Thoracic cage; b) Thoracic cage with organs inside; c) Complete human body model. 22

3.1 Fringe effect in patch antennas [44] 26
3.2 Patch impedance. 28
3.3 Patch Antenna and the variables in study. 29
3.4 S_{11} parameter with the antenna optimized. 29
3.5 Smith chart with the antenna optimized. 30
3.6 S_{11} parameter of the antenna varying the patch width. 30
3.7 S_{11} parameter of the antenna varying the patch length. 31
3.8 S_{11} parameter of the antenna varying the patch feeding point. 31
3.9 Smith chart varying the feeding point. 32
3.10 Body in vicinity of the patch antenna. 32
3.11 S_{11} parameter of the antenna radiating in free space (blue) and radiating on a body (orange). 33
3.12 First prototype of a simple patch textile antenna operating at 2.45 GHz in free space. 34
3.13 S_{11} parameter of the textile antenna optimized. 34
3.14 Smith chart of the textile antenna optimized. 35
3.15 S_{11} parameter from the textile antenna varying the distance from the human body. 35
3.16 S_{11} parameter from the textile antenna having a 5.3 mm distance from the human body. 36
3.17 Smith Chart from the textile antenna having a 5.3 mm distance from the human body. 37
3.18 S_{11} parameter from the textile antenna having a 2.650 mm distance from the human body. 37

3.19 Smith Chart from the textile antenna having a 2.650 mm distance from the human body. 38

3.20 S_{11} parameter from the textile antenna using a 5.3 mm superstrate. . . . 38

3.21 Smith Chart from the textile antenna using a 5.3 mm superstrate. 39

3.22 S_{11} parameter from the textile antenna using a 2.650 mm superstrate. . . 39

3.23 Smith Chart from the textile antenna using a 2.650 mm superstrate. . . . 40

3.24 Representation of the triangular patch antenna with slots [45]. 40

3.25 Representation of the simple triangular patch antenna [45]. 41

3.26 Representation of the simple triangular patch antenna in CST Studio. . . 41

3.27 S_{11} parameter for the optimized triangular patch antenna radiating at 2.45 GHz in free space. 42

3.28 Smith chart for the optimized antenna radiating at 2.45 GHz in free space. 42

3.29 Representation of the antenna optimized using a 20 mm superstrate. . . 43

3.30 S_{11} parameter for the optimized antenna using a 20 mm superstrate.. . . 43

3.31 Smith chart for the optimized antenna using a 20 mm superstrate.. . . . 43

3.32 Representation of the antenna using inset feed optimized using a 10 mm superstrate. 44

3.33 S_{11} parameter for the optimized antenna using a 10 mm superstrate. . . 44

3.34 Smith chart for the optimized antenna using a 10 mm superstrate. 45

3.35 Representation of the antenna using inset feed optimized using a 5.3 mm superstrate. 45

3.36 Antenna without the inset feed optimized using a 5.3 mm superstrate. . 46

3.37 S_{11} parameter for the optimized antenna using a 5.3 mm superstrate . . 46

3.38 Smith chart for the optimized antenna using a 5.3 mm superstrate 46

4.1 Patch antenna with slots in study. 50

4.2 Final design of the textile antenna using horizontal slots in the patch and ground. 55

4.3 S_{11} parameter from the patch antenna with slots varying W3. 55

4.4 S_{11} from the patch antenna with slots parameter varying W6. 56

4.5 S_{11} parameter from the patch antenna with slots varying L4. 56
4.6 S_{11} parameter from the patch antenna with slots varying L9. 57
4.7 Front and back view of the optimized Patch Antenna with slots radiating at 433.32 MHz in free space. 57
4.8 S_{11} parameter of the optimized patch antenna with slots. 58
4.9 S_{11} parameter of the optimized antenna using a superstrate of 10 mm. . 59
4.10 S_{11} parameter of the optimized antenna using a superstrate of 7.93 mm. 59
4.11 S_{11} parameter of the optimized antenna using a superstrate of 5.3 mm. . 60
4.12 S_{11} parameter of the optimized antenna using a superstrate of 2.650 mm. 60
4.13 Smith chart of the optimized antenna using a superstrate of 2.650 mm. . 61
4.14 Side and perspective view of the antenna close to the human body model 61
4.15 S_{11} parameter of the optimized antenna using a superstrate of 1.325 mm. 62
4.16 S_{11} parameter of the optimized antenna using a superstrate of 0.8 mm. . 62
4.17 Final design for the textile antenna using a patch with slots. 63
4.18 Illustration of the movement of the body deforming. 64
4.19 Textile antenna setup for deformation test. 64
4.20 S_{11} parameter for different radius of deformations. 65
4.21 $S11$ parameter phase varying the lungs properties. 66
4.22 Corrected Textile patch antenna with slots corrected operating at 433.32 MHz. 66
4.23 Illustration of the movement of the body. 68
4.24 Reflection coefficient phase depending of the lung thickness varying relative permittivity. 68
4.25 Reflection coefficient phase depending of the lung thickness varying electric conductivity. 69
4.26 Reflection coefficient phase depending on the lung thickness. 69
4.27 Reflection coefficient phase depending of the lung thickness varying electric conductivity and relative permittivity. 70
4.28 Illustration of the movement of the body. 71

4.29 Reflection coefficient phase depending of the lung width varying relative permittivity. 71
4.30 Reflection coefficient phase depending of the lung width varying electric conductivity. 72
4.31 Reflection coefficient phase depending on the lung width. 72
4.32 Reflection coefficient phase depending of the lung width varying electric conductivity and relative permittivity. 73
4.33 Illustration of the movement of the body. 73
4.34 Reflection coefficient phase depending of the lung height varying relative permittivity. 74
4.35 Reflection coefficient phase depending of the lung height varying electric conductivity. 74
4.36 Reflection coefficient phase depending on the lung height. 75
4.37 Reflection coefficient phase depending of the lung length varying electric conductivity and relative permittivity. 76
4.38 Illustration of the total movement of the body: a) Width and thickness; b) Height; c) Width and thickness view from above. 77
4.39 Reflection coefficient phase varying permittivity, electric conductivity depending on the lung thickness. 77
4.40 Movement of the heart. 78
4.41 Reflection coefficient phase depending on the heart dimensions. 78

5.1 Textile antenna using slots in the patch and ground: a) Back view of the antenna; b) Side view of the antenna. 81
5.2 Phase Network Analyzer. 82
5.3 Devices used from BIOPAC [47]: a) Chest band with respiration transducer; b) Data acquisition unit. 82
5.4 Setup for the tests. 83
5.5 Keysight N7555A CalKit [48]. 83
5.6 S_{11} parameter of the designed antenna for five different subjects. 84
5.7 Respiration from subject 1. 85
5.8 Respiration from subject 2. 86

5.9 Respiration from subject 3. 86
5.10 Respiration from subject 4. 87
5.11 Respiration from subject 5. 87

List of Tables

2.1 Examples of textile antennas designed for low frequency. 13

2.2 Dipole antennas. 15

2.3 Patch antennas. 16

2.4 Values of relative permittivity, and conductivity (S/m) for various tissues at four frequencies from [36]. 20

2.5 Dimensions for the simple three layer model. 21

2.6 Dimensions for the thoracic cage and organs within. 22

3.1 Patch specifications 29

3.2 Parameters of the patch with the textile antenna optimized 34

3.3 Parameters of the patch with the textile antenna optimized with a 5.3 mm distance from the human body. 36

3.4 Parameters of the patch with the textile antenna optimized with a 2.650 mm distance from the human body. 37

3.5 Parameters of the patch with the textile antenna optimized using a 5.3 mm superstrate. 38

3.6 Parameters of the patch with the textile antenna optimized using a 2.650 mm superstrate. 39

3.7 Dimensions of the triangle patch antenna [mm]. 41

4.1 Dimensions for the antenna in study [mm]. 50

4.2 Designs of the antenna adding the slots to the patch. 51

4.3 S_{11} parameter from the antennas with slots in the patch. 52
4.4 Designs of the antenna adding the slots to the ground. 53
4.5 S_{11} parameter from the antennas with slots in the ground. 54
4.6 Dimensions of the optimized patch antenna with slots [mm]. 58
4.7 Dimensions of the final optimized patch antenna with slots [mm]. 63
4.8 Reflection coefficient phase values density variation according with the chest wall movement. 67
4.9 Phase values in condition of the movement. 67

5.1 BMI and perimeter of each subject. 84
5.2 Respiration frequency from each subject and each device. 88

1

Introduction

Wearable technology and their applications have advanced considerably from a technical perspective, but most of its work has been stagnated due to barriers that the human body causes. The constant movement, the sweat a human body produces etc. This technology ignited a new type of human–computer interaction with the rapid development of information and communication technology. Having created new applications for humans to have technology at their hand, an example of its use can be shown of Figure 1.1.

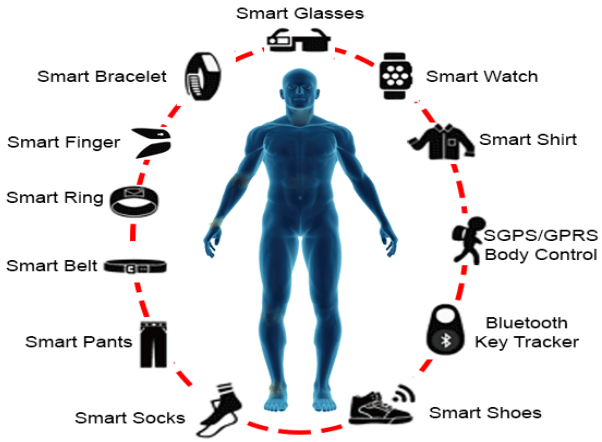

Figure 1.1: Example of wearables [1].

Wearables that possess antennas, it is essential to consider the interaction between the human body and the antenna, when designing the antenna. Most of this technology,

some years ago, was only machine-to-machine but along the years more studies have been made to make more machine-to-person interactions especially in medicinal areas. This new human-machine interaction aims to improve the quality of life using the combination of textile and electronics in human clothes. Introducing textile antennas as a result of this combination. An example of a textile antenna is shown on Figure 1.2.

Figure 1.2: Example of a textile antenna embedded in clothes [2].

The attention on textile antennas has been increasing due to their stretchable and deformable materials. Thus the applications using this type of antennas has been increasing as well. Applications varying from healthcare to entertaining [3]. With this said and having the potential for more applications, a textile antenna to detect vital signs will be the application to be done in this work. Normally an antenna is manufactured using on solid materials and radiating to an open-air atmosphere. But in this case, the antennas will be based on textile material, and they will be developed to radiate towards the human body in order to detect the vital signs. Vital signs as most people know, consist of checking blood pressure, temperature, pulse rate and respiratory rate [4]. There are multiples ways of checking them, as through blood pressure monitors (some of them give pulse rate as well as blood pressure), oximeters and infrared thermometers which are very commonly used nowadays due to COVID-19. Traditionally, it results in the hospitalisation of the patient, with expensive equipment and medical personnel on hand. In some cases, the patient may remain at home, but the use of bulky and expensive equipment still remains required. Normally at hospital, the vital signs are measured with various small sensors attached to the human body, that are connected to a monitor in order to display the measured values corresponding to each sensor. An example of a vital sign monitoring display is shown on Figure 1.3.

In medical area, advanced wireless diagnosis and treatment technologies have been greatly researched using body-centered antennas such as wearables, indigestible or implanted antennas. This textile antenna will have a different way of detecting vital signs from the conventional projects. In [6], vital signs are monitored using a method where

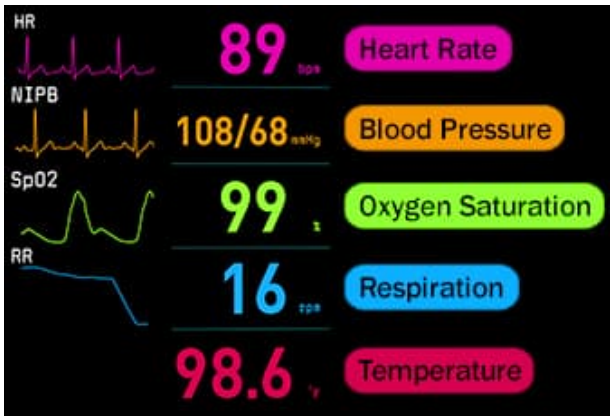

Figure 1.3: Example of vital signs monitoring [5].

the reflection coefficient phase of the antenna will be used. Basically when breathing or when the heart is beating, the organs dielectric properties will change, resulting on a change on the reflection coefficient phase of the antenna. In this work the same method as in [6] will be used but instead of a rigid antenna, a textile antenna will be used. The design and simulations of the textile will be made using the software CST Studio 2018.

1.1 Motivation

Being in a time where technology is constantly evolving, there is always some gaps on studies where certain fields were still not properly studied and there is still a vast source of information about textile antennas to be studied and tested. Obtaining vital signs through these antennas is a matter of subject that has low fluency of study and needs to be expanded. The combination of the human body with textile antennas presents some challenges regarding its design, the materials selection, and the antenna efficiency considering the proximity with the human body.

Antennas such as the microstrip will be used within this study. Microstrip antennas are one of the most successful and revolutionary technology, being introduced in the 1950s but only set to use in 1970s. Microstrip antennas are the most common used antennas [7]. These antennas present as advantages such the low cost, light weight, superior portability amongst many more. There is a wide number of articles reporting microstrip antennas for different applications. However there is a lack of studies focused on medicinal applications using textile antennas. Microstrip antennas are a discrete and low-profile solution to be used on textile technology since it can be easily integrated with clothes. Having these antennas integrated in clothes, would allow a

less invasive monitoring of vital signs. Antennas such as these are able to capture vital signs through the chest movement due to respiration or, due to heart pulse. The end goal would be a thin and discrete antenna able to be integrated in clothes and capable of detecting vital signs.

1.2 Objectives

The main objective of this dissertation is to design cardiopulmonary textile antennas using the superstrate method. This work is divided in to the following stages:

- Expand this field using Tariq´s work [6];
- Design a textile antenna to operate on free space;
- Design a textile antenna to operate near the human body;
- Test on a human body to be able to validate the results and measure cardiac and respiratory pulse;

1.3 Contribution of this work

Accepted papers:
T. Cunha, P. Pinho, C. Loss, C. Gouveia, D. Albuquerque , "Textile Cardiopulmonary Antenna Design", for the 17th European Conference on Antennas and Propagation, 26 March - 31 March, at Florence, Italy.

2

Vital signs acquired by textile antennas

Monitoring vital signs its a very important component of nursing care, as they are essential to identify clinical events, so it should be performed continuously constant measurement they need constant measurement. As years go by, various numbers of applications were studied and developed to improve monitoring of the of the vital signs, and to give a more practical and comfortable way to get these measurements correctly. Since the evolution of wireless on-body communications is increasing with time, so are its possibilities to progress on newer and better wireless monitoring applications for the vital signs measurements. In this dissertation the main vital signs that will be focused on are the human respiration and the cardiac pulse. With antennas being the main source of communication, has grown the need of it to have certain characteristics such as comfort and portability. Along with specifications such as bandwidth, smaller size and high gain. Having a human as a medium of propagation has its troubles that will be brought up in this chapter. This chapter will be divided by several sections. In Section 2.1 , it will be defined the vital signs that are going to be captured , in this case the heart beat and respiratory rate. In section 2.2 , it will be shown types of a textile antennas and types of materials that can be used. In the last two sections of this chapter, the human body theme will be approached when it comes to wearables and the on-body radiation using textile antennas.

2.1 Human vital signs

Monitoring of vital signs is a growing area of research, becoming more sophisticated and less invasive as the years progress. The monitoring of the human respiration and cardiac pulse is an important process to obtain information about the health status of the patient. For them to be detected, a search has to be done about the cycle of each vital sign (in this case, heart and respiration rate) and the induced changes in the human body.

2.1.1 Respiration rate

Starting with the human respiration and its rate, this is a process consisting of the cyclical inflation and deflation of the lungs. It is also the cycle where carbon dioxide is removed from the lungs and oxygen is replenished. Breathing (or respiration) is an important physiological task in living organisms. Breathing rate (BR) is a vital sign used to monitor the progression of illness and an abnormal BR is an important indicator of serious illness. Variation in BR can be used to predict potentially serious clinical events such as heart attack [8] [9]. In the course of this cycle where air is coming and going, there are changes in the volume of the thorax which cause a chest-wall motion. When we breathe, muscles contract and cause the chest wall to move outward. These muscles are shown in Figure 2.1 and include the diaphragm, the intercostal muscles (the muscles between the ribs), the neck muscles, and the abdomen muscles. One important matter when studying this process is the dielectric properties.

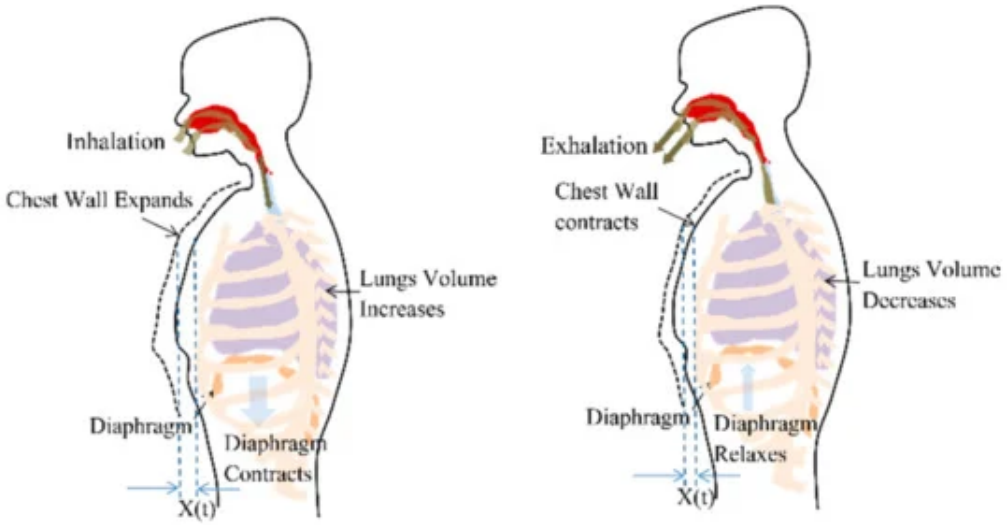

Figure 2.1: Chest wall motion resultant due to the contraction and relaxation of diaphragm. [10].

The dielectric properties of lung tissue depend on the degree of inflation and therefore vary with the physical state [11] as will be shown in section 2.3.
For this work the dielectric properties will be the main deal when trying to detect vital signs. As the lungs tend to inflate and deflate their properties will change and that causes a shift in the reflection coefficient phase of the antenna. In this way it can be detected when a person is inhaling or exhaling. In most of the cases, in clinical research, conventional non-invasive monitoring of respiration rate is performed by impedance pneumography and inductive plethysmography. Impedance pneumography measures the impedance change between two electrodes placed on the chest. Although this technique measures the movement of the chest caused by the respiration cycle, the impedance pneumography is prone to errors from posture changes and motion. Inductive plethysmography, on the other hand, employs two copper wires: one is placed around the abdomen, the other placed on the chest. During the respiration cycle, volumetric differences occur and this causes self-induction of the two wires. Inductive plethysmography is a more reliable technique compared to impedance pneumography [12].

2.1.2 Cardiac pulse

The cardiac activity involves changes in shape, dimension, and dielectric properties of the heart muscle. When the heart contracts to generate the pressure that drives blood flow, it moves within the chest cavity, hitting the chest wall, and creating a measurable displacement at the skin surface [10].

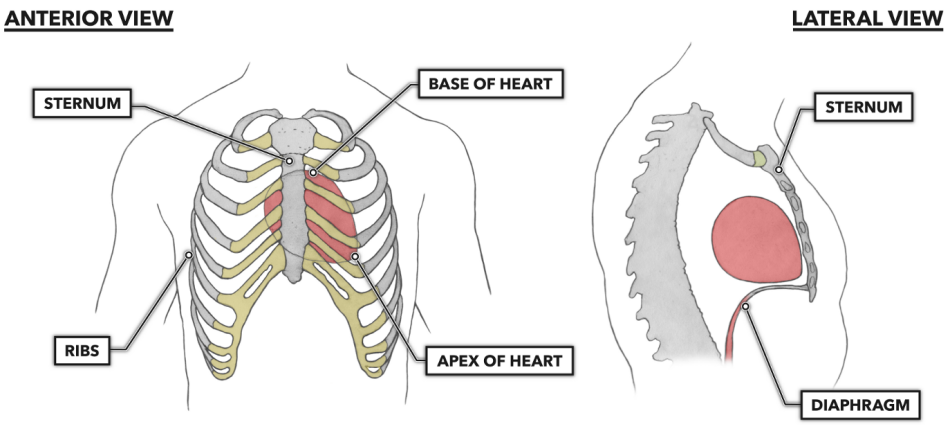

Figure 2.2: Example of the position of the heart in relation to the rib cage [13].

Each side of the heart is responsible for providing blood to different parts of the body. The left side pumps blood to organs and tissues, while the right side pumps blood to the lungs [6]. Figure 2.2 shows a representation of the heart within the rib cage. The heart rate is the number of processes (heartbeats) per unit of time, typically expressed as beats per minute.

The displacement of the heart and movement of the ribs and tissues near the heart are caused by the cycle of contractions formed by the depolarization and polarization. For the work in progress, this movement of the heart will make a small change on the reflection coefficient phase of the textile antenna.

The conventional monitoring of cardiac activity can be performed in a clinical setting in real-time, by recording electrocardiograph (ECG) signals. Monitoring the heart activity through ECG signals is a very common technique and it is performed by placing at least three electrodes to the skin to measure the electrical activity of heart.

Traditionally, Holter monitors are used for ambulatory monitoring, during the recovery period after cardiac surgeries [14]. Although Holter monitors are capable of providing continuous monitoring, the central unit of these monitors is bulky and each electrode is connected to the central unit with wires. Therefore, the Holter monitor usage interrupts the daily routine of the patient and it is not feasible for unobtrusive continuous monitoring. Over the past few years, with the advancement in wireless technologies, Holter monitors have been miniaturized and evolved into complete wire-free monitoring devices. Although ambulatory wire-free devices look promising for continuous monitoring, there is still a need for further development of such devices in order to make them more discrete, practical and still functional [12].

2.2 Textile Antennas

The conventional antenna design process presents some differences when compared with the textile antenna design. When designing a microstrip antenna for conventional substrates, characteristics such as efficiency and bandwidth are very important since those will define the composition of the antenna and (normally) will radiate to normal opened up environment. A textile antenna that is supposed to radiate to a human body is a bit more complex since the materials and the environment of radiation is completely different from a solid microstrip antenna that is radiating to open space. On a conventional antenna the important factor is its performance, but on a textile antenna there are more factors besides performance, such as its resistance to water, malleability, etc. Choosing the materials for the textile antenna is a very important part

of the design since materials have different characteristics, each would have different strength levels under stress, different water resistance, and these are important subjects because they can influence the antenna behaviour [3]. Researching about these materials and figuring out which ones to use can be one of the fundamental keys to design a functional textile antenna.

2.2.1 Textile materials

The textile antennas that were already proposed in literature have usually a conductor as the radiating element and the substrate is made by cloth-based material (cotton, foam, nylon, etc.). The textile materials that are used as antennas substrates can be divided into two main categories: natural and man-made fibers as shown in Figure 2.3 [15].

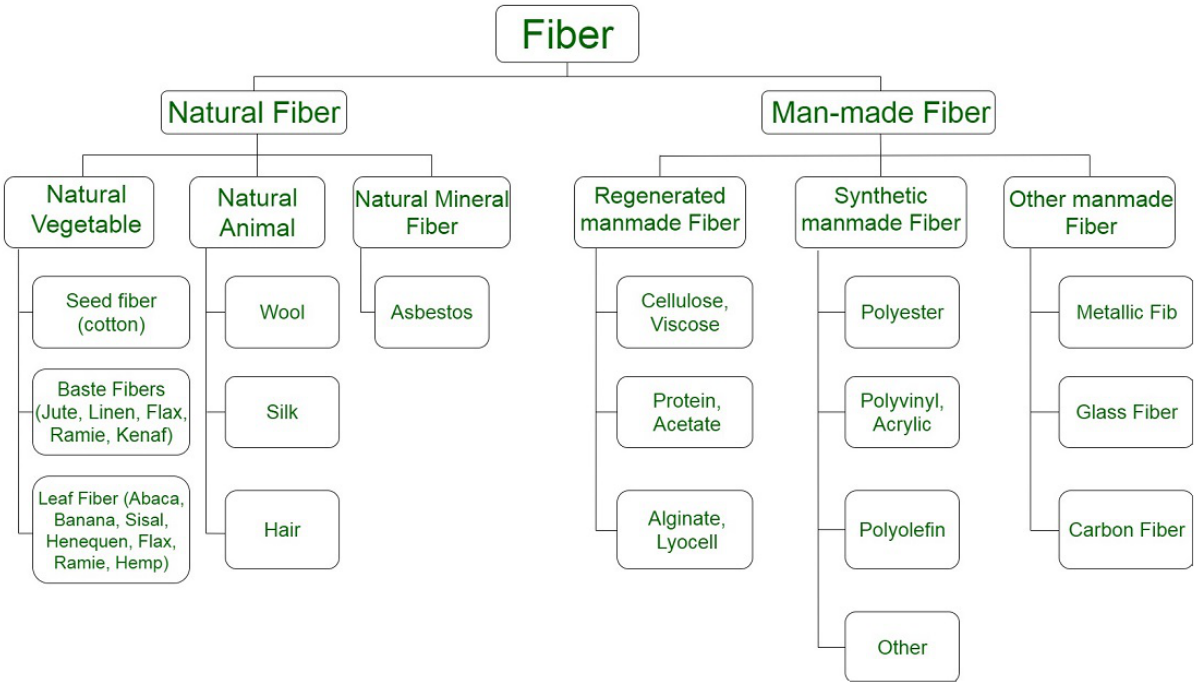

Figure 2.3: Diagram of synthetic and natural fibers [15].

Textiles are composed by fibres, which are generally made of long chain polymers and have high length and diameter ratio. They are generally considered as insulators, since the electrical conductivity of these polymers is very low [2].

When choosing these materials it is needed to have in mind these important features of the textile fabrics [2]:

1. Dielectric constant and thickness;
2. Surface resistivity;
3. Conductivity;
4. Moisture content;
5. Mechanical deformations of the dielectric.

2.2.1.1 Dielectric constant and thickness

The dielectric constant of the fabrics represents the ability to transmit fast changing signals across the textile transmission line. This parameter is expressed as the coming equation [16]:

$$\varepsilon = \varepsilon_0(\varepsilon_r' - j\varepsilon_r'') \tag{2.1}$$

where $\varepsilon_0 = 8.854 \times 10^{-12}$ F/m is the permittivity of vacuum and ε_r its the relative permittivity. The dielectric properties of materials can be affected by the frequency, temperature, and surface roughness and also on the moisture content, purity and homogeneity of the material. The textile materials dielectric behavior depends on the properties of the constituent fibres and polymers, and on the fiber packing density in the fibrous material [17].

The thickness of the material and its dielectric constant are the ones that determine the efficiency and bandwidth of planar microstrip antenna [2]. Textile materials have a very narrow range of permittivity values, so thickness may present much larger variations and determine the bandwidth. It also influences geometric size of the antenna [18].

In [17] and [19] has been shown that when a material is chosen for the substrate many characteristics that matter will differ in the wearable like bandwidth, efficiency, dielectric constant, thickness, temperature, conductivity, etc.

2.2.1.2 Surface resistivity and conductivity

Fabrics are planar materials and therefore their electrical behaviour may be quantified by the surface resistance and characterized by the surface resistivity [18]. It is the ratio between the DC voltage drop per length unit with the surface current per width unit.

This property of the material and does not depend on the configuration of electrodes used for measurement [2].

Passing on to conductivity, the choice of the conductive fabric for the patch and ground planes. It is one of the most important aspects to assure the good performance of the antenna. This characteristic is inversely proportional to the surface resistivity and thickness [2].

2.2.1.3 Absorption of Moisture

The moisture changes the antenna performance parameters dramatically when a fabric antenna absorbs water because water has a higher dielectric constant than the fabric. The fibers are constantly exchanging water molecules with the air, which changes the dynamic equilibrium with the temperature and humidity of the air surroundings. The sensitivity of the fabric to moisture is expressed as a percentage. This percentage is the ratio of the mass of absorbed water in specimen to the mass of the dry specimen [17].

Since fabric antennas are used near the skin, the occurrence of fabric wetness due to human sweat becomes a high possibility. In addition, wearable systems can be mounted on top of jackets or suits also susceptible to rain or washing the textile materials. Beyond these effects, when textile fibers absorb water they swell transversely and axially, causing tightening of the fabrics [17].

2.2.1.4 Deformations of the dielectric

The material deformations caused by stretching, bending or compressing is typical since they are not solid materials. On this matter, stretching and bending, influences the permittivity and thickness of the dielectric hence affecting the bandwidth as well as the resonant frequency of the antenna [2]. Having this variable in mind, makes it difficult to have a precise definition and cut of the shape of the components. The types of fabrics that have more stability in terms of higher geometrical accuracy are the wovens and nonwovens since they are a stern material [17].

In [20] a miniaturized textile antenna was made using denim, strip line and SMA connector at 2.4 GHz. It was subjected to different kinds of deformations to check its performance and the results were satisfying since the deterioration was negligible. Another project is [21] where a dual-band wearable textile antenna was made using the EBG substrate which is present in common clothing fabrics. The antenna was designed to operate at the 2.45 and 5 GHz bands. The antenna was tested in terms of deformation and washing cycles. When it comes to deformation this antenna was tolerant to

it, having slight changes of performance differing on the way that it was deformed. When subjected to washing cycles apparently in this case the fabric shrunk a bit after several washes, concluding that the best solution for this case was to waterproof the antenna in order to avoid that problem.

2.2.2 Types of textile antennas

The textile antennas have different kinds of applications such as monitoring vital signs in firefighter helmets [22], ECGs [23], GPS [24]. Thus these antennas will differ from ones to anothers and on this section it will be presented some of them.

2.2.2.1 Induction antennas

Starting with the induction antennas, normally these antennas function on low band frequency used on Near-field communications (NFC). In [25] the fabric area network (FAN) was based on 125 kHz RFID (Radio-Frequency Identification) (figure 2.4a). Antennas were routed to the trouser pockets (front and back), shirt pockets, cuffs of the trousers, sleeves, the back of the shirt and other locations. These antennas can then be used to communicate with transponder chips that are embedded in the wallet, shoes, pens, watches, accessories or personal items in a back-pack (figure 2.4b).

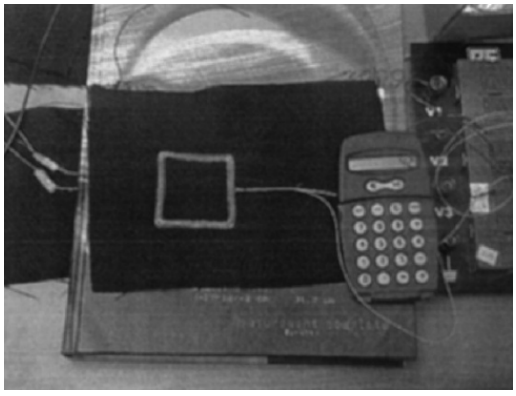

(a) Wireless transfer of RF energy across two antenna coils built on fabrics

(b) Base-station layer supplying power to devices attached on clothing (left) and set up of wireless communications with a bag containing contents (such as cellphones) that have transponder chips embedded (right).

Figure 2.4: Example of Fabric area network [25].

This project was made in order to show how a network of emission-safe, low-power and low-cost wireless links can be easily implemented on clothing [25]. Because the range of the RF communications is restricted to the surfaces of the clothing, interference of bandwidth and data security can be easily controlled. The wireless links can supply power to devices on the clothing.

In low frequency, there are other uses as the ones proposed in [23], where textile sensors were used for wireless electrocardiograms (ECG) and respiration rate monitoring of hospitalised children. The wireless transmission is made by the primary coil that is within the mattress and the secondary coil on the clothes (figure 2.5).

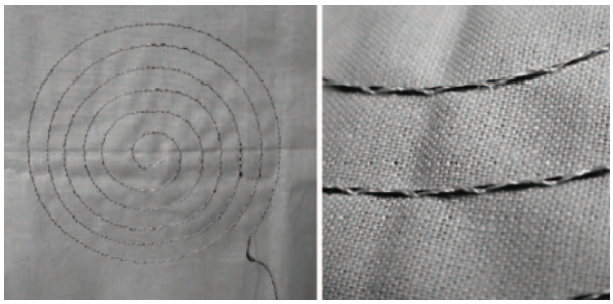

Figure 2.5: Textile coils for ECG monitoring suits: sewn coils of stainless steel yarn for inductive links [23].

More examples of antennas for low frequency are presented in Table 2.1.

Table 2.1: Examples of textile antennas designed for low frequency.

Low frequency antennas				
Antenna type	**Frequency (MHz)**	**Fabrication Method**	**Size (cm)**	**Applications**
Square coil [25]	0.125	Attachment of 15 turns of 0.25-mm insulated wire	5x5	FAN
Square coil [26]	6.78	15 turns of conductive yarn (27 μH)	-	WBAN for locomotion analysis
Circular coil [23]	0.7	Sewn 6-turn spiral inductor (diameter: 12.5cm)	12.5	Operating distance of 6 cm at 700 kHz
Circular coil [27]	0.132	Embroidery of a stainless steel filament wrapped copper core yarn	10	WBAN

The antennas presented in Table 2.1 work for low distances and with induction.

2.2.2.2 Conventional antennas

In this case these antennas work in higher frequency bands, they are more focused on external communications. The most common antennas used are the following:

1. Dipole antennas;
2. Patch antennas;
3. Ultra-wideband antennas;
4. Coplanar antennas.

Textile Dipole antennas have a lot of applications, fabrication methods , and they can be divided in three known types:

1. Folded dipole antennas;
2. Bow-tie dipole antennas;
3. Spiral dipole antennas.

Examples of each type are shown in figure 2.6

(a) (b) (c)

Figure 2.6: Examples of dipoles: a) Log-periodic folded dipole array [28]; b) Bow-tie antenna [29]; c) embroidered conductive yarn spiral [29].

Table 2.2 presents different works focused on the development of dipole textile antennas for different frequencies, manufacturing method and sizes.

In Table 2.2 presents the various applications for dipoles antennas. With antennas having wider bandwidths and better radio frequency performances.

Table 2.2: Dipole antennas.

Dipole antennas				
Antenna type	**Frequency (GHz)**	**Fabrication Method**	**Size (cm)**	**Applications**
Log-periodic folded dipole array [28]	2.45	Hand embroidery of stainless steel yarn on cotton fabric	-	Wider bandwidth
Multi-resonant folded dipole [30]	0.087-0.107	MCEY CNC embroidery on polyester woven fabric	144 x 10	Broadband
Copper-coated-fabric patched bow-tie antenna [29]	0.1-1	Copper coated	-	Better RF performance
Equiangular spiral [31]	2-4	Ni-Cu-Ag nylon (Nora1, 0.03O/sq) spiral antenna sewn on polyester cloth	6.09 (outer radius)	Broadband, space suit

On the other hand Patch antennas are the most common and well known type of antennas, and their implementation in textile encompass:

1. Microstrip patch antennas;

2. Microstrip patch antenna array.

These antennas have a lot of advantages, such as the easy optimization, low cost fabrication, light weight, etc.

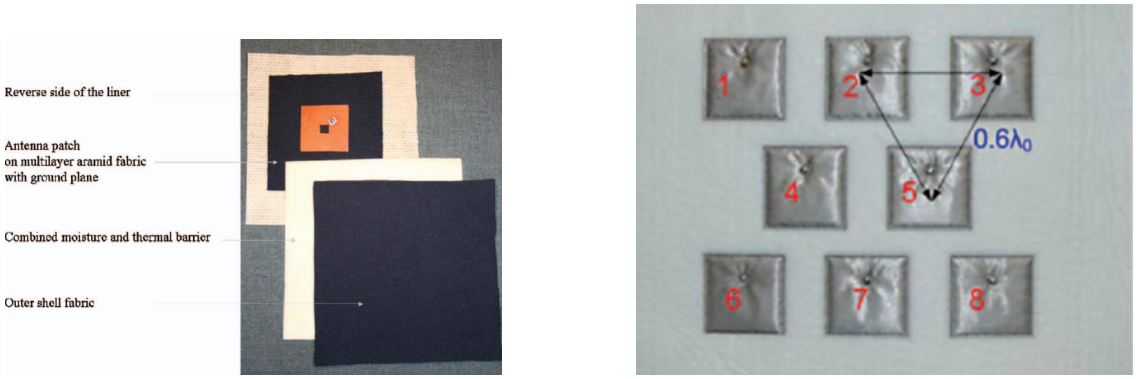

(a) (b)

Figure 2.7: Examples of each type of Patch antennas: a) Microstrip Patch antenna [32], b) Microstip patch antenna array [33]

Table 2.3 presents some microstrip patch antennas developed to different applications.

Table 2.3: Patch antennas.

Patch antennas				
Antenna type	**Frequency (GHz)**	**Antenna composition**	**Size [L× W] (mm)**	**Applications**
Truncated corner microstrip patch [22]	2.4-2.4835	Metal-coated fabric antenna patch and ground: fire-resistant/ water-repellent foam substrate	50×46	Firefighter's vital sign monitoring (Proetex project)
Microstrip patch [24]	1.563,1.587	Metal-coated fabric antenna patch and ground: fire-resistant /water-repellent foam substrate	73.5×69.5	Global Positioning System (GPS) (Proetex project)
LTCC based slotted patch antenna [34]	0.915	Dupont 951 LTCC substrate (1 mm), copper patch and ground	25×25	Biomedical applications

In Table 2.3 is possible to verify the various types of applications that patch antennas can execute. Such as biomedical applications, monitoring vital signs, and even Global Positioning Systems.

In this project the antenna used in [34] will be one of the models to be simulated. The model is represented in Figure 2.8.

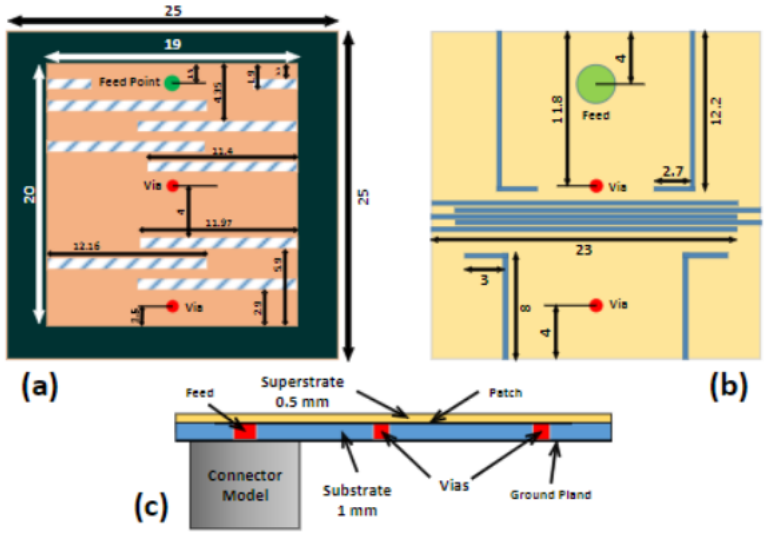

Figure 2.8: Antenna used in [34]: (a) Top view of patch, (b) Bottom view with slots on the ground plane, (c) Side view of the antenna.

This antenna has a resonant frequency of 915 MHz, with a dimension of 25×25×1.5 mm, Since this antenna will be used on biomedical applications, this antenna also uses a superstrate shown in Figure 2.8 (c), because in this project the antenna is close to the body as well. In Figure 2.9 is represented the S_{11} parameter for the study done in [34].

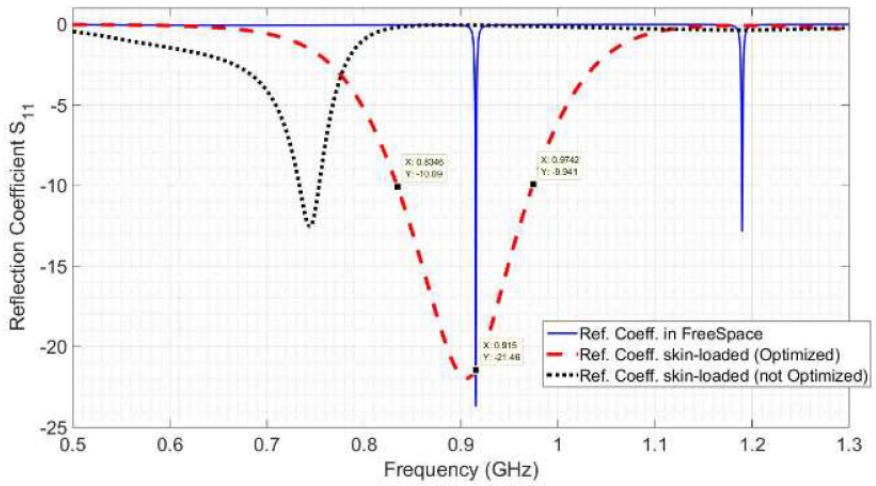

Figure 2.9: S_{11} parameter of the antenna presented in [34].

In Figure 2.9 is represented the S_{11} parameter of the antenna in free space, on-body optimized and on-body not optimized. In [34] is used a peculiar design on the patch

and ground, is used slots in the patch and also on the ground. The slots used on the ground are used to optimize the resonant frequency of the antenna and to increase current path which will decrease the resonant frequency. Textile antennas literature also includes applications that require UWB. For instance in [35] a UWB antenna was developed to work in WBAN, more specifically for breast cancer imaging. The proposed solution is shown in Figure 2.10.

(a) (b)

Figure 2.10: Example of a UWB antenna [35]
: a) Prototype UWB antenna, b) measurement setup on chest.

In the final type of antennas used in far-field communication, there is the coplanar antenna, where it has a much wider bandwidth comparing with a microstrip patch antenna. An example of a coplanar antenna was proposed in [21] and it is shown in Figure 2.11. This antenna is a dual-band coplanar designed on a eletromagnetic band-gap (EBG) substrate. The EBG array was designed to act as a high-impedance plane for the low profile antenna, to reduce the backward scattering wave towards the body and possibly minimize the coupling between an antenna and other nearby antennas [21].

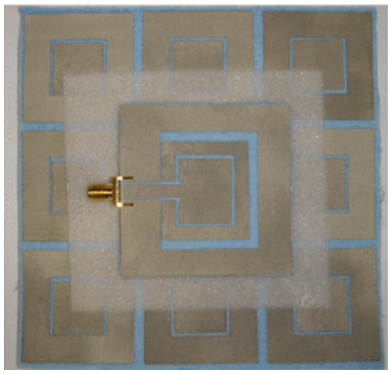

Figure 2.11: Dual-band coplanar antenna on EBG plane [21].

After reviewing some examples of textile antennas that had applications on the medical area it was possible to realize that the most common frequency band used was 1 - 5 GHz. In further work, when choosing the material to compose the textile antenna, a study towards the material will be needed. The selection of the material will have a impact on the antenna since its malleability, water resistance and other aspects mentioned before will impact the antenna performance.

2.3 Impact of human body in the antenna performance

In this case of study, an antenna is being designed to operate close to a human body, which normally it is designed to operate in an open space. The problem is the fact that electrical properties on human tissues are completely different from air or vacuum. The propagation in human bodies is not like it is in vacuum or air, since a human body possesses different layers such as skin, fat, muscle, bone and internal organs, each one with different properties as can be seen in Table 2.4. In Figure 2.12 are presented two examples of biological models considered to design on-body antennas. These two models are examples of what can be used to test the antenna when designing it.

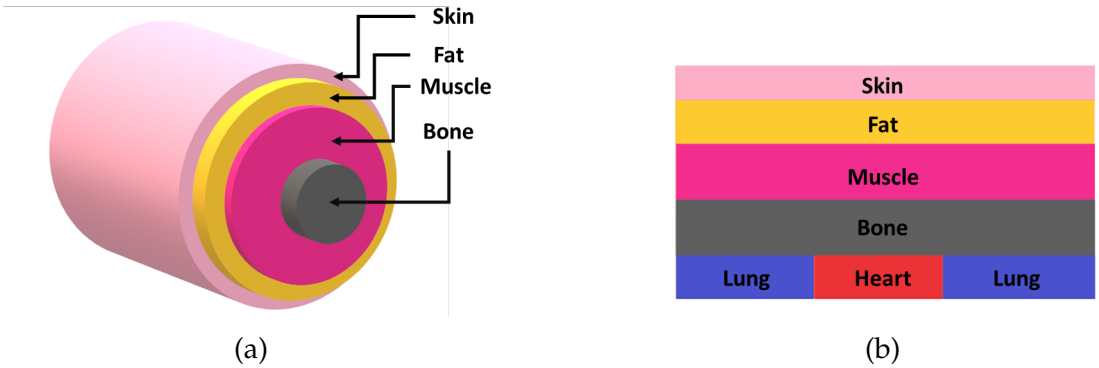

(a) (b)

Figure 2.12: a) A cylindrical model; b) A stacked model.

The on-body propagation environment is, in some ways, similar to that in both indoor and outdoor environments, since it is affected by scattering from the local environment [37]. However, the scattering effect is worsened by the change in body posture [37]. In fact, changes in the posture affects on-body propagation dramatically, including during even the simplest daily activities. The movement of the body parts causes variability in the antenna properties such as frequency; for example, antennas placed on a hand, show dramatic variability [38], since it is one of the most common body part to move.

Table 2.4: Values of relative permittivity, and conductivity (S/m) for various tissues at four frequencies from [36].

	Frequency					
	433.92 MHz		2.45 GHz		5.8 GHz	
Material	ε_r	σ	ε_r	σ	ε_r	σ
Bone (Cancellous)	22.3	0.241	18.5	0.805	15.4	2.15
Bone (Cortical)	13.1	0.0944	11.4	0.394	9.67	1.15
Fat	11.6	0.0822	10.8	0.268	9.86	0.832
Heart muscle	65.3	0.984	54.8	2.26	48.9	5.86
Lung (deflated)	54.2	0.695	48.4	1.68	43.8	4.82
Lung (inflated)	23.6	0.380	20.5	0.804	18.5	2.08
Muscle	56.9	0.805	52.7	1.74	48.5	4.96
Skin	46.1	0.702	38	1.46	35.1	3.72

When the antenna is located closer to the human body, all common antenna parameters, including resonant frequency, radiation pattern, bandwidth, and efficiency, may change radically.This is due to the high relative electric permittivities from the human body. Hence, the off-body (free space) design may not be a suitable approach for these cases [39].

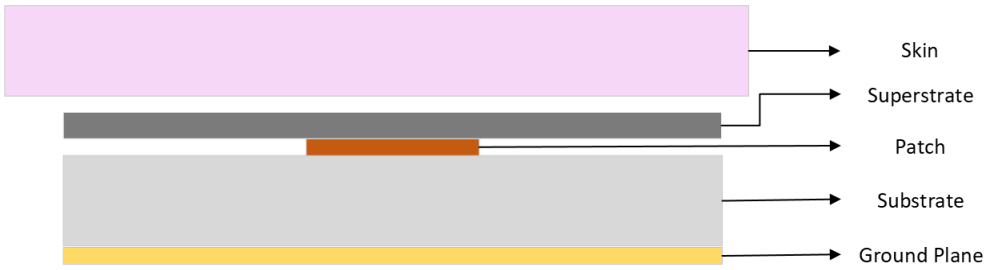

Figure 2.13: Microstrip patch antenna design with superstrate.

So in order to design the antenna it will be used one strategy named superstrates in order to adapt the antenna [40]. The design is demonstrated in Figure 2.13.

2.3.1 Considered body models

In this work, three types of body models were used in simulations in CST Studio. The phantoms became more complex as the final model of the textile antenna was reached.

The first model consists of three layers: skin, fat and muscle. When searching for the antenna design to use, this was the model working on simulations. This is due to the fact that as a simple model, the simulation would run more quickly. As the

antenna design had not yet been chosen, it was important not to waste time with long simulations. The model in question is represented in Figure 2.14.

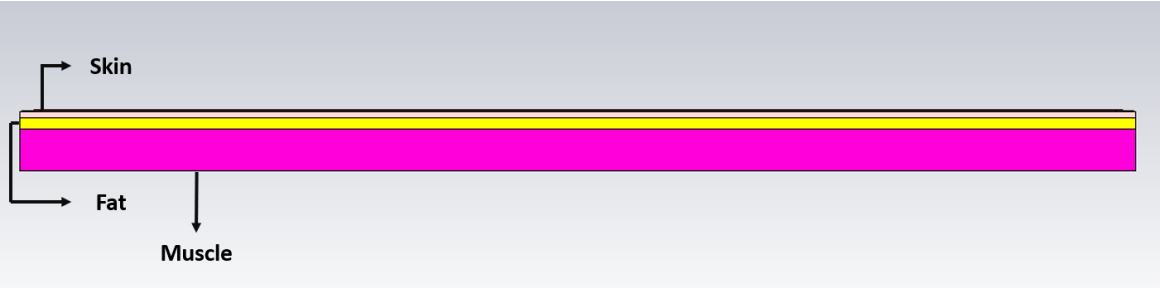

Figure 2.14: Simple three layer model of a human body.

In Table 2.5 is displayed the thickness and dimensions used for these layers.

Table 2.5: Dimensions for the simple three layer model.

	Skin	Fat	Muscle
Thickness [mm]	2.3	3.99	15
Dimensions (W x L)[mm]	300x300	300x300	300x300

As the antenna was reaching to its final design, the model suffered changes, becoming more complex in order to become more realistic. Using the model from Figure 2.14, it was made the addition of organs such as lungs and heart, and the front side of the thoracic cage. For this model, only air is between the organs and ribs. The example of the model is shown in Figure 2.15.

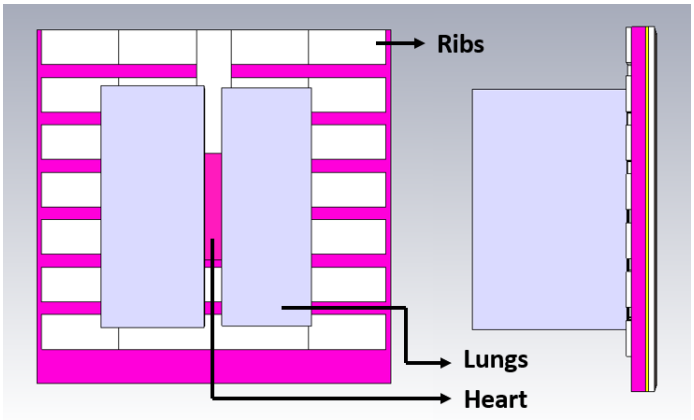

Figure 2.15: Human body model containing front side of rib cage, the lungs and the heart.

In Table 2.6 are the dimensions of each organ and the ribs of the thoracic cage.

Table 2.6: Dimensions for the thoracic cage and organs within.

	Heart	Left Lung (inflated)	Right Lung (inflated)	Ribs	Sternum
Thickness [mm]	60	171	170	5.74	5.74
Width [mm]	85	110	124	87.5	39.17
Length [mm]	120	270	274	39.16	200

The dimensions of the thoracic cage and the organs within vary depending on the person. It depends if it is a child, an adult, tall, short, the values presented in Table 2.6 were based on [41],[42], considering an average person.

The third and last model to be used is the most complete type of body model. When comparing to the last model, this last one has a complete thoracic cage and the layers go around the said thoracic cage.

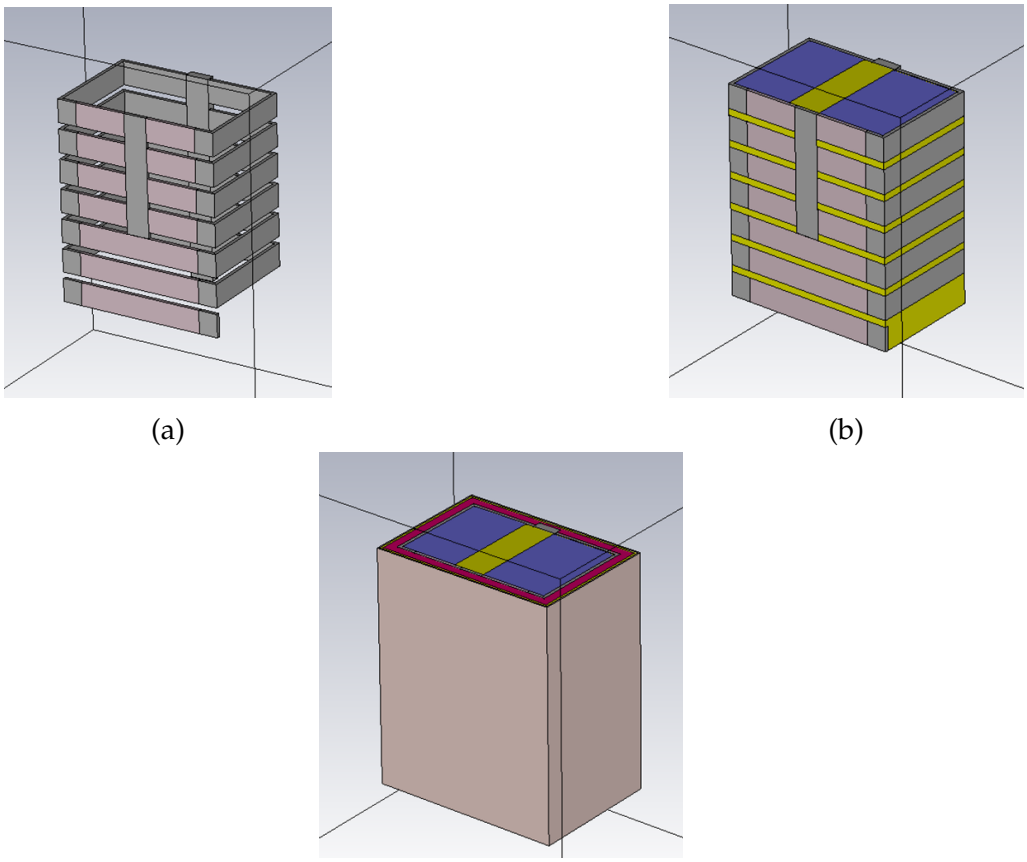

(a) (b)

(c)

Figure 2.16: Body models: a) Thoracic cage; b) Thoracic cage with organs inside; c) Complete human body model.

In Figure 2.16 is possible to see how the body will be displayed. The thoracic cage was completed by adding a vertebral column and filled with visceral fat on empty spaces

between bones and organs. The column has the same properties as the bones and the visceral fat the same as the layer of fat presented in Table 2.4 This last model will be used to simulate the respiratory and cardiac pulse.

2.4 State of the Art Conclusions

This document intends to review the state of the art concerning the use of textile antennas in order to detect vital signs and the effect that the human body has on the antenna performance. This study began with a small study on vital signs, in this case the cardiac and respiration signals. In order to detect them it was proceeded to understand which changes the heart and lungs go through in each cycle, their motions and dielectric properties. The next step was to approach the textile antennas. The first matter to be attended was the textile antennas materials and their properties. Properties such as dielectric constant, surface resistivity, conductivity, absorption of moisture and its endurance in terms of deformations. One could conclude that the absorption of water and the deformations are the most important on the antenna designing, since the antenna will be in constant moving and susceptible to sweat if in contact with a human body. Those two properties can change certain aspects of the antenna parameters such as the frequency and the bandwidth. Finishing the textile antennas overview, it was verified various types of textile antennas and its applications. Finishing this chapter was last approached the impact that the human body has on the antenna. It was studied in this section the dielectric properties of the human organs, the effects that they have on the antenna and a way to adapt the antenna to this matter. This section was studied as well the body models that will be used in the simulations.

3

On-body textile antenna design

This chapter will present the tasks made in order to obtain a textile antenna capable of operating close to a human body. This design, starts by a simple conventional microstrip patch antenna that was made in order to be familiarized to the software used, the CST Microwave Studio. This first antenna was used to understand how the width, the length and the feeding point of the patch would influence the behavior of the antenna. The first antennas that were made, were optimized to work in ISM band (2.4-2.5 GHz), in this case more specifically to work at 2.45 GHz. After understanding how the patch antenna works, the same was done using textile substrate.

3.1 Study of a simple microstrip patch antenna

A simple microstrip patch antenna was created using a conventional substrate and optimized in order to understand the behavior that each variable has on the antenna performance and to be familiarized with the software in use. Before that the microstrip patch antenna has to be design and its dimensions calculated.

3.1.1 Dimensions of the patch

To obtain initial values for the design of this patch antenna, some calculations have to be done. These calculations will be made with the main goal of obtaining the best

reflection coefficient possible for the antenna, that value would have to tend to -∞. The first equation to be considered is displayed in Equation 3.1 [43].

$$W = \frac{c}{2 \times f_r \times \sqrt{\frac{\epsilon_r+1}{2}}} \tag{3.1}$$

Where:

- W = Patch width;
- c = Speed of light;
- f_r = Resonance frequency;
- ϵ_r = Relative permittivity of the substrate of the antenna.

In patch antennas occurs the fringe effect phenomenon, represented in Figure 3.1.

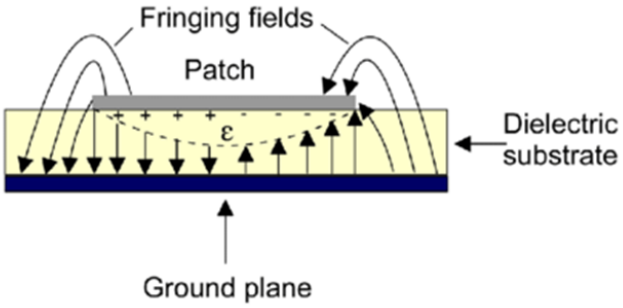

Figure 3.1: Fringe effect in patch antennas [44]

Due to the limits of the antenna, the electromagnetic waves pass through air and the substrate. In a perfect case these waves would only pass through the substrate. Thus it is necessary to handle the air and the substrate as only one. To do that each permittivity of the air and the substrate will be homogenized becoming the parameter ϵ_{ref}. The Equation 3.2 [43] will obtain the ϵ_{ref} parameter.

$$\epsilon_{ref} = \frac{\epsilon_r + 1}{2} + \frac{\epsilon_r - 1}{2} \times (1 + 12 \times \frac{h}{W})^{-0.5} \tag{3.2}$$

Where:

- h = height of the substrate;

In Equation 3.2, $\frac{W}{h}$ has to be greater then 1. The reason behind this relation is for the radiation to be more predominant then the transmission.

Having homogenized the two mediums as one, the effective wavelength can now be obtained. Equation 3.3 [43] calculates the effective wavelength (λ_{eff}).

$$\lambda_{eff} = \frac{c}{f_r \times \sqrt{\epsilon_{ref}}} \tag{3.3}$$

Half of the value of the effective wavelength is equivalent to the effective length of the patch [43]. This last statement is presented in Equation 3.4.

$$L_{eff} = \frac{\lambda_{eff}}{2} \tag{3.4}$$

The fringe effect causes a curve effect in the electric field lines in the borders of the patch. Therefore, the dimensions of the patch seem to be bigger then the real dimensions. Thus the calculation of the length excess is necessary to eliminate this contribution of the effective length. As presented in Equation 3.5, [43].

$$\Delta L = 0.412h \times \frac{(\lambda_{eff} + 0.3) \times (\frac{W}{h} + 0.264)}{(\lambda_{eff} - 0.258) \times (\frac{W}{h} - 0.8)} \tag{3.5}$$

This effect occurs from both sides of the patch width, having to eliminate both contributions. The length of the patch can now be concluded with Equation 3.6, [43].

$$L = L_{eff} - 2 \times \Delta L \tag{3.6}$$

3.1.2 Feeding of the patch

The feed locations in the patch produces different input impedance. In Figure 3.2 is possible to verify three different locations of the feed and how the impedance will vary.

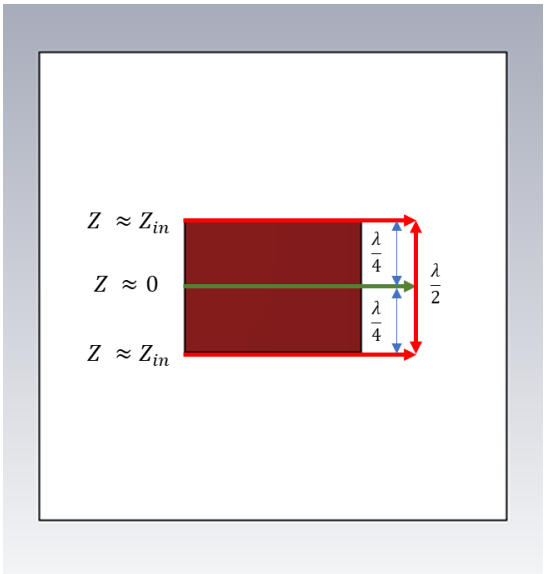

Figure 3.2: Patch impedance.

If the feed location is in the borders of the patch, the impedance reach the value. The minimum impedance will be reached if the feed location $\lambda/4$ from the border of the patch (assuming $L \approx \lambda/2$). The λ is referring to the wavelength at the substrate.

The input impedance of the patch must be equivalent to the characteristic impedance of the feed, so the antenna can be optimized. The input impedance can be obtained using Equation 3.7.

$$Z_{in} = \frac{60 \times \lambda_0}{W} \tag{3.7}$$

Where:

- Z_{in} = Input impedance
- λ_0 = Wavelength in vacuum

The feeding must be done in the location where the input impedance of the patch is the same as the characteristic impedance of the feeding device (typically at 50 Ω).

3.1.3 Design of the simple patch antenna

In Figure 3.3 is the representation of the antenna created using CST Studio.

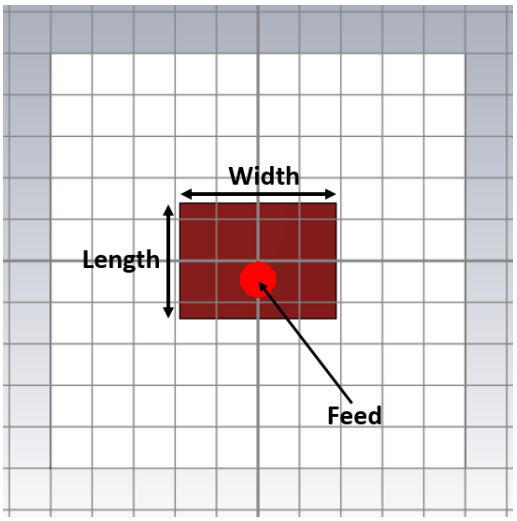

Figure 3.3: Patch Antenna and the variables in study.

The presented antenna needs to work at a frequency of 2.45 GHz using a FR4 substrate with a $\epsilon_r = 4.14$. It also uses PEC (perfect electric conductor) material for the patch and ground. Adding to that, this antenna will radiate to free space. In Table 3.1 is presented the patch specifications calculated and the values that optimized the antenna.

Table 3.1: Patch specifications

	Theoric	Simulated
W [mm]	37.6	37.9
L [mm]	29.2	28.02
Feed Point [mm]	8.126	9.5

The Figure 3.4 and Figure 3.5 shows the S_{11} parameter and the Smith Chart of the antenna optimized, respectively.

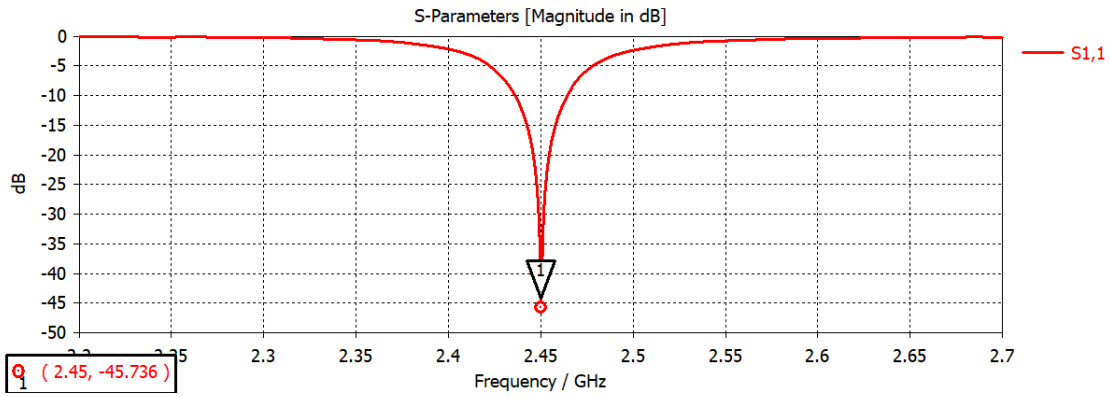

Figure 3.4: S_{11} parameter with the antenna optimized.

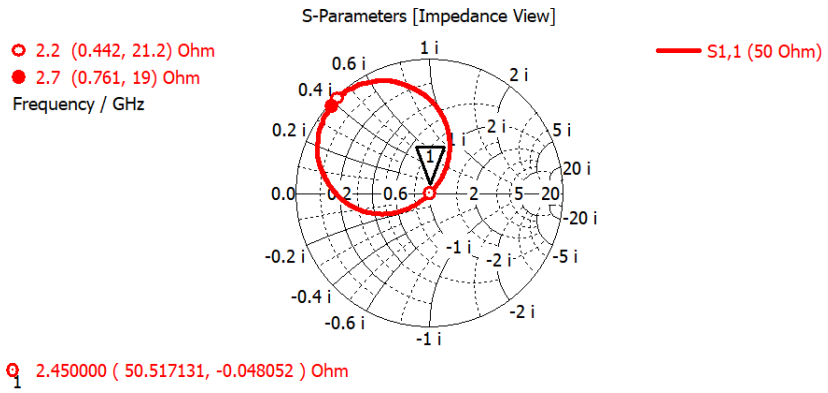

Figure 3.5: Smith chart with the antenna optimized.

The next step being taken is the study of the variables of the patch. Meaning the study of the the width, the length and the feeding point of the patch.

3.1.4 Width of the patch

This parameter study started with the width of the patch. In order to understand how this will affect the S_{11} parameter, the width was varied between 35 mm and 40 mm, using 1.25 mm step. The results are shown in Figure 3.6.

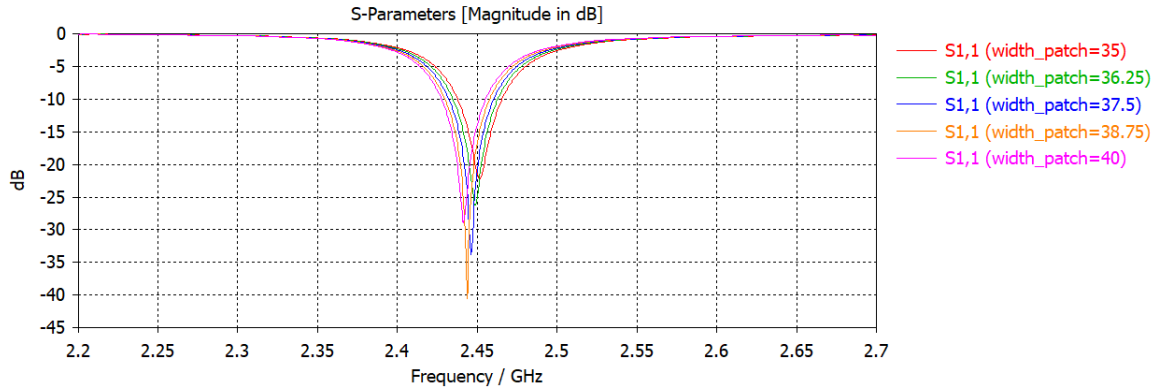

Figure 3.6: S_{11} parameter of the antenna varying the patch width.

In Figure 3.6 is possible to observe that this parameter will have a strong impact on the magnitude S_{11} parameter. On the other hand the resonant frequency will suffer a slight variation when varying the width of the patch. When the patch width increases the resonance slightly decreases and vice-versa.

3.1.5 Length of the patch

Succeeding is the study of the length of the patch. In order to understand how this will affect the S_{11} parameter, the length was varied between 26 mm and 30 mm, using 1mm steps. The results are shown in Figure 3.7.

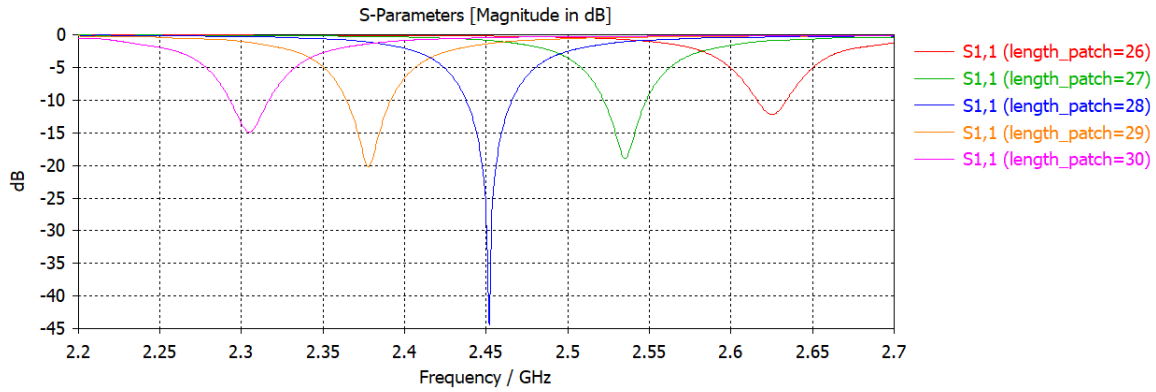

Figure 3.7: S_{11} parameter of the antenna varying the patch length.

In Figure 3.7 is possible to observe that this parameter will have a strong impact on the resonant frequency. As the length increases the resonant frequency decreases, and as the length decreases the resonant frequency increases.

3.1.6 Feeding point of the patch

The last parameter at study is the position of the feed in the patch. This parameter will vary the feeding position of the antenna. Thus the feeding point will be related to the length of the patch. This variation will go from 7 mm to 11 mm which means that 7 mm is closer to the edge of the patch and 11 mm closer to the center of the patch.

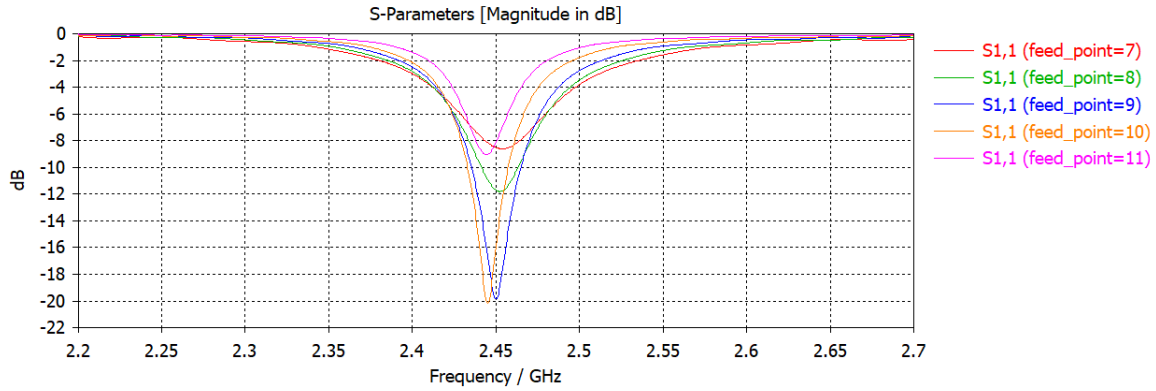

Figure 3.8: S_{11} parameter of the antenna varying the patch feeding point.

In Figure 3.8 are the results from the variation of the feed point. This parameter will influence more the S_{11} magnitude value than the frequency. In this case the feeding point will have its weight to adapt the antenna as it shows in Figure 3.9.

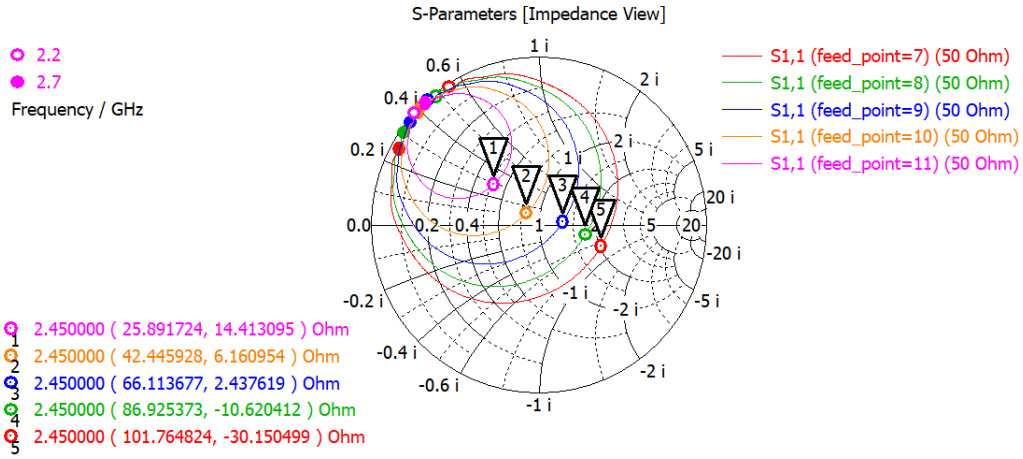

Figure 3.9: Smith chart varying the feeding point.

In this case as the feed point increases so does the impedance decreases and vice versa.

3.2 The impact of the body on the antenna

Mentioning the previous Section 3.1, it was said that the patch antenna was radiating to free space. Thus, the next step is to add the simple three layer model of a human body displayed in Section 2.3.1 in Figure 2.14. This model will stand in front of the microstrip patch antenna and radiate towards it. This step is to understand how the body will impact a optimized antenna. Those three layers being the skin, fat and muscle having the properties specified on Table 2.4 at a resonant frequency of 2.45 GHz. The representation of the body in relation to the antenna is shown in Figure 3.10.

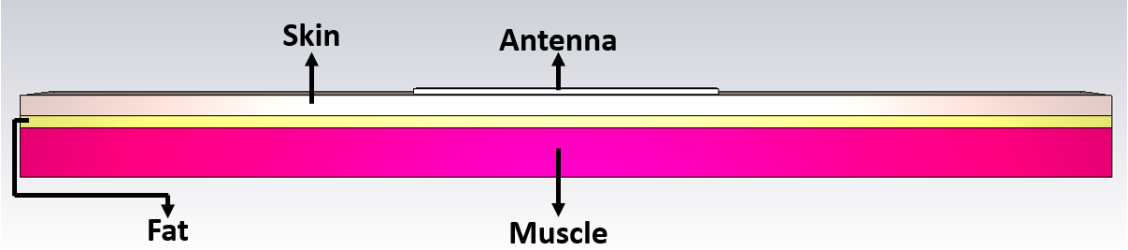

Figure 3.10: Body in vicinity of the patch antenna.

In Figure 3.10 is the simple three layer model represented in 2.3.1 in Figure 2.14 with the dimensions displayed in Table 2.5

Onto the next step, having the model created and each property defined, was made a simulation where the antenna is close to the body. The antenna in this case had no type of protection (or a superstrate), meaning that the patch was in contact with the body. The results of the S_{11} parameter of the simulation is shown on Figure 3.11.

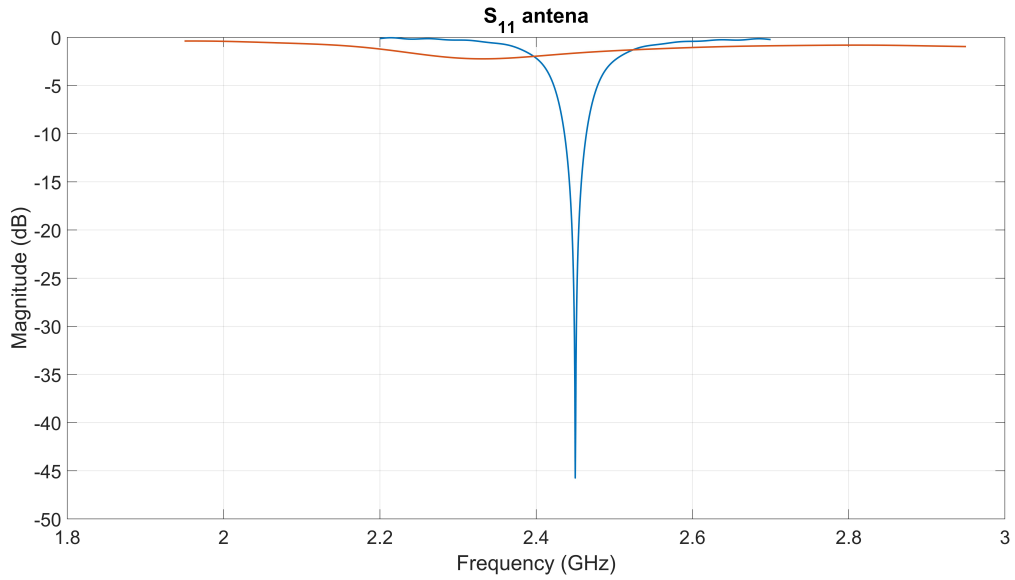

Figure 3.11: S_{11} parameter of the antenna radiating in free space (blue) and radiating on a body (orange).

Observing Figure 3.11 is possible to verify that the body had a massive impact on the antenna S_{11} parameters. These results were the expected, like it was explained on Section 2.3, the body has completely different properties comparing to free space.

3.3 Textile patch antenna

After understanding how the microtstrip patch antenna works in terms of its parameters and how the human body will affect it, a textile antenna is the next step to be taken. In this case it will be used real materials that were already used for textile antennas. For the substract it will be used the 3D Spacer Knit with a thickness of 2.650 mm and a relative permittivity of 1.13 @ 2.45 GHz. The patch and the ground will be made of Pure Copper Polyester Taffeta Fabric with a thickness of 0.08 mm and a conductivity of 62600 S/m. The initial parameters used in this antenna were calculated the same way as for the conventional antenna. Said that the consequent textile antenna was made, the representation of that antenna is shown in Figure 3.12.

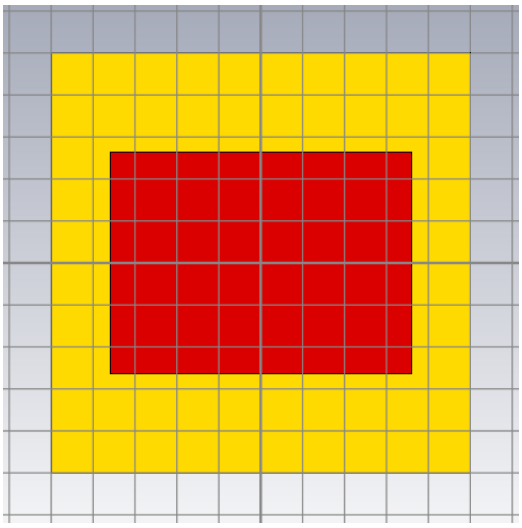

Figure 3.12: First prototype of a simple patch textile antenna operating at 2.45 GHz in free space.

In Table 3.2 are the parameters of this antenna optimized to a resonant frequency of 2.45 GHz.

Table 3.2: Parameters of the patch with the textile antenna optimized

Length [mm]	Width [mm]	Feed Point [mm]
52.57	72	9.7

The S_{11} parameters and the Smith chart for this antenna radiating in free space are displayed in Figures 3.13 and 3.14 respectively.

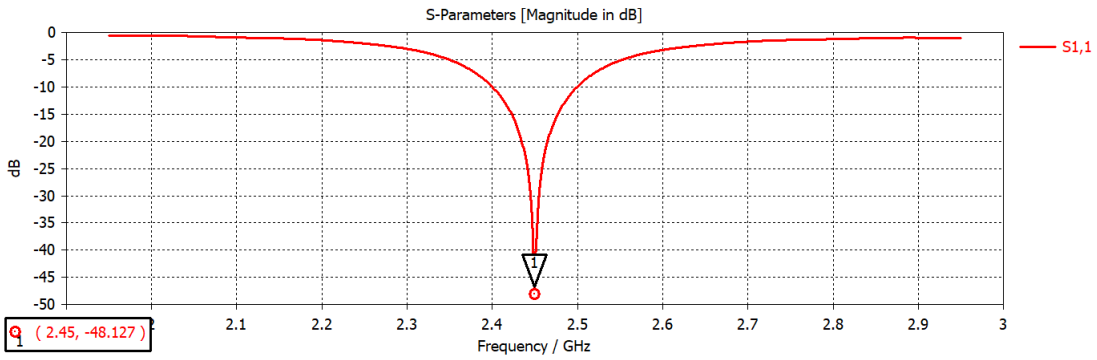

Figure 3.13: S_{11} parameter of the textile antenna optimized.

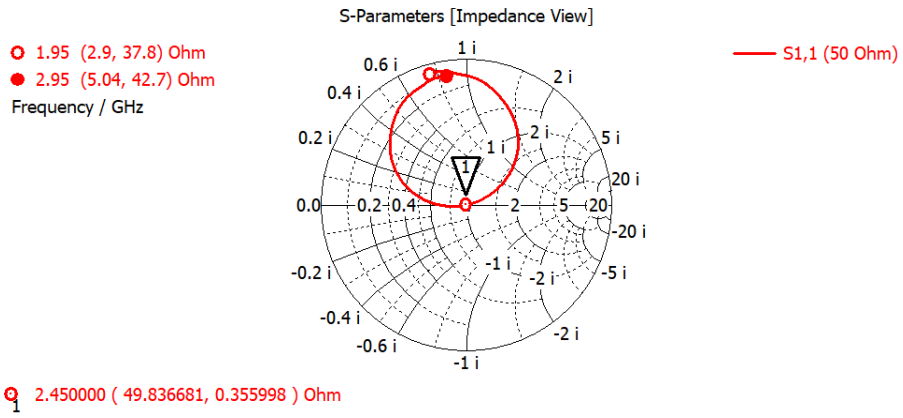

Figure 3.14: Smith chart of the textile antenna optimized.

3.3.1 Textile antenna in vicinity of the human body

In the previous Section 3.2 the simple patch antenna was subjected to radiate close to a human body, and so will the textile patch antenna. The textile antenna will be tested varying the distance between the body and the antenna from 0 mm to 7 mm in order to understand how the distance will affect the performance of the antenna. And just like the Section 3.2, this antenna will not have a protection from the body.

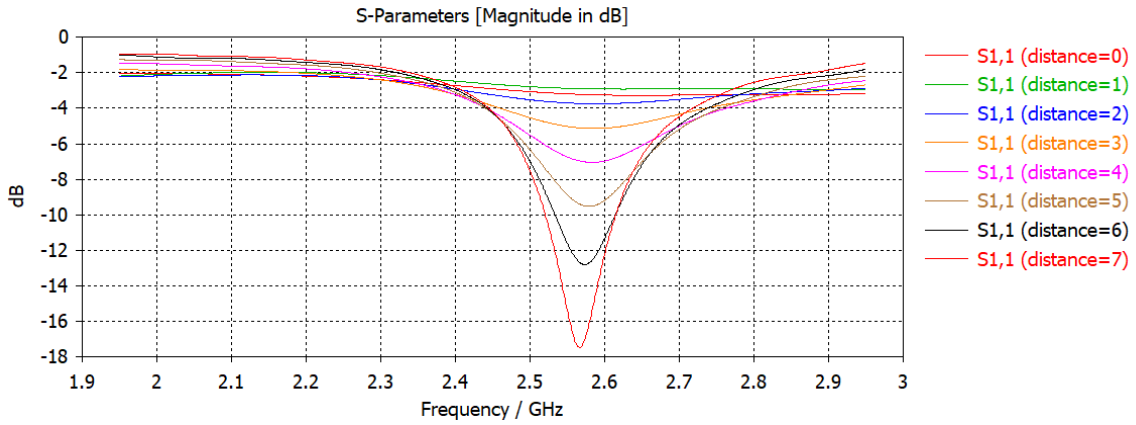

Figure 3.15: S_{11} parameter from the textile antenna varying the distance from the human body.

The Figure 3.15 displays the S_{11} parameter result from the variation of the distance between the textile antenna and the human body. Examining Figure 3.15, the antenna gradually gets optimized as the distance from the body keeps increasing. This is expected since the antenna was optimized to operate in free space, if the distance kept on increasing the antenna would be optimized. The next step was to understand the limitations of a simple patch antenna when close to a human body. The simulations

made next are to understand how the superstrate will help to optimize the textile antenna. Thus, textile antennas were first simulated without superstrates and then using superstrates to compare.

3.3.1.1 Optimizing the textile antenna without a superstrate

Consequently, a textile antenna was placed in a distance of 5.3 mm (which is equivalent of two layers of the 3D Spacer knit fabric) of the body. This distance was chosen because in Figure 3.15 at a distance of 5 mm the antenna had almost -10 db of magnitude. This value was obtained with the antenna not being optimized, meaning that if the antenna got optimized a good result could be achieved. The optimized textile antenna achieved the associated results on Figure 3.16 and 3.17. The dimensions of the patch are displayed in Table 3.3.

Table 3.3: Parameters of the patch with the textile antenna optimized with a 5.3 mm distance from the human body.

Length [mm]	Width [mm]	Feed Point [mm]
56.1	47	2.5

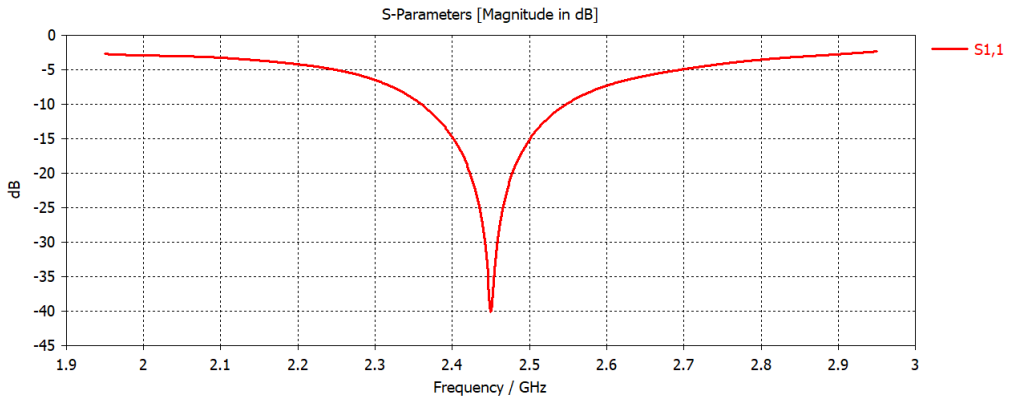

Figure 3.16: S_{11} parameter from the textile antenna having a 5.3 mm distance from the human body.

The optimization of this antenna took quite a while to be accomplished. This might be due to the lack of a medium to facilitate the optimization between the antenna and the body. The final results seem to be good, and observing Figure 3.16, the bandwidth becomes a bit wide. Following this, the distance from the body was reduced until it got to 2.650 mm (half of the last distance).

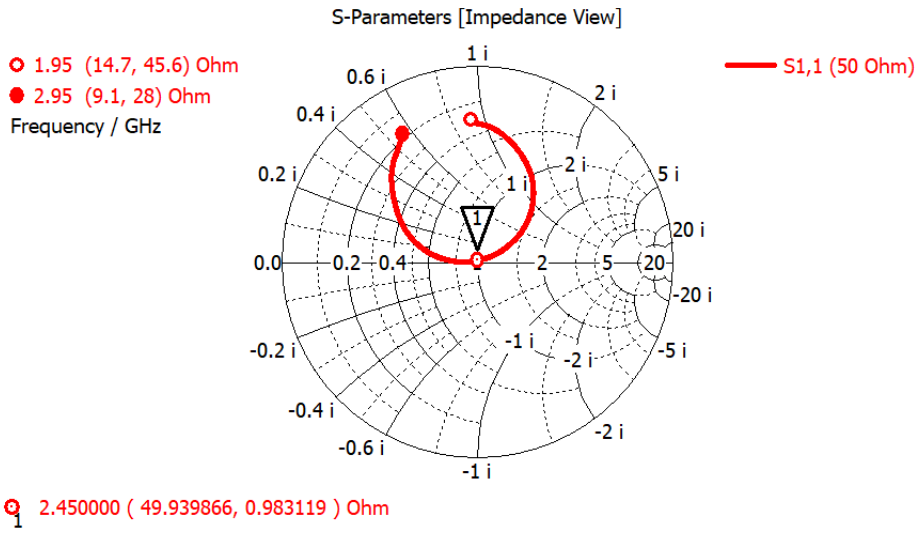

Figure 3.17: Smith Chart from the textile antenna having a 5.3 mm distance from the human body.

In this case the optimization got more difficult but decent results were achieved. The results are shown in the Figure 3.18 and 3.19. Thus the dimensions of the patch of the optimized antenna in Table 3.4.

Table 3.4: Parameters of the patch with the textile antenna optimized with a 2.650 mm distance from the human body.

Length [mm]	Width [mm]	Feed Point [mm]
59.1	15.71	2.6

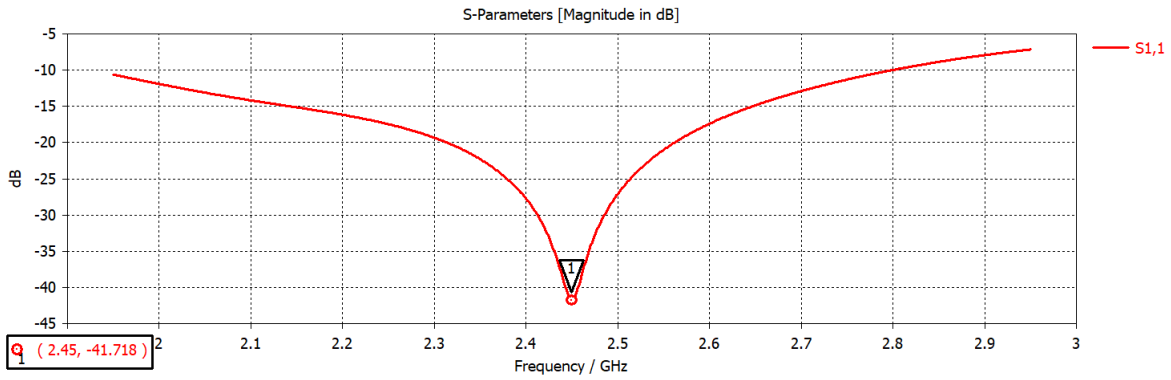

Figure 3.18: S_{11} parameter from the textile antenna having a 2.650 mm distance from the human body.

Adding the fact that the width of the patch antenna tends to gets smaller when the body gets closer to the antenna. Comparing Table 3.3 and 3.4 is possible to see that.

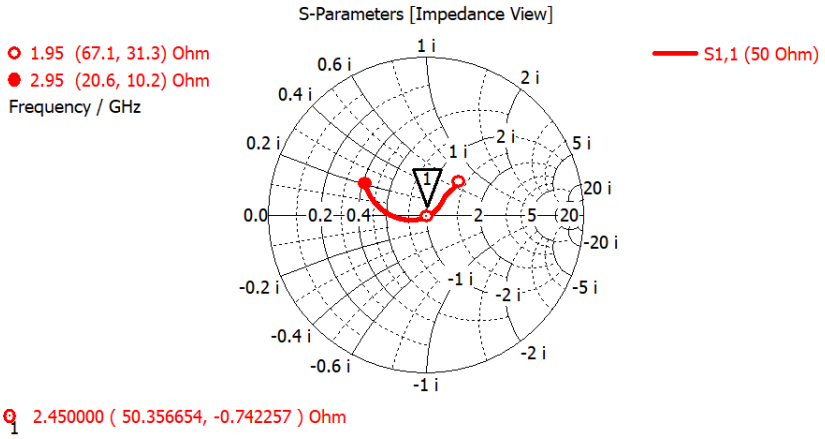

Figure 3.19: Smith Chart from the textile antenna having a 2.650 mm distance from the human body.

3.3.1.2 Optimizing the textile antenna with a superstrate

Just like said before, now the simulations in vicinity of the body will use a superstrate. Equivalent to the substrate of the antenna, the superstrate will be made of the same material. Hence the supestrate is made of 3D Spacer Knit. In Section 3.3.1.1, the tests began with a distance from the body of 5.3 mm and in this section it will start using that distance as well. The results are basically the same when comparing the antennas without superstrate. In Table 3.5 are the dimensions of the patch and the feed point and Figures 3.20 and 3.21 present the results for this case.

Table 3.5: Parameters of the patch with the textile antenna optimized using a 5.3 mm superstrate.

Length [mm]	Width [mm]	Feed Point [mm]
56.1	47	2.5

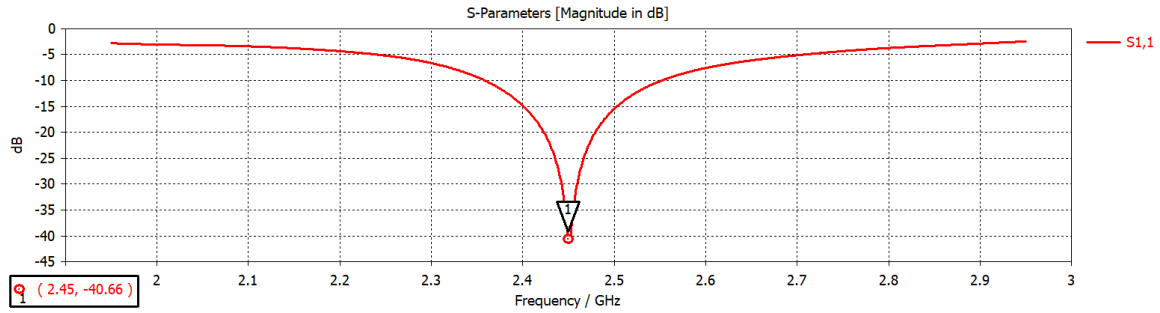

Figure 3.20: S_{11} parameter from the textile antenna using a 5.3 mm superstrate.

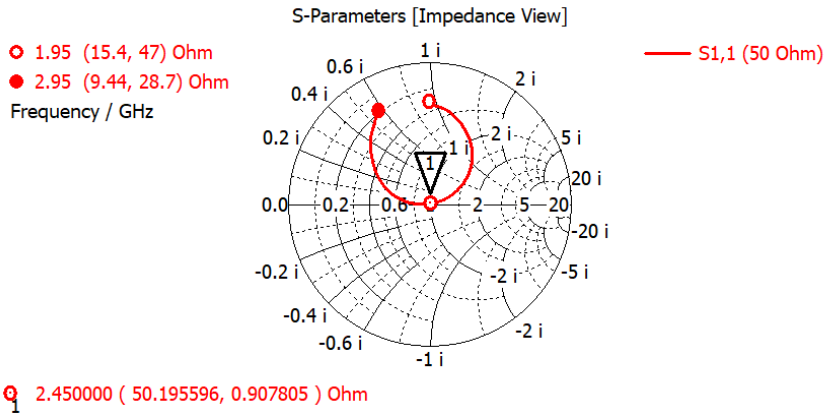

Figure 3.21: Smith Chart from the textile antenna using a 5.3 mm superstrate.

Next the superstrate thickness will be reduced to 2.650 mm, meaning only one layer of 3D Spacer Knit. Once again the optimization is easier using the superstrate and the results are not that different from the optimized antenna without superstrate. The results are shown in Figure 3.22 and 3.23 and the dimensions of the patch and its feeding point are in Table 3.6.

Table 3.6: Parameters of the patch with the textile antenna optimized using a 2.650 mm superstrate.

Length [mm]	Width [mm]	Feed Point [mm]
59.09	16	2.7

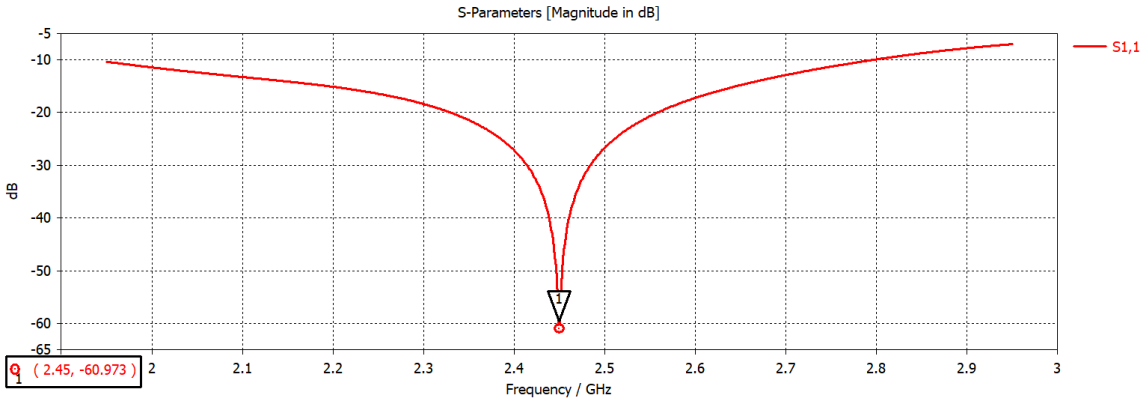

Figure 3.22: S_{11} parameter from the textile antenna using a 2.650 mm superstrate.

The antenna is optimized as it can be seen on Figures 3.22 and 3.23. When comparing to the results obtained in Subsection 3.3.1.1, the results are almost the same although when using a superstrate the optimization process is easier. The same issue occur here

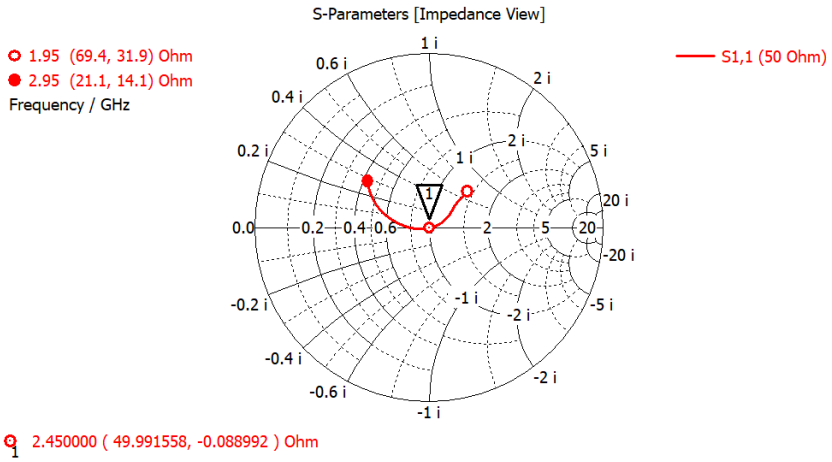

Figure 3.23: Smith Chart from the textile antenna using a 2.650 mm superstrate.

as well, since the width of the patch gets smaller as the distance between the antenna and the body is shortened. Concluding, this simple design won´t work for this project and the search of another design has to be continued.

3.4 Textile triangle patch antenna

The next implemented design was inspired in [45], specifically the first design presented. This design was chosen because the studies made revealed good robustness to the human body and to structural deformations, making it a candidate for flexible and body-worn devices [45] .The full design presented a triangular patch antenna with slots that were used to reduce its size and also slots on the ground in order improve the bandwidth of the antenna. The antenna mentioned is shown in Figure 3.24. Since the design was too complex the first design is a simple patch antenna using a inset feed line. The representation of the antenna is presented in Figure 3.25.

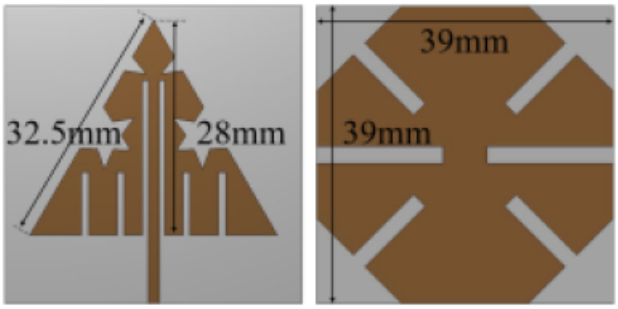

Figure 3.24: Representation of the triangular patch antenna with slots [45].

In Figure 3.25 is the starting design used in [45]. Before making any test in vicinity of

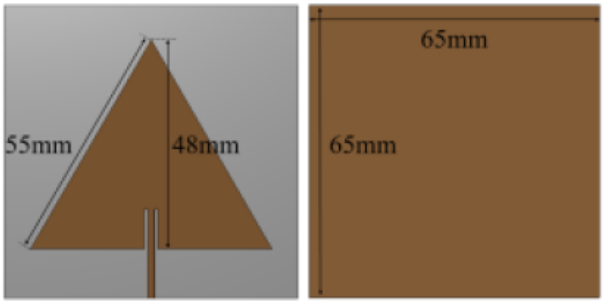

Figure 3.25: Representation of the simple triangular patch antenna [45].

a human body model, first the antenna needs to be optimized radiating on free space. The antenna simulated in CST Studio is represented in Figure 3.26

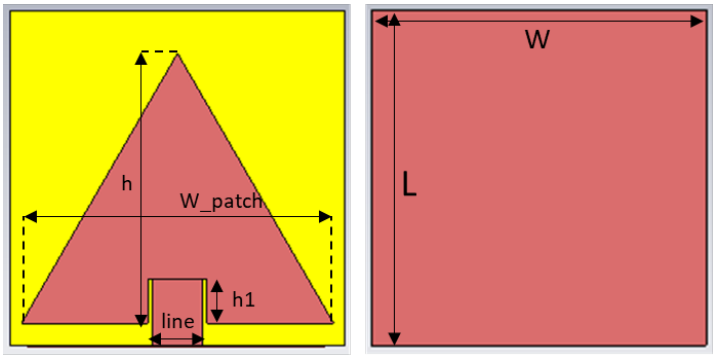

Figure 3.26: Representation of the simple triangular patch antenna in CST Studio.

The optimization of this antenna uses the same principle of the simple patch antenna. The width is used in order to optimize the S_{11} absolute value and the length (in this case height) of the patch to variate the resonance frequency. The only difference is the type of feeding which is the inset feed method. The inset is to match the microstrip line impedance to the patch impedance. The principle for the inset is the same as the one explained in Section 3.1.2 in Figure 3.2. Thus, as the inset approaches the center the impedance gets close to 0 and as it approaches the lower border of the patch the impedance reaches the maximum value. With the antenna optimized to operate in free space, the results are presented in Figures 3.27 and 3.28.

In Table 3.7 indicates the dimensions of the antenna mentioned.

Table 3.7: Dimensions of the triangle patch antenna [mm].

W	L	W patch	h	h1	line
75	75	68	60.1	10	11.4

The antenna is now optimized in free space, passing onto optimizing it to operate close

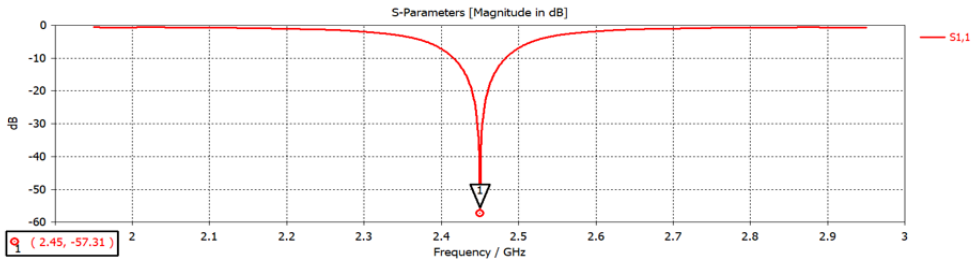

Figure 3.27: S_{11} parameter for the optimized triangular patch antenna radiating at 2.45 GHz in free space.

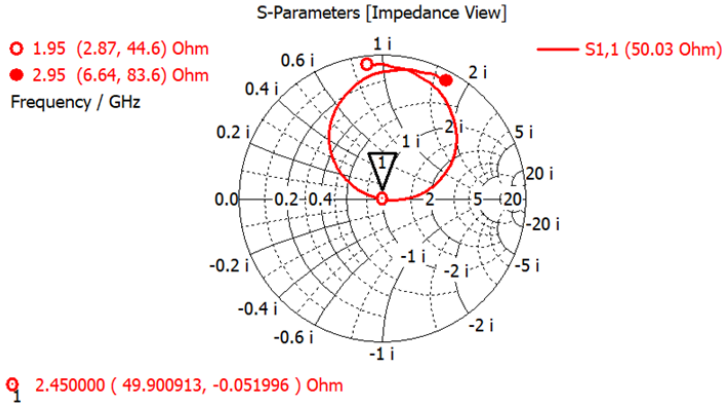

Figure 3.28: Smith chart for the optimized antenna radiating at 2.45 GHz in free space.

to a human body.

3.4.1 Optimizing the antenna in vicinity of the human body

Taking conclusions from section 3.3.1 it is easier to optimize an antenna using a superstrate. In this manner, the optimizations close to the human body will begin already using a superstrate.

The first antenna in contact with the human body model used a superstrate with a thickness of 20 mm. After the antenna being optimized, the antenna took the shape showed in Figure 3.29.

The results for the antenna with a superstrate of 20 mm are arranged in Figures 3.30 and 3.31.

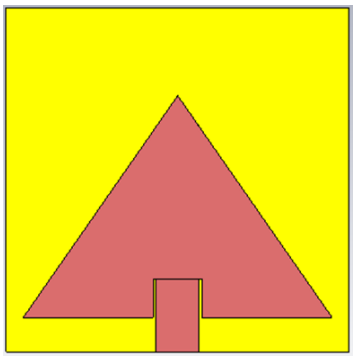

Figure 3.29: Representation of the antenna optimized using a 20 mm superstrate.

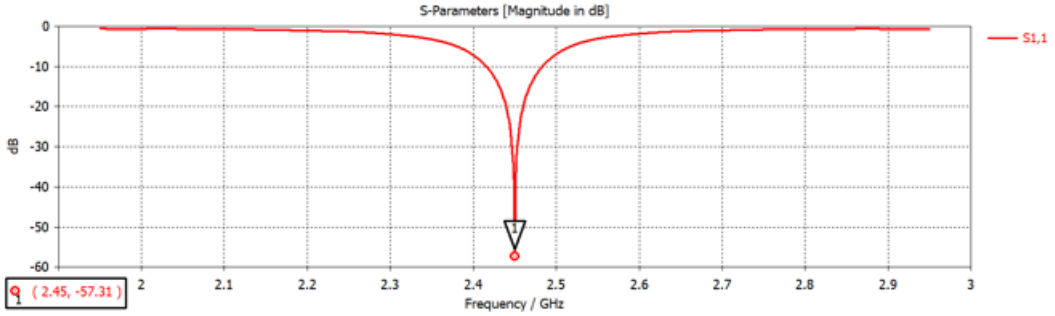

Figure 3.30: S_{11} parameter for the optimized antenna using a 20 mm superstrate..

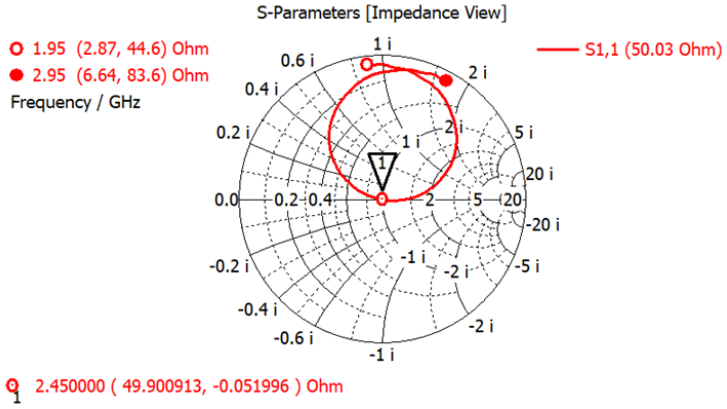

Figure 3.31: Smith chart for the optimized antenna using a 20 mm superstrate..

From this point on the superstrate will be reduced to the minimum possible as it was done in the previous design. The superstrate is now reduced to 10 mm thick, the antenna obtained from the optimization is shown in Figure 3.32.

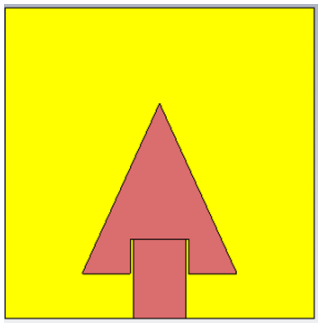

Figure 3.32: Representation of the antenna using inset feed optimized using a 10 mm superstrate.

This antenna is having the same effect as the simple patch antenna. As the body gets closer to the antenna, the thinner the antenna turns. The outcome for this antenna is shown in Figures 3.33 and 3.34.

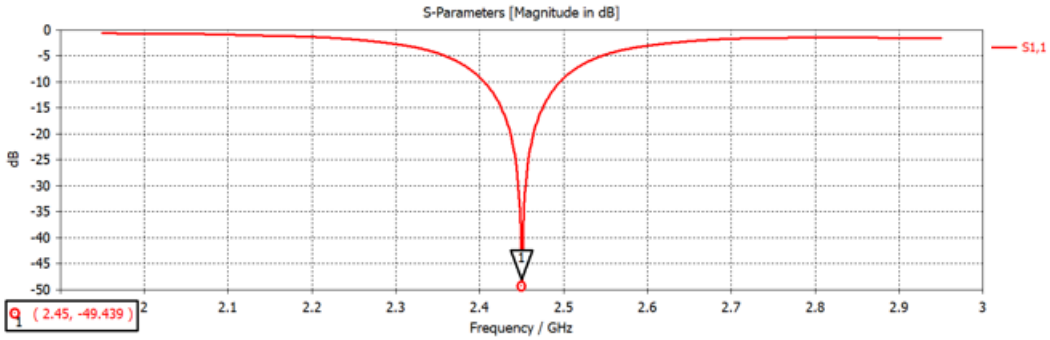

Figure 3.33: S_{11} parameter for the optimized antenna using a 10 mm superstrate.

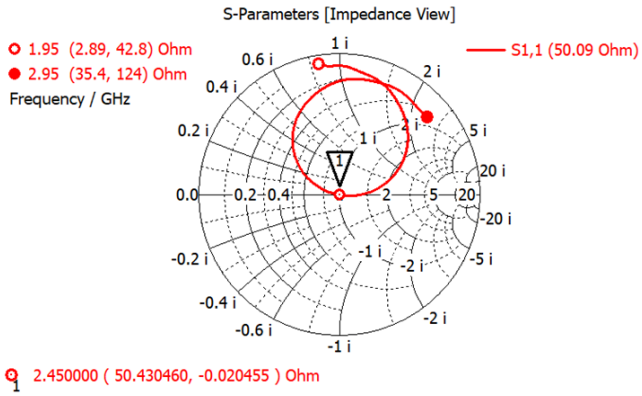

Figure 3.34: Smith chart for the optimized antenna using a 10 mm superstrate.

Based on these results if the antenna reduces even more the superstrate the patch will be even more thin. The other problem is the fact that since will be using textile material, there is a limitation due to the manufacturing process. In the manufacturing process of the antenna, its elements (such as the patch) are laser cut and for that reason, there has to be some room for manoeuvre. Another problem to be addressed is the line thickness, as the line cannot be too thin or else the line might rip. is the lines and their thickness If a cut makes a bit of the copper material that is less then 1.5 mm, there is a probability that it will get burned.

The next optimization has an example to be better explained. The next antenna for this case is optimized using a superstrate of 5.13 mm thick. The representation of this antenna is shown in Figure 3.35

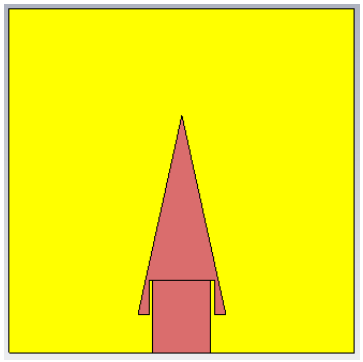

Figure 3.35: Representation of the antenna using inset feed optimized using a 5.3 mm superstrate.

Checking Figure 3.35, as expected, the antenna got to thin and there are parts in its design where it cannot be cut due to material limitations.

The inset feed line for this case is not the best choice since it causes in the triangle spots which are too thin. Meaning that it will not be possible to produce this design. Adding

to that last affirmation, the objective of this project would not be completed since one of the objective is to get the antenna as close to the human body as possible, needing an even thinner layer of superstrate.

The same design was tried without the inset feed as a feeding method and just being a simple patch in a shape of triangle. In Figure 3.36 is shown how the design is without the inset feed.

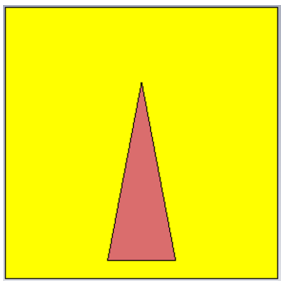

Figure 3.36: Antenna without the inset feed optimized using a 5.3 mm superstrate.

The results provinient from the matched antenna are shown in Figures 3.37 and 3.38

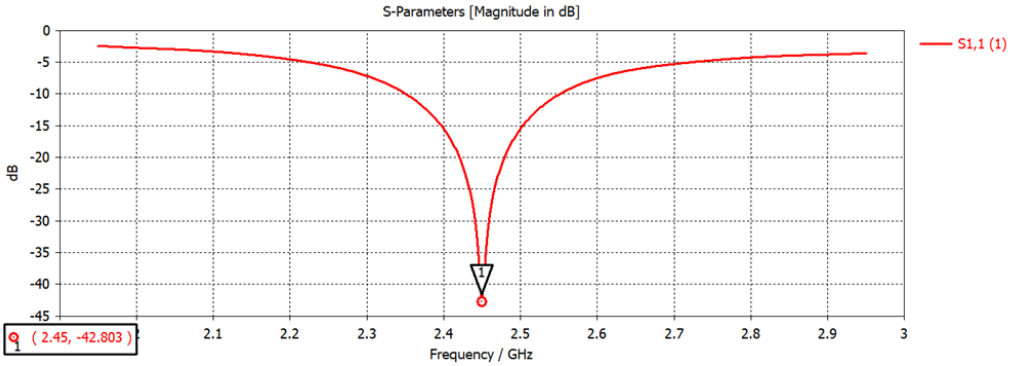

Figure 3.37: S_{11} parameter for the optimized antenna using a 5.3 mm superstrate

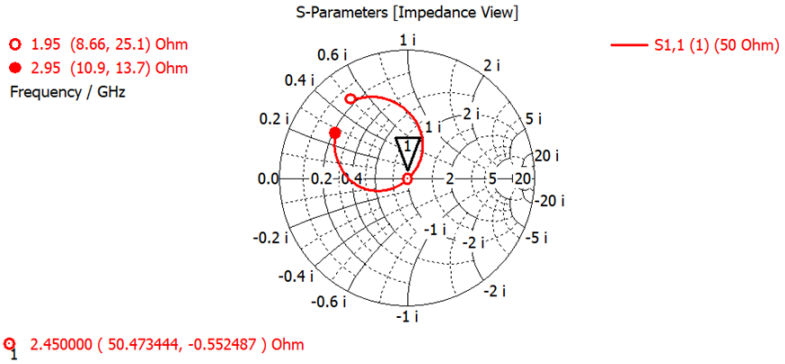

Figure 3.38: Smith chart for the optimized antenna using a 5.3 mm superstrate

The results when comparing to the antenna with inset feed are basically the same, in

this case the problem of the material limitations is solved. Although the antenna is still to small and will eventually be too thin just like the design in Section 3.3

4

Textile patch antenna with slots

In this chapter, presents the chosen design and which is based on [34], this works had biomedical applications and had potential to fulfill the objective of this dissertation. The antenna design chosen uses slots in order to reduce its size and to optimize the resonance at the desired frequency [34].The chapter will begin with a study in how the slots will affect the S_{11} parameter. Starting with slots just in the patch and next with slots just on the ground in order to figure out the final design to be used in this work. After choosing the design, the optimization will begin. Following with simple tests operating in free space and then working it out to radiate close to a human body using the superstrate. Having everything in order with the antenna operating close to the human body, the variation in the lungs and heart will be the next tests to be made in order to understand how the antenna will behave to capture vital signs.

The frequency used on previous designs was 2.45 GHz but in this case it is being design an antenna in order to work on a frequency of 433.32 MHz. The change in frequency is due to the fact that, shown in the previous sections, the patch would become too small as the body comes close with a high frequency, the frequency is reduced in order to have a decent sized patch close to the human body. Adding to these reasons, the fact that a lower frequency has a higher capacity of tissue penetration. Changing the frequency will bring changes such as in the properties of the dielectric and body itself. The material used on the substrate and in superstrate, the 3D Spacer Knit, will change its dielectric property from 1.13 to 1.083 since the frequency changed. These values were obtained using the Microstrip Resonator Patch Method [46]. The properties in

the human body that will change have already been exposed in Section 2.3 in Table 2.4.

4.1 Studying of the slots in the antenna

The antenna created in [34] uses slots on the patch and the ground to decrease the size of the antenna in order to be functional and size-reduced at a low frequency. Thus these slots will have a major impact when optimizing the antenna, in this section will be shown how the slots impact the performance and the optimization of the antenna. The first tests for this matter happened on the patch. Starting with a simple patch antenna $50 \times 50 \times 2.650$ mm radiating in free space without superstrate.

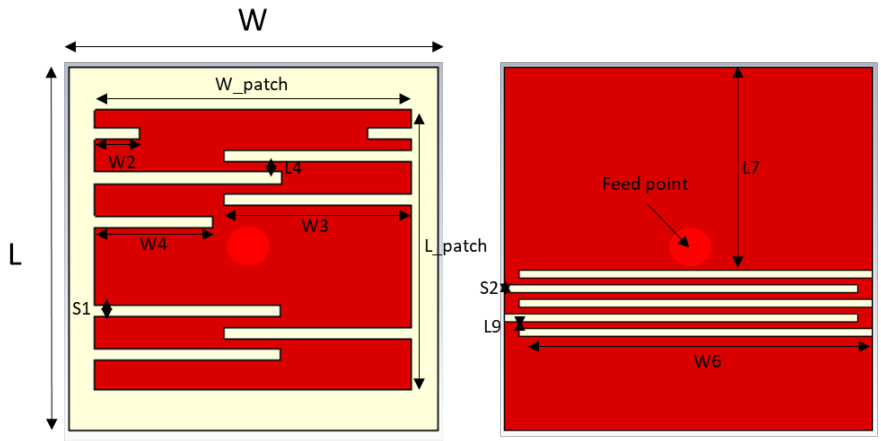

Figure 4.1: Patch antenna with slots in study.

The Figure 4.1 shows the antenna in study and its variables. These variable will be the ones who will help optimizing the antenna in further steps.

Table 4.1: Dimensions for the antenna in study [mm].

W	L	W_patch	L_patch	W2	W3	W4	W6	L4	L9	S1	S2	Feed
75	75	50	35	3	12.7	8	23	0.7	0.2	0.8	0.3	19

The dimensions of this antenna are exhibited on Table 4.1, these values are the starting point for this antenna.

4.1.1 Variation of the slots on the patch

The tests made were similar as the tests made in [40]. The slots were added to the antenna and were made tests to see the effect that it would have on S_{11} parameter. In this subsection it will be tested just the slots in the patch, having a simple ground plane. In Table 4.2 is shown how the slots were added to the patch to simulate the antenna.

Table 4.2: Designs of the antenna adding the slots to the patch.

Antenna Design				
a)	b)	c)	d)	e)
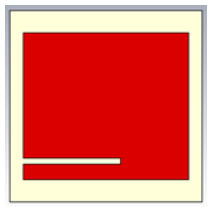	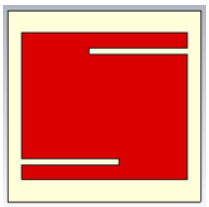	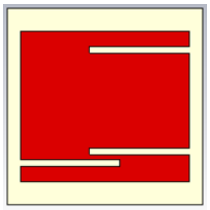	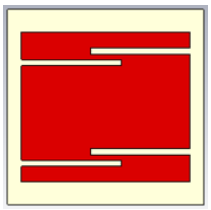	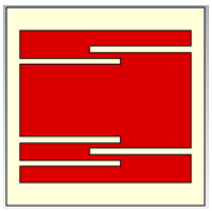
f)	g)	h)	i)	j)
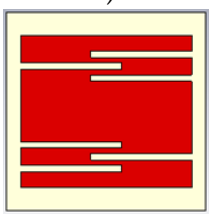	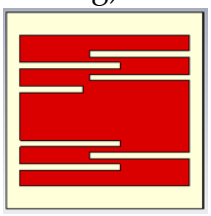	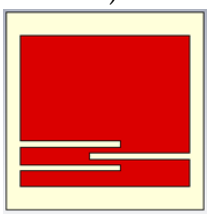	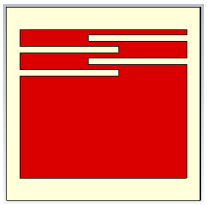	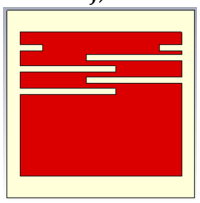

The antennas represented in Table 4.2 labeled from a) to h) were simulated radiating to free space. The S11 parameters obtained from the simulations are represented in Table 4.3 with each label from the respective antenna. When adding slots to the patch the resonance frequency seems to reduce.

As an example of the last affirmation when comparing antenna a) with antenna h), the antenna with more slots (antenna h)) has a lower frequency of work. Comparing antennas i), and j) both have a low frequency, but in order to have a more simplified antenna, antenna i) will be the design to be used on the patch antenna. Antenna i) is more simplified since, comparing with antenna j), will have less variables to be dealt with (check Figure 4.1).

Table 4.3: S_{11} parameter from the antennas with slots in the patch.

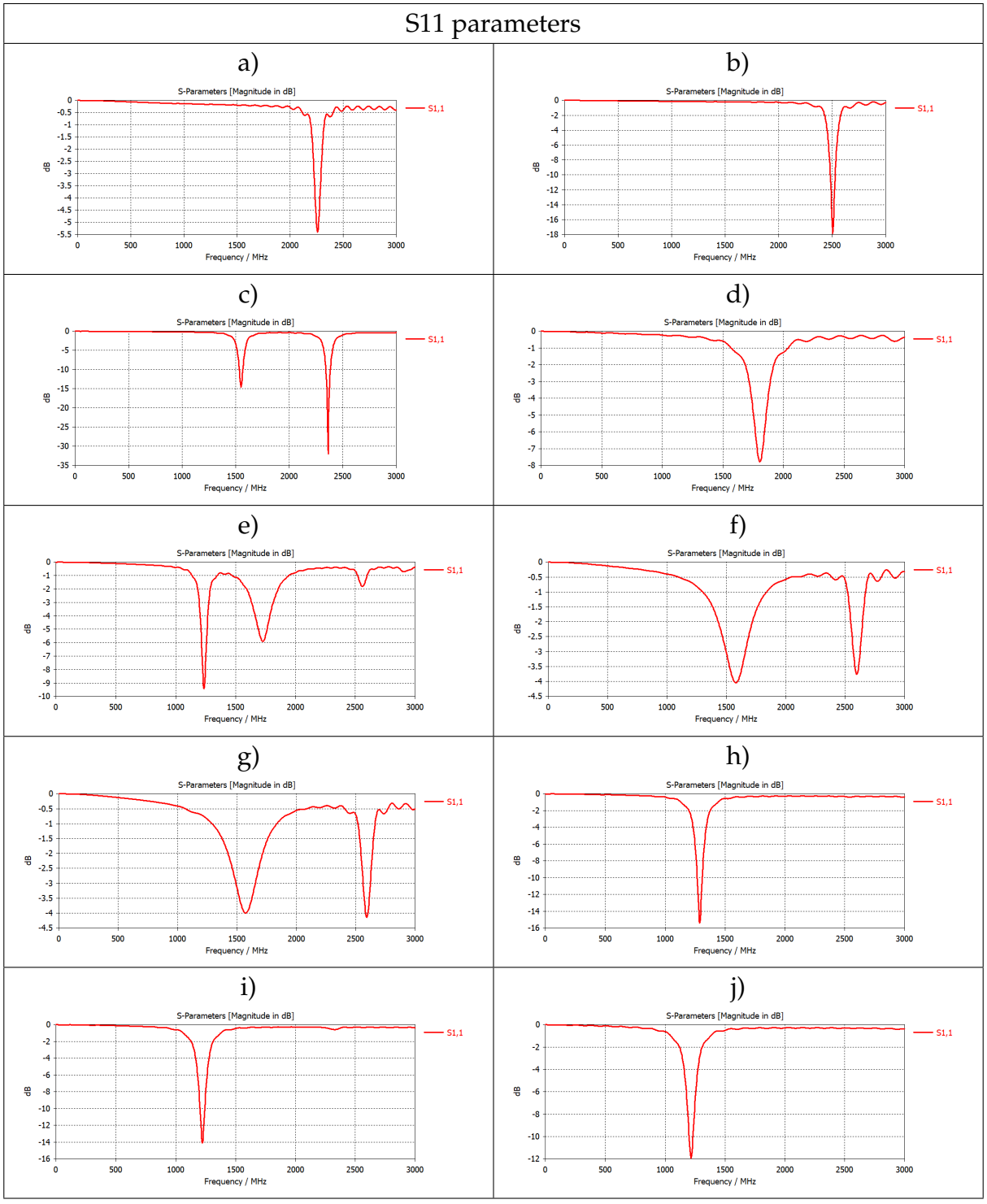

4.1.2 Variation of the slots on the ground plane

Succeeding the tests using slots on the patch and choosing the design for it, in this subsection will be tested just the slots in the ground plane, using a simple patch. In Table 4.4 are the designs of the ground using slots.

Table 4.4: Designs of the antenna adding the slots to the ground.

Antenna Design		
a) 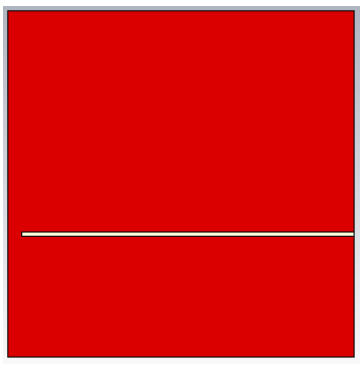	b) 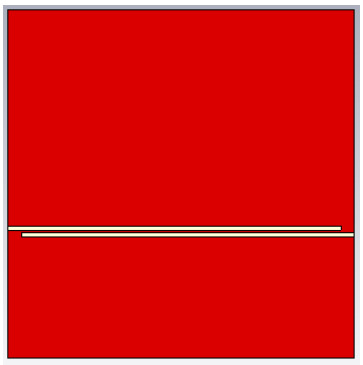	c) 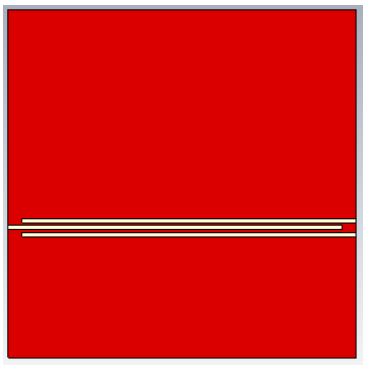
d) 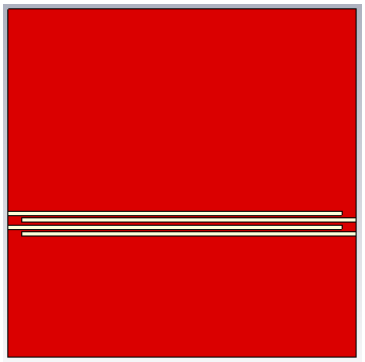	e) 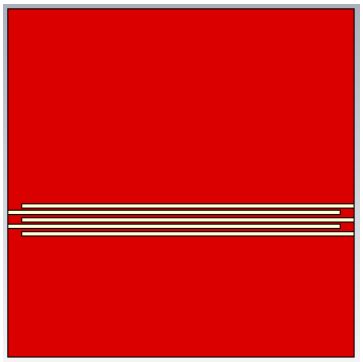	

In [34] the ground plane has L shaped slots in the ground plane, but due to the results from [40], those slots were not considered for these tests as they would not have a big influence in the performance of the antenna. The antennas represented in Table 4.4 labeled from a) to e) were simulated radiating to free space. The S_{11} parameters obtained from the simulations are represented in Table 4.5 with each label from the respective antenna. Just like the patch, in this case as the slots get added, the resonance frequency tends to decrease. In this case the antenna with more slots will be the chosen since has the lowest resonance frequency. The value W6 (which is slots width) helps to obtain the pretended resonance frequency as it will be seen in Section 4.1.3. But can only go as big as the substrate width and the slots can help decreasing the frequency if W6 is not enough. In this case the simplicity factor does not apply as much as in the

case of the patch. That is due to the fact that these slots only work under two variables, as it can be seen in Figure 4.1.

Table 4.5: S_{11} parameter from the antennas with slots in the ground.

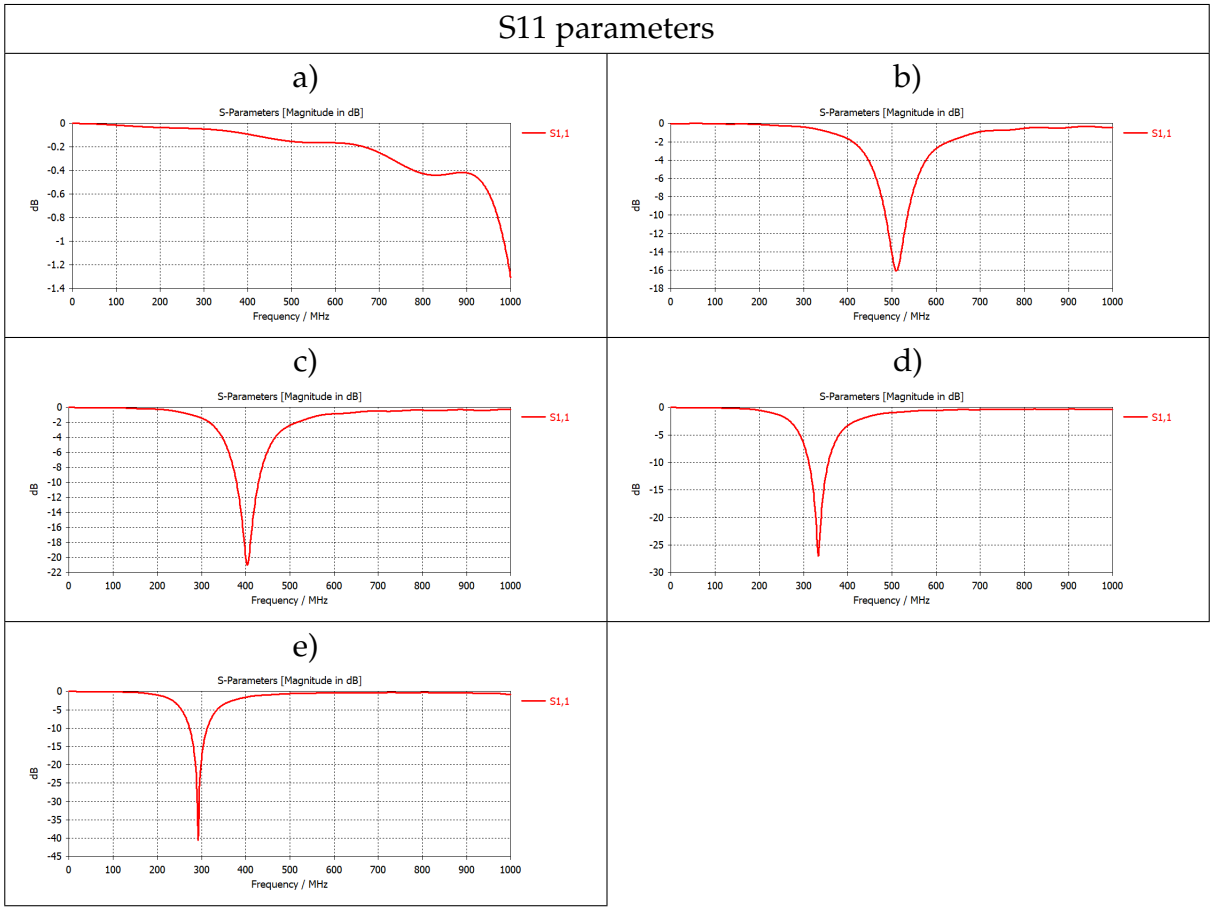

Concluding this subsection the design chosen at end is the design presented in Figure 4.2.

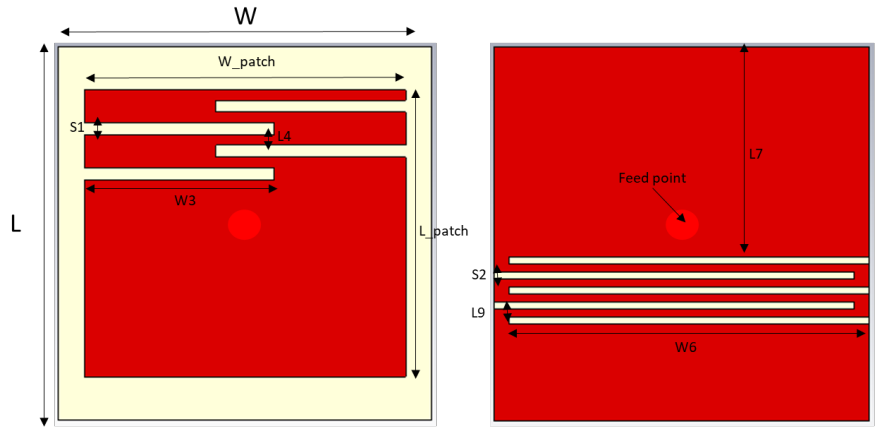

Figure 4.2: Final design of the textile antenna using horizontal slots in the patch and ground.

4.1.3 Parametric study about the variables of the antenna

Having the design finished it is important to understand more about the antenna itself and how the optimization will be made. A last study is made about the slots. Tests involving the length and width of the slots, the space between them etc. The variables that will be tested are represented in Figure 4.2 in the last Subsection 4.1.1.

Starting with the width of the slots. The first test is going to be made in W3 (slot width in the patch), represented in Figure 4.3

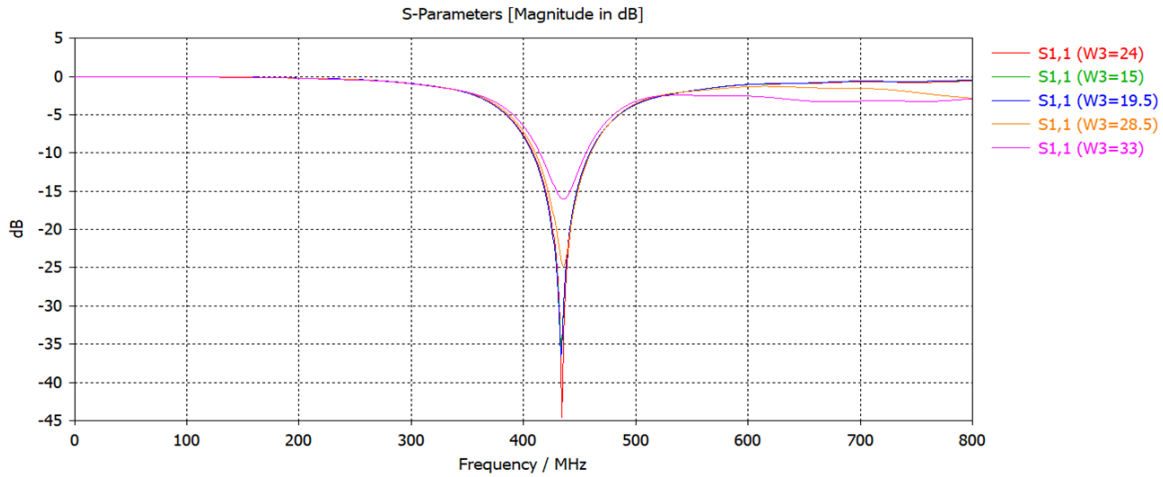

Figure 4.3: S_{11} parameter from the patch antenna with slots varying W3.

This property will help to optimize the value of the S_{11} parameter. The next test to be made is about the width of the slots in the ground, W6. Represented in Figure 4.4

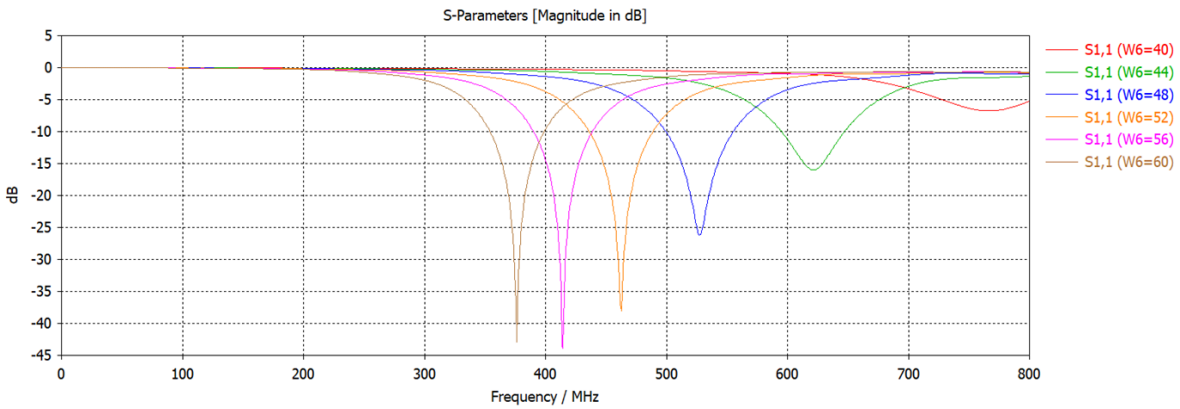

Figure 4.4: S_{11} from the patch antenna with slots parameter varying W6.

The width of slots located in the ground will help to choose the resonance frequency of the antenna. Analyzing Figure 4.4, when W6 increases, the frequency decreases and vice versa.

Passing onto the length of the slots. Beginning with L4, that is the length of the slots located in the patch, Figure 4.5 represent the variation of the variable in question.

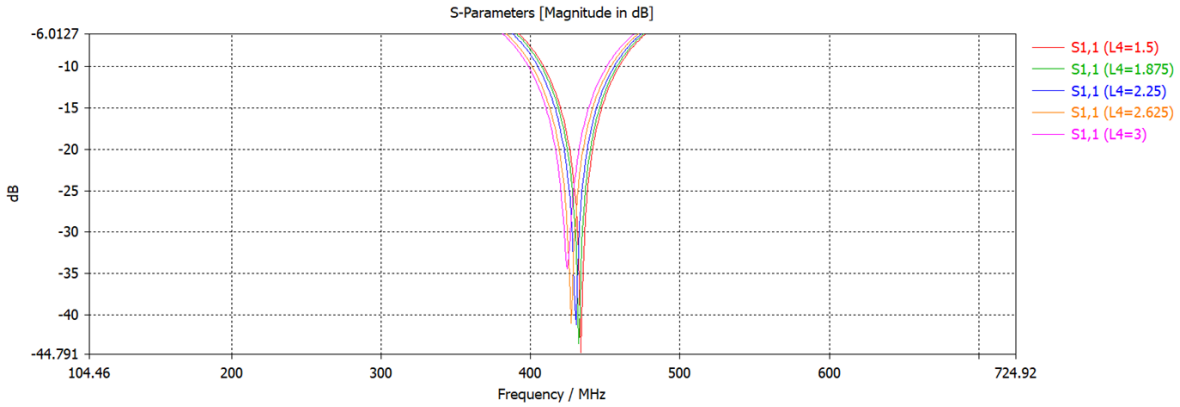

Figure 4.5: S_{11} parameter from the patch antenna with slots varying L4.

The results obtained in Figure 4.5 shows that this variable will not have much impact on the antenna S_{11} parameter. Moving to the length of the slots on the ground, variable named L9. The results are previewed in Figure 4.6.

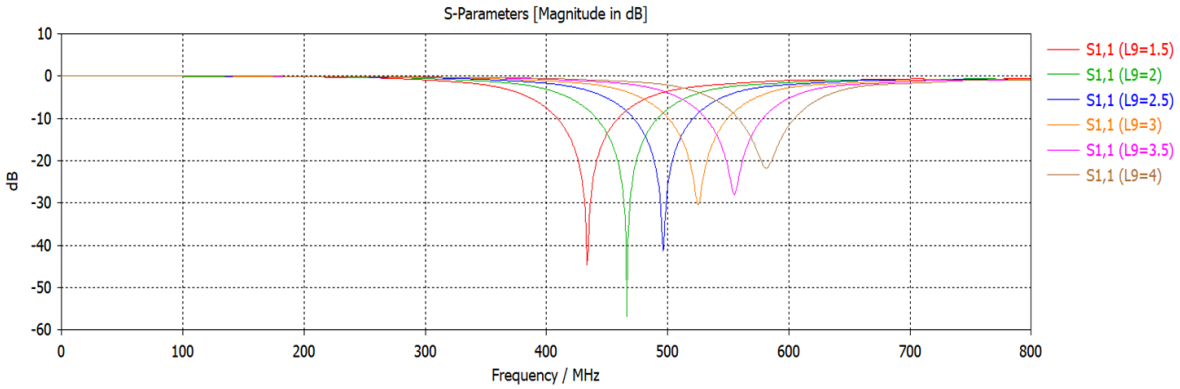

Figure 4.6: S_{11} parameter from the patch antenna with slots varying L9.

The parameter L9 will have a greater impact when comparing to L4. This parameter will have some impact on the resonance frequency, since this value goes up, so does the frequency. These two last variables have a limitation because of the material that the patch and the ground will be built in. The limitation is that these variables cannot be lower then 1.5 mm since the material can get burned or have a rupture when the slots are being cut.

After finishing the study of the slots and how they would affect the antenna, is time to finally start to optimize the antenna. Having the design chosen and just like previous antennas, the first tests will start by having the antenna radiating to open space.

So the first optimized antenna is the antenna represented in Figure 4.7 with the result of the S_{11} parameter presented in Figure 4.8.

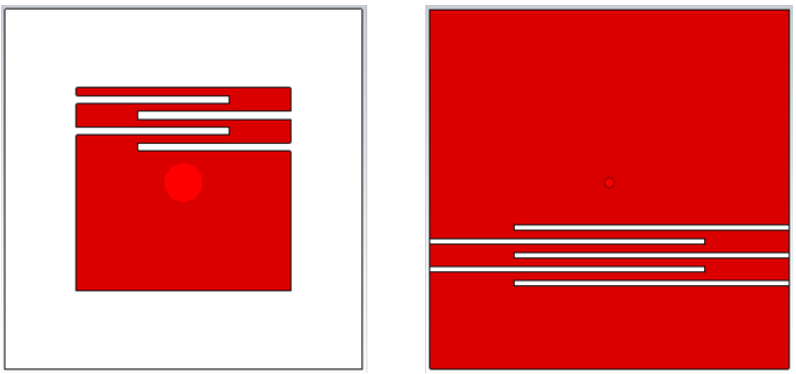

Figure 4.7: Front and back view of the optimized Patch Antenna with slots radiating at 433.32 MHz in free space.

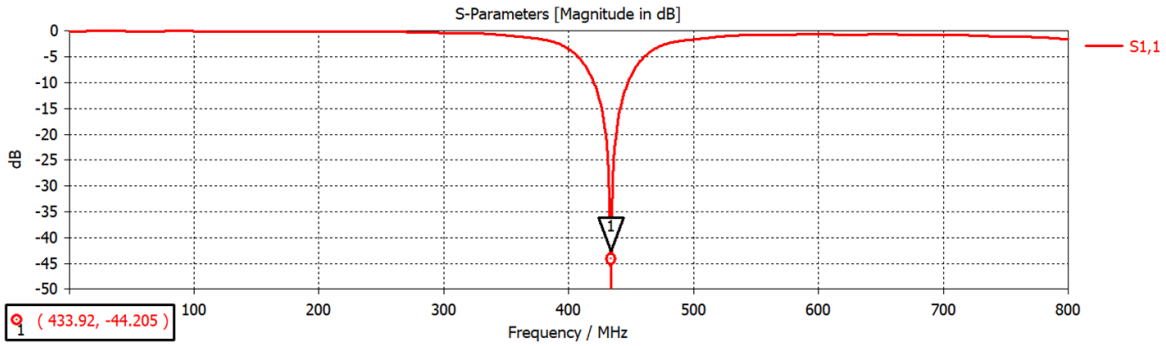

Figure 4.8: S_{11} parameter of the optimized patch antenna with slots.

The dimensions of the antenna are represented in Table 4.6.

Table 4.6: Dimensions of the optimized patch antenna with slots [mm].

W	L	W_patch	L_patch	W3	W6	L4	L9	S1	S2	Feed
70	70	49	32.4	30	53.67	1.53	1.63	1.534	1.06	19

The optimization for this antenna has more complexity when compared to a simple patch antenna. The use of variables like W3, W6, air and air2 are the main ones to be changed when optimizing the antenna. After understand the role of each variable, the optimization gets easier. Concluding the section is now possible to try to optimize the antenna to radiate close to a human body model.

4.2 Optimizing the antenna in proximity of a body

The last step for this textile antenna with slots in the patch and the ground plane, is to optimize the antenna in a vicinity of a human body.

For this purpose, the version with the human body represented in Figure 2.15 in Subsection 2.3.1 will be used. First of all, a superstrate with 10 mm of thickness was used and the antenna optimizations were developed considering as final goal the thickness reduction. Figure 4.9 present the results for the antenna optimized using a superstrate with 10 mm of thickness.

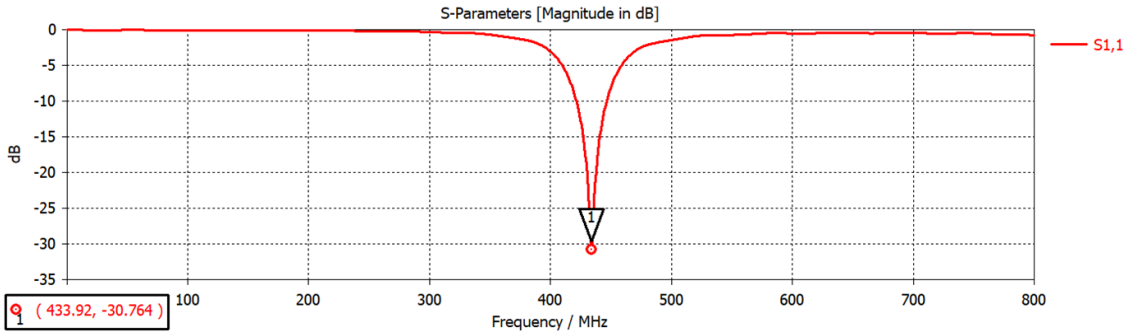

Figure 4.9: S_{11} parameter of the optimized antenna using a superstrate of 10 mm.

Comparing with the antenna radiating in free space, shown in Figure 4.7, the properties that had to change were only the slots. For this antenna were kept the width and length of the patch, since the other designs as the body gets closer those properties would not change. Meaning that this antenna can get close to a body and still have a decent width and length for the patch.

The superstrate was reduced to 7.93 mm (which is equivalent to three layers of the fabric 3D Spacer Knit) and the antenna was optimized accordingly to the results shown in Figure 4.10.

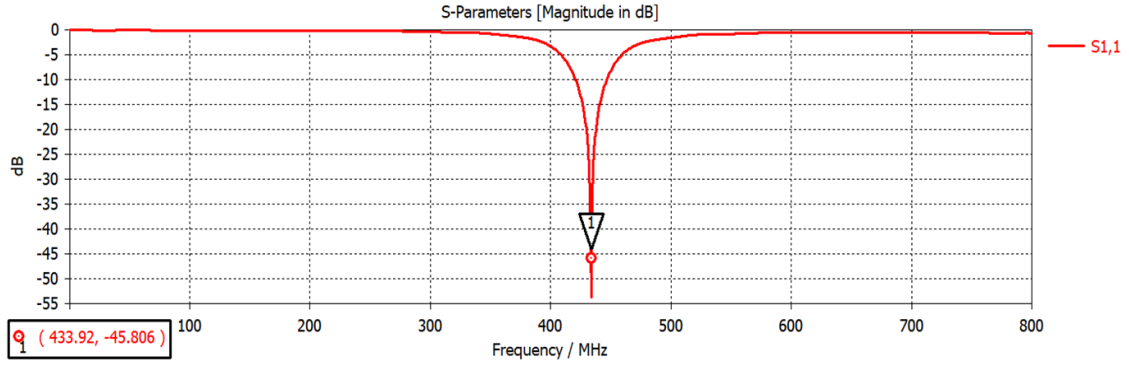

Figure 4.10: S_{11} parameter of the optimized antenna using a superstrate of 7.93 mm.

Finally, the superstrate decreased into 5.3 mm (meaning two layers of the fabric 3D Spacer Knit). Results of the optimized antenna are presented in Figure 4.11.

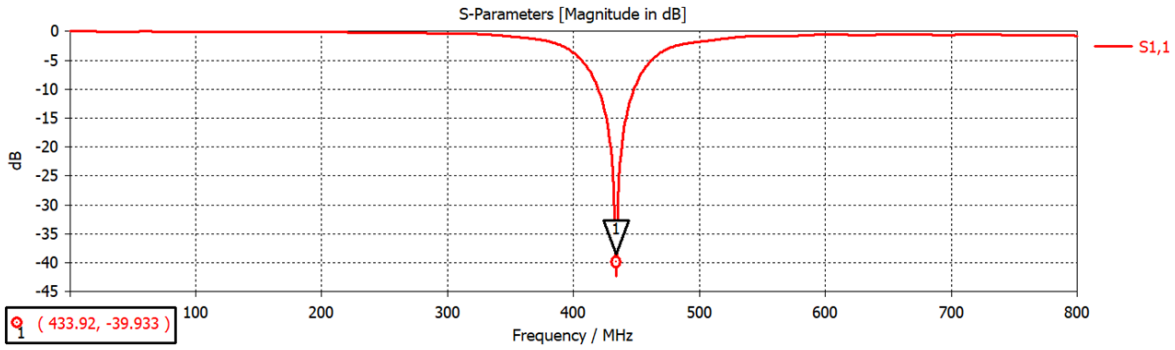

Figure 4.11: S_{11} parameter of the optimized antenna using a superstrate of 5.3 mm.

As said before only the slots changed in order to optimize the antenna, which will not compromise the patch size. Therefore having obtained great results using this design it is worth to use the complete and final body model, represented in Figure 2.16 in Subsection 2.3.1, to validate the last designed antennas.

In this test, it will only be used one layer of 3D Spacer Knit as superstrate, meaning 2.650 mm thick. Obtaining the results shown in Figures 4.12 and 4.13.

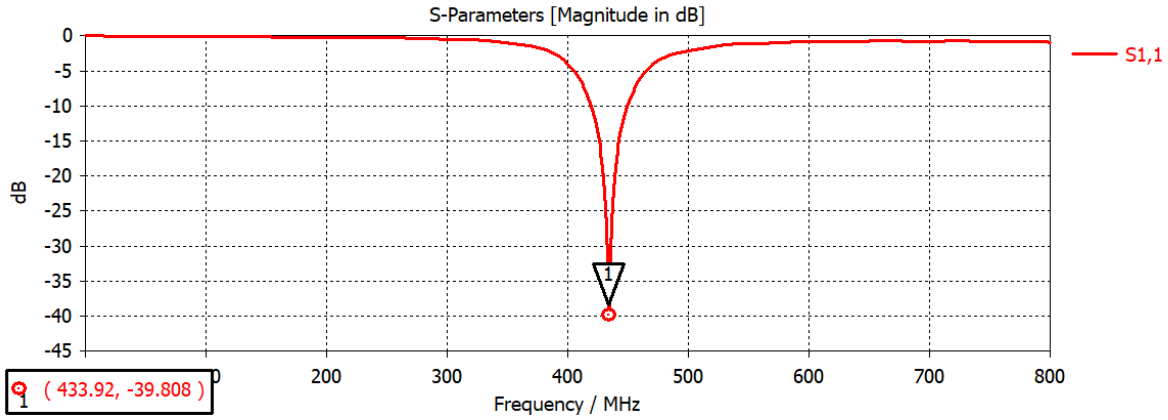

Figure 4.12: S_{11} parameter of the optimized antenna using a superstrate of 2.650 mm.

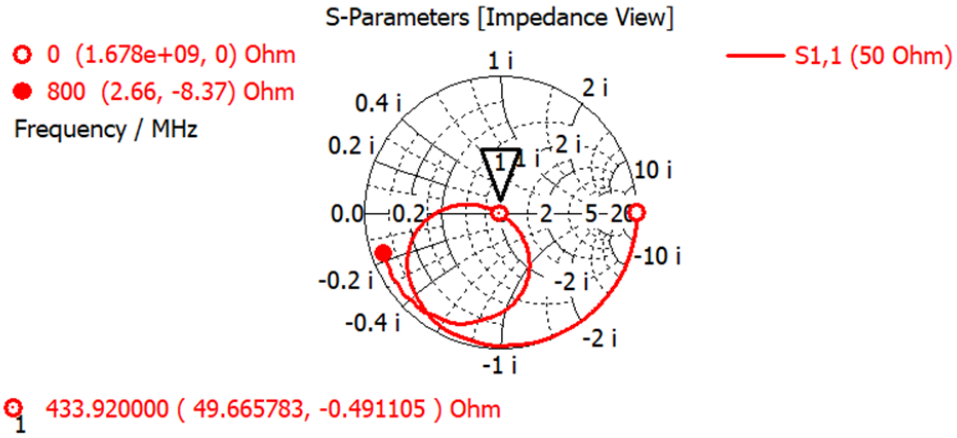

Figure 4.13: Smith chart of the optimized antenna using a superstrate of 2.650 mm.

Checking this Figures is possible to conclude that this antenna can radiate and be optimized close to a human body using only one layer of superstrate. In Figure 4.14 is possible to observe the body model used for these last simulations and the antenna close to it.

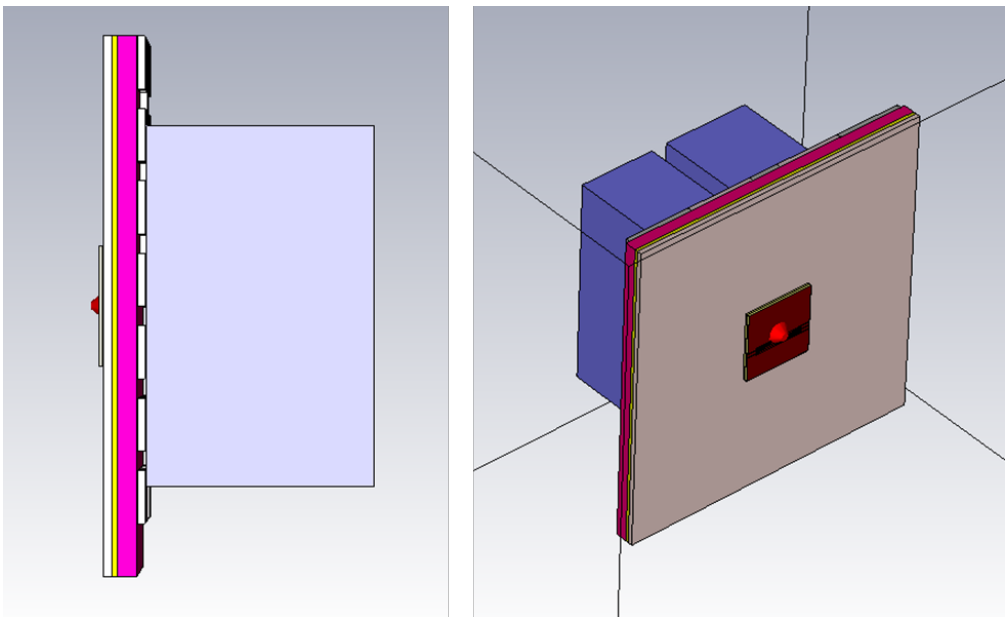

Figure 4.14: Side and perspective view of the antenna close to the human body model

The material has a physical thickness of 2.650mm, but in order to understand the limitations of this antenna more simulations were done. Although it is not physically possible to reduce the thickness of the superstrate, tests were made with a supertstrate with thinner thickness. Simulations were done using a superstrate of 1.325 mm and 0.8 mm thick, and the results are shown the following Figures. Starting with Figure 4.15,

are the results for the optimized antenna using a superstrate with a thickness of with 1.325 mm.

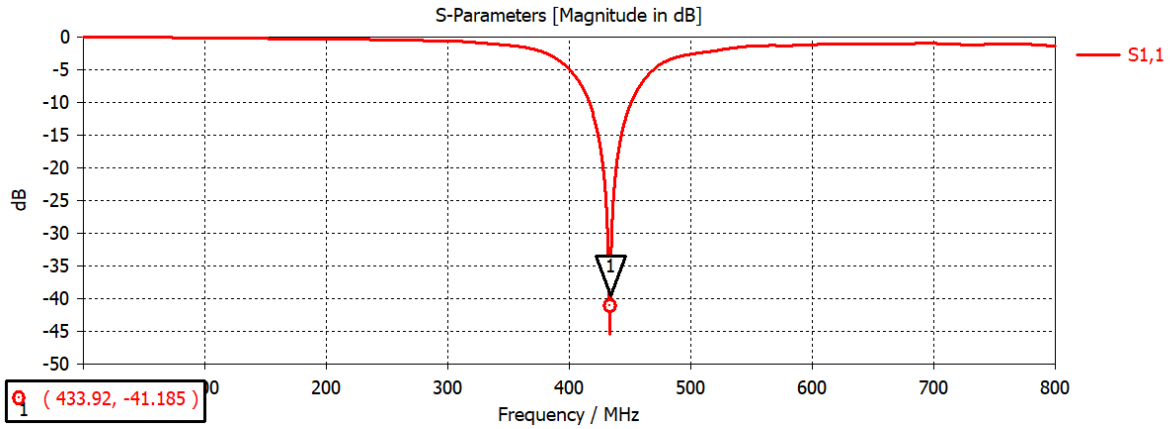

Figure 4.15: S_{11} parameter of the optimized antenna using a superstrate of 1.325 mm.

The last antenna with a superstrate with a thickness of 0.8 mm, has the results exhibited in Figure 4.16.

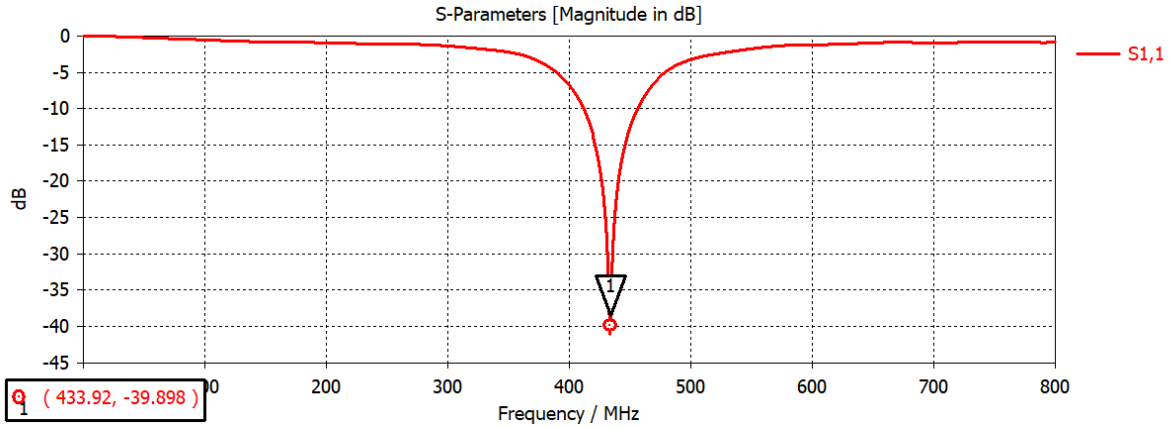

Figure 4.16: S_{11} parameter of the optimized antenna using a superstrate of 0.8 mm.

These two antennas will not be constructed due to not have the availability to use these materials for this dissertation. Thus this proof that this antenna can function in a close proximity to the human body.

Concluding this chapter, the textile antenna that has been chosen to be used as the final prototype will be the one designed using a superstrate 2.650 mm thick. These antennas have been using a discrete port in the simulations, hence to be realistic, a coaxial connector was designed to be used in this antenna. Using the Equation 4.1 was possible to design a coaxial cable with an impedance of 50 Ω.

$$Z_0 = \frac{60}{\sqrt{\epsilon_r}} \times \ln \frac{b}{a} \tag{4.1}$$

Where Z_0 is the impedance of the coaxial cable, b the coaxial external radius of the conductor and a the internal radius of the conductor. Having ended up with a and b respectively being 0.635 mm and 2.12 mm.

Finalizing with the following textile patch antenna showed in Figure 4.17 with the dimensions presented in Table 4.7.

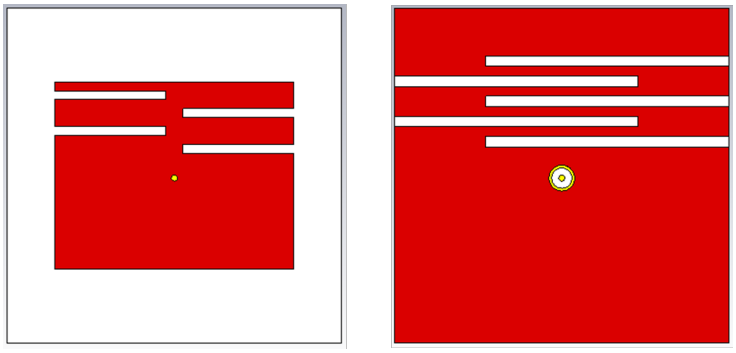

Figure 4.17: Final design for the textile antenna using a patch with slots.

Table 4.7: Dimensions of the final optimized patch antenna with slots [mm].

W	L	W_patch	L_patch	W3	W6	L4	L9	S1	S2	Feed
70	70	50	39.09	22	51.05	1.875	2.015	1.85	2.2	19

With the antenna fully optimized to work in the vicinity of a human body in order to detect vital signs, the antenna can now be built to operate for the matter.

4.3 Simulating Deformations in the antenna

One advantage that a textile antenna has over a conventional antenna is the fact that the textile antenna can be malleable. This advantage comes with a bad side which can cause a deformation in the patch meaning it will have an effect on its performance. This part of the work is to demonstrate how the antenna will be affected by the deformations that a human body can cause. A simple three layer model will be used for this test since the purpose for this simulation is only to test the effect of deformations.

The deformations in the simulation will be performed as showed in Figure 4.18. Starting with the form presented in Figure 4.18a and gradually transform into the form in

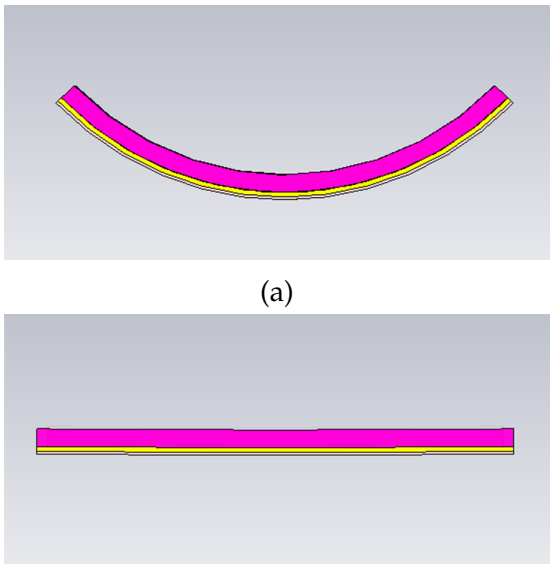

(a)

(b)

Figure 4.18: Illustration of the movement of the body deforming.

Figure 4.18b. The Figure 4.19 is displayed to exemplify how the antenna is mounted in this setup.

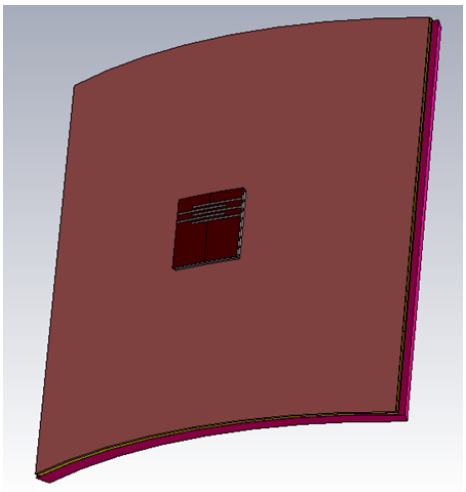

Figure 4.19: Textile antenna setup for deformation test.

The outcome from this deformations is presented in Figure 4.20.

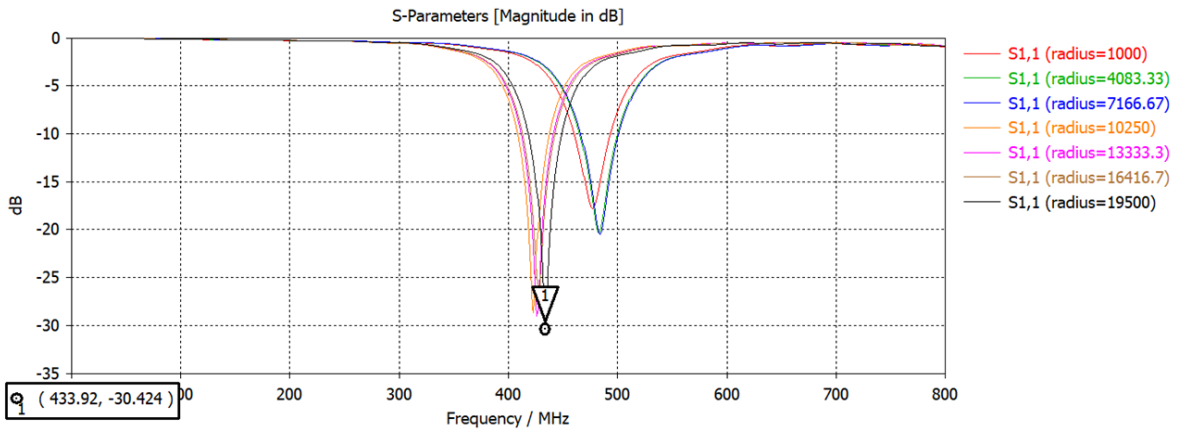

Figure 4.20: S_{11} parameter for different radius of deformations.

The variable 'radius' for this case dictates the level of deformation of the antenna. Basically, as the radius increases, the more the antenna gets close to having no deformations. The point where the antenna is optimized is where the body does not have deformations, having a totally plane body. The results observed on Figure 4.20 are as expected since as the radius keeps increasing so does the antenna gets closer to the optimized point in the resonance frequency of 433.92 MHz. Therefore the plausible limit value for the radius is about 19500 mm.

4.4 Simulating vital signs

This first section is a brief study about how the antenna will behave when there is changes in the body properties, in this case simulating respiration and cardiac pulse. Before simulating the full motion and the full change in the dielectric properties, there will be a division in this process. The body will be moving in three different axis before the full movement, in this case, simulating the X, Y and Z axis movement separately. The vital signs will be detected via help of the reflection coefficient phase of the antenna, as the respiratory or cardiac cycle occurs, the reflection coefficient phase will change. When verifying the reflection coefficient phase of the antenna a problem was observed. In Figure 4.21 it can be seen that the reflection coefficient phase had a discontinuity and with that, would not be possible to have a correct reading of the vital signs.

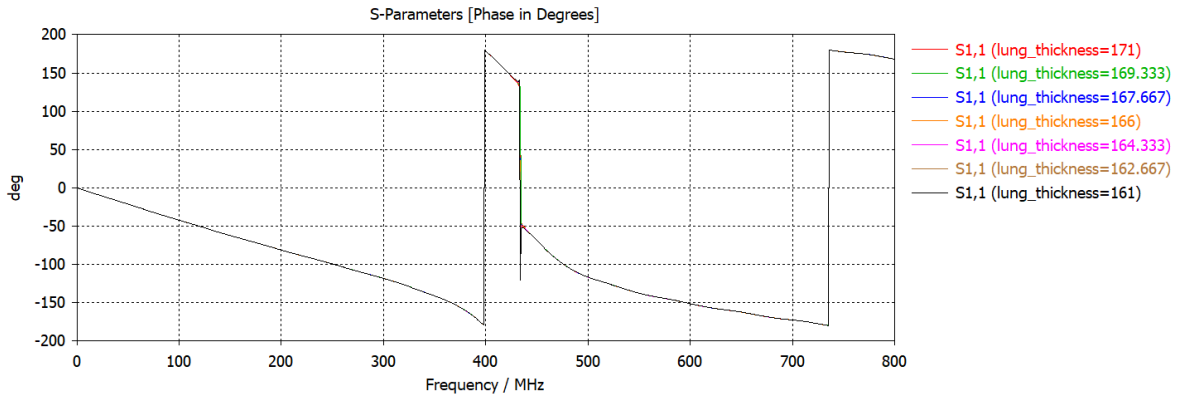

Figure 4.21: $S\,11$ parameter phase varying the lungs properties.

The antenna then had to suffer some changes in order to correct this issue, it was observed that the width of the slots in the patch had an impact on how the reflection coefficient phase would respond. Thus that the correct reflection coefficient phase was achieved varying W3. With that out of the way, the antenna with the modifications is displayed in Figure 4.22.

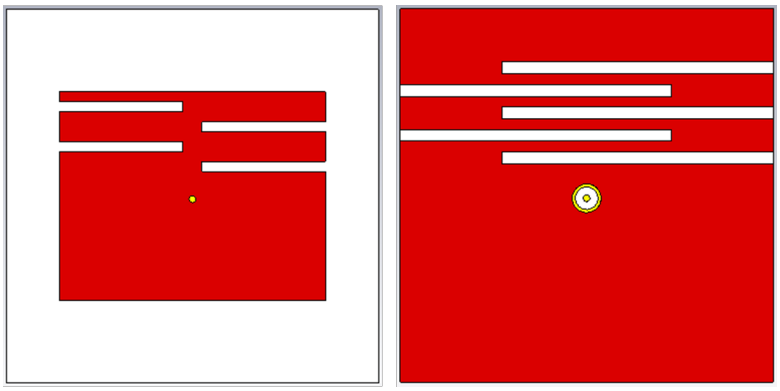

Figure 4.22: Corrected Textile patch antenna with slots corrected operating at 433.32 MHz.

Comparing Figure 4.22 with Figure 4.17, it seems to not have major changes. The problem was resolved by changing varying W3. Since the antenna has various variables the antenna has more then one way to be optimized.

Meter novas medidas

As the problem been solved, the respiratory and cardiac pulse can now be simulated. There are three properties in lungs that changes throughout the respiratory cycle: relative permittivity, electric conductivity and density. Density does not have much influence over the phase, as shown in Table 4.8. In both tables the movement is being

made in Z axis but in Table 4.8 density is being varied as well and in Table 4.9 only the movement is varied.

Table 4.8: Reflection coefficient phase values density variation according with the chest wall movement.

Density [kg/m3]	394	525,2	656,4	787,6	918,8	1050
Phase [º]	71,099	71,148	71,207	71,267	71,332	71,403

Table 4.9: Phase values in condition of the movement.

Lung thickness [mm]	100	97,6	95,2	92,8	90,4	88
Phase [º]	71,099	71,148	71,207	71,267	71,332	71,403

In this case was varied the Z axis Analyzing the Tables 4.8 and 4.9 it can be seen that the values are the same meaning that the reflection coefficient phase is only varying due to the movement of the body. Each axis will be having four tests before making the full movement of the respiratory cycle. Two tests consist on varying the relative permittivity and the electric conductivity both in simultaneous with the movement of the lungs. One test just for the movement and the last one with these properties in simultaneous. These properties will suffer a variation to simulate the breathing action for each axis. This is to analyze which axle or which property has the more influence over the reflection coefficient phase of the antenna. The starting point for every simulation will be when the lungs are full with air and the last point with the lungs fully deflated. Each movement from each axis will be varying from around 8-12 mm [6]

4.4.1 Variation of the lungs in Z axis

Starting with the Z axis which referrers to the thickness of the lungs. The representation of the movement is shown in Figure 4.23.

The lungs for this case will be varied 10 mm [41]. The highest value means the lungs will be inflated and the lowest value meaning the lungs will be deflated.

The first results provided by the simulation varying the relative permittivity depending on the thickness of the lung are in Figure 4.24.

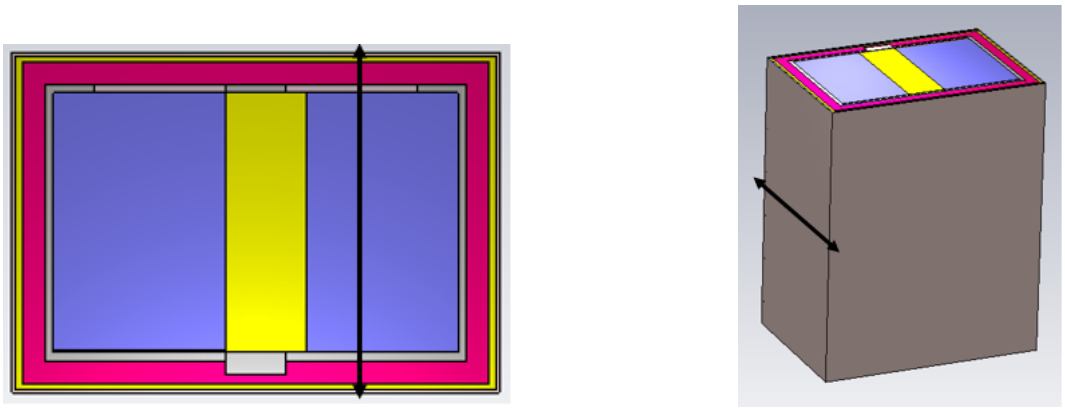

(a) (b)

Figure 4.23: Illustration of the movement of the body.

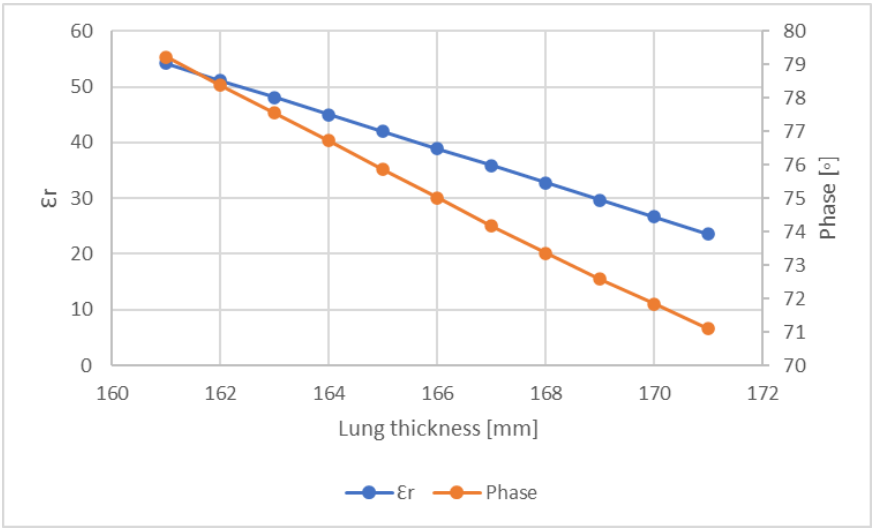

Figure 4.24: Reflection coefficient phase depending of the lung thickness varying relative permittivity.

The difference of reflection coefficient phase that takes place in Figure 4.24 is from about 8.127 degrees. As the relative permittivity reduces so does the phase.

The next one is electric conductivity depending on the thickness of the lung. The results are displayed of Figure 4.25.

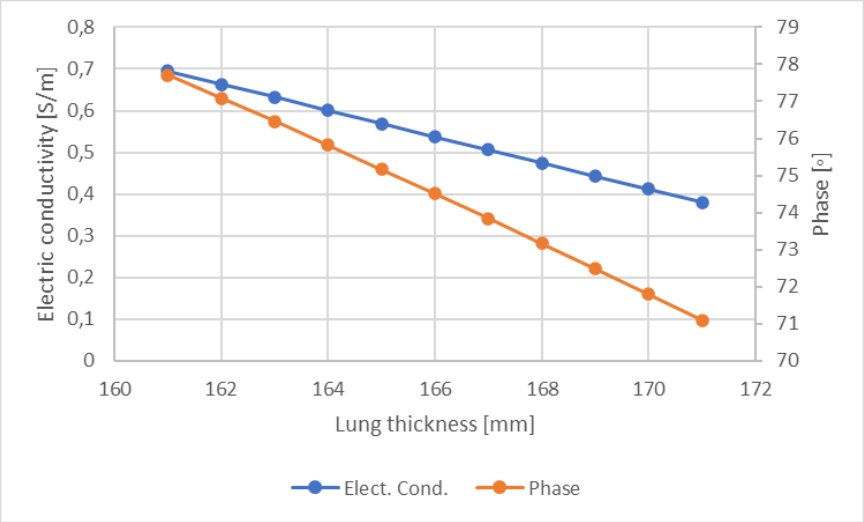

Figure 4.25: Reflection coefficient phase depending of the lung thickness varying electric conductivity.

The difference of reflection coefficient phase that takes place in Figure 4.25 is from about 6.614 degrees. The same event occurs in this case, as the electric conductivity is decreasing so does the phase.

Before combining these properties, this next Figure 4.26, represents the phase of the antenna just depending on the lung thickness and without varying any other property.

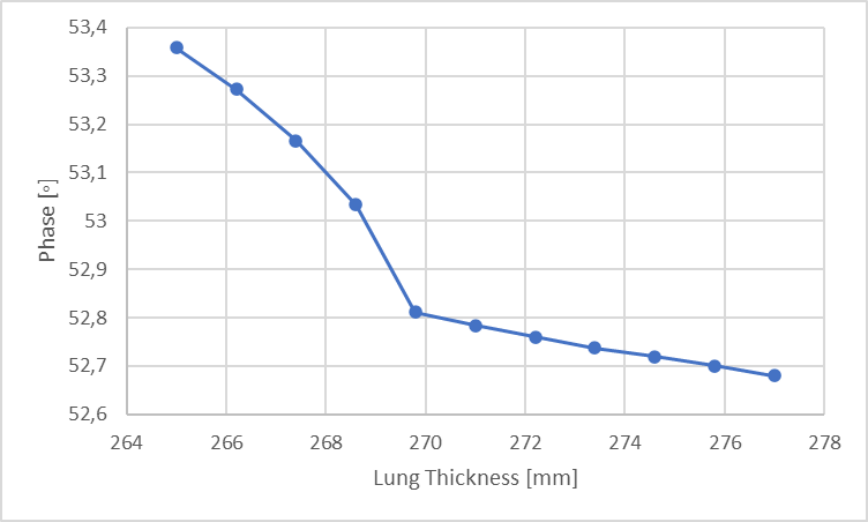

Figure 4.26: Reflection coefficient phase depending on the lung thickness.

The difference of reflection coefficient phase that takes place in Figure 4.26 is from about 0.679 degrees. The movement from the Z axis does not seem to have a big influence on the phase.

The Figure 4.27 is the last from this section and shows the reflection coefficient phase of the antenna when relative permittivity and electric conductivity are simultaneously depending on the lung thickness.

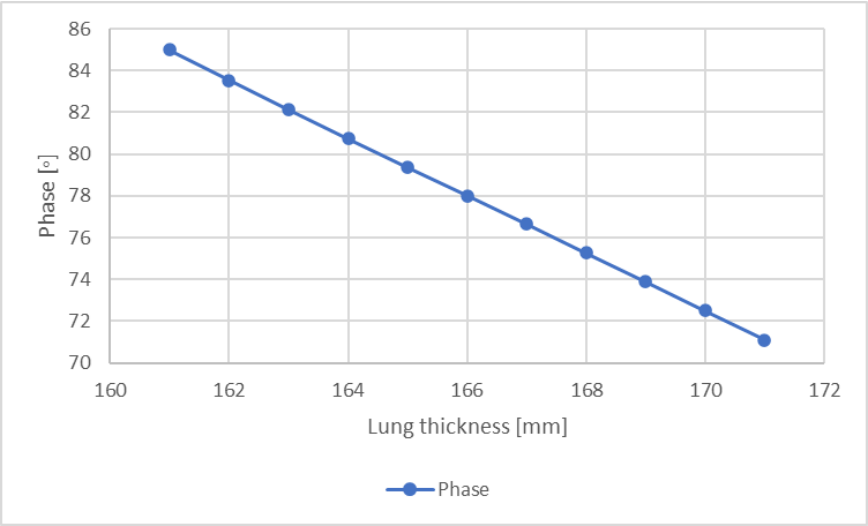

Figure 4.27: Reflection coefficient phase depending of the lung thickness varying electric conductivity and relative permittivity.

The difference of reflection coefficient phase that takes place in Figure 4.27 is from about 14.889 degrees. Concluding the simulations in the first axis, good results were achieved. The antenna has a significant change in the phase.

4.4.2 Variation of the lungs in X axis

The next movement being varied is the width of the lungs. The representation of the movement explained is displayed in Figure 4.28.

When varying the width of the lungs, the variation will have a difference of 12 mm [41]. Having 100 mm when the lungs are inflated and 88 mm when deflated [6].

The first results provided by the simulation varying the relative permittivity depending on the width of the lung are on Figure 4.29.

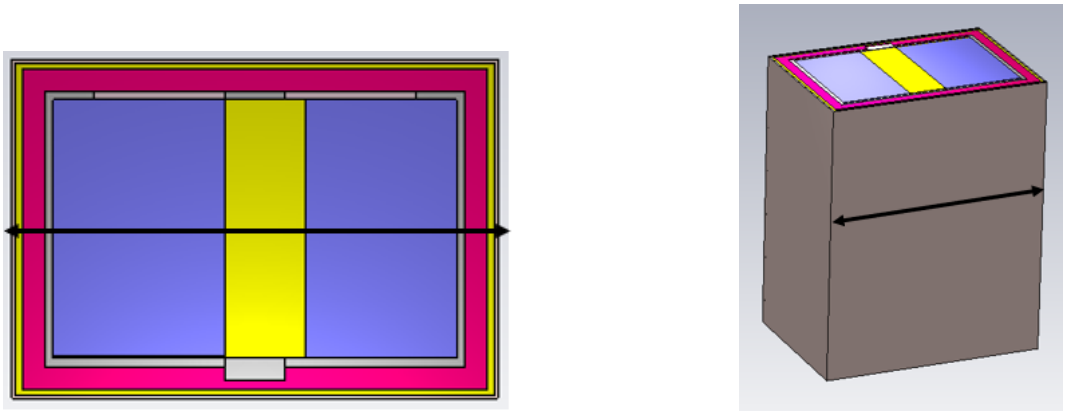

(a) (b)

Figure 4.28: Illustration of the movement of the body.

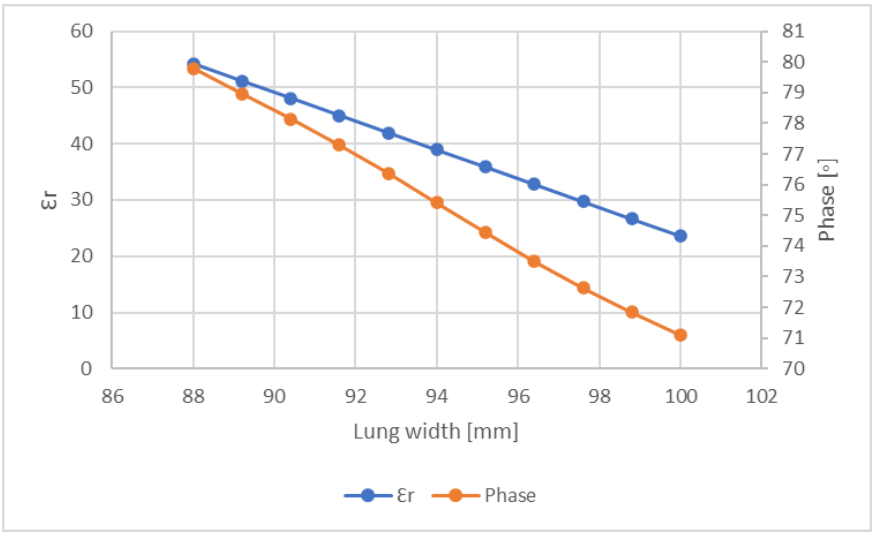

Figure 4.29: Reflection coefficient phase depending of the lung width varying relative permittivity.

The difference of reflection coefficient phase that takes place in Figure 4.29 is from about 8.69 degrees. From the last section, relative permittivity had the most influence in the difference of the phase, and for this case the same happens.

The next one is electric conductivity depending on the width of the lung. The results are displayed of Figure 4.30.

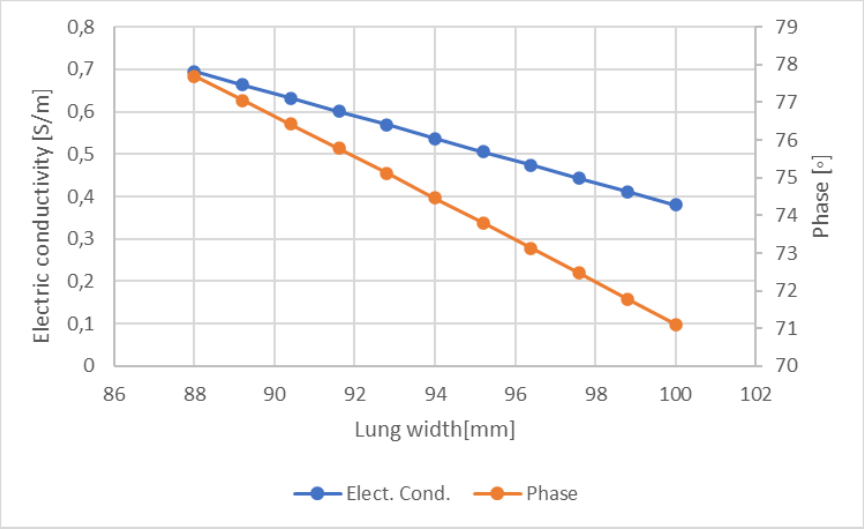

Figure 4.30: Reflection coefficient phase depending of the lung width varying electric conductivity.

The difference of reflection coefficient phase that takes place in Figure 4.30 is from about 6.583 degrees. Before combining these properties, Figure 4.31 represents the reflection coefficient phase of the antenna depending just on the lung width.

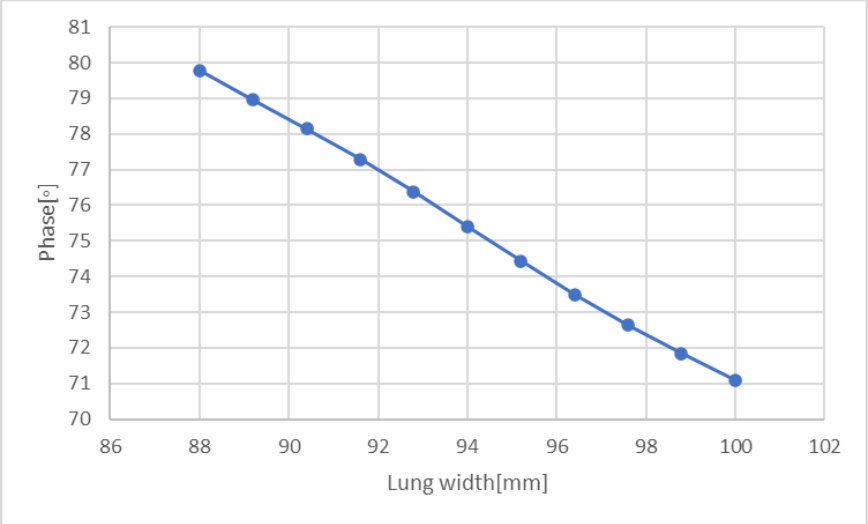

Figure 4.31: Reflection coefficient phase depending on the lung width.

The difference of reflection coefficient phase resulted in Figure 4.31 is from about 8.691 degrees. When the width of the lungs changes size, the shift in reflection coefficient phase will be more noticeable comparing to the movement on section 4.4.1. Therefore width has more influence then the thickness of the lungs. The Figure 4.32 shows the reflection coefficient phase of the antenna when relative permittivity and electric conductivity are simultaneously depending on the lung width.

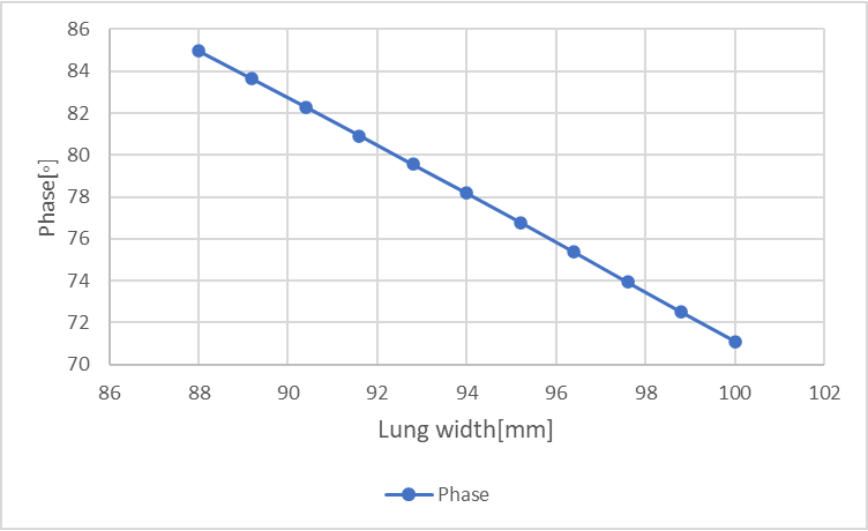

Figure 4.32: Reflection coefficient phase depending of the lung width varying electric conductivity and relative permittivity.

The difference of reflection coefficient phase that takes place in Figure 4.32 is from about 13.866 degrees. The variation in reflection coefficient phase from this final result is not that different from the final result obtained in the Z axis. Although in this axis the movement had much more impact in the phase.

4.4.3 Variation of the lungs in Y axis

The last movement being varied is the height of the lungs. The representation of the movement explained is displayed on Figure 4.33.

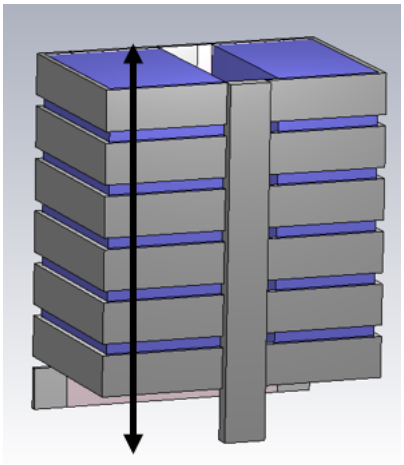

Figure 4.33: Illustration of the movement of the body.

For this movement, the height will be changed from about 12 mm [41]. The difference from this one is the fact that the highest value is when the lungs are deflated and

the lowest value when the lungs are inflated. When inhaling, the diaphragm goes up towards the thoracic cage, decreasing the lungs length. The first results provided by the simulation varying the relative permittivity depending on the length of the lung are in Figure 4.35.

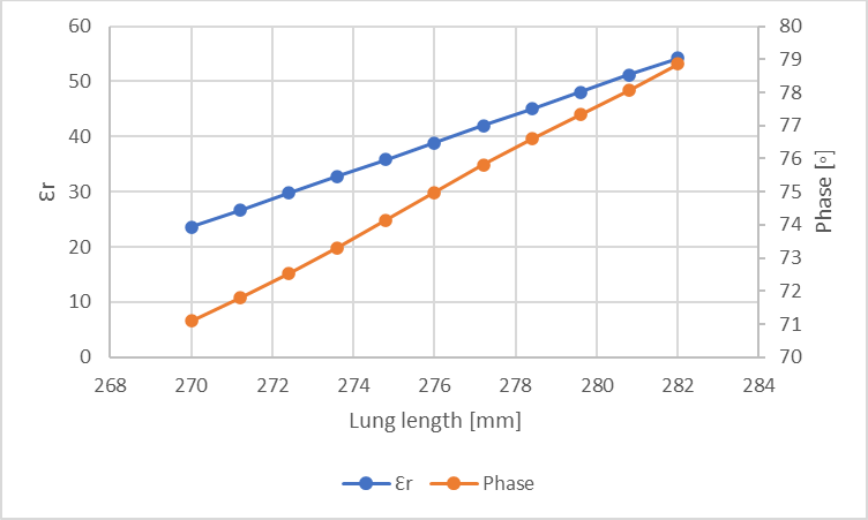

Figure 4.34: Reflection coefficient phase depending of the lung height varying relative permittivity.

The difference of reflection coefficient phase that takes place in Figure 4.34 is from about 7.765 degrees. As this one is also the highest value of difference in phase, it can be concluded that relative permittivity will have the most impact for the reflection coefficient phase of the antenna. The next one is electric conductivity depending on the height of the lung. The results are displayed of Figure 4.35

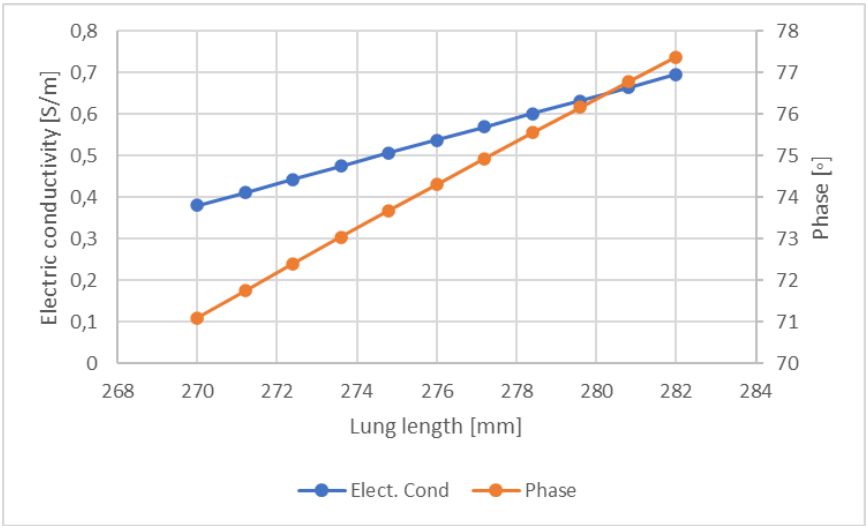

Figure 4.35: Reflection coefficient phase depending of the lung height varying electric conductivity.

The difference of reflection coefficient phase that takes place in Figure 4.35 is from about 6.268 degrees. The length of the lung is the only property being varied in Figure 4.36.

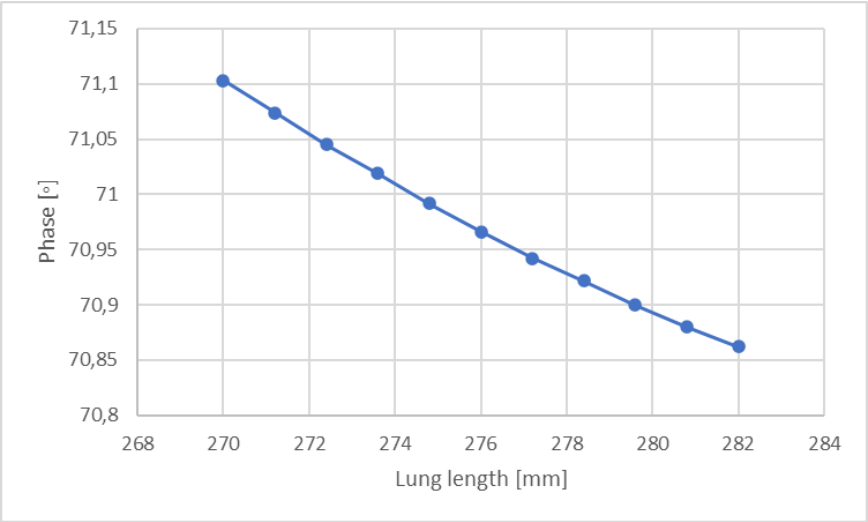

Figure 4.36: Reflection coefficient phase depending on the lung height.

The difference of reflection coefficient phase that takes place in Figure 4.36 is from about 0.241 degrees. This last simulation depending just on the change of the lung dimension makes possible the conclusion that the width of the lungs provokes the most shifting in the reflection coefficient phase of the antenna. The Figure 4.37 is the last from this section and shows the reflection coefficient phase of the antenna when relative permittivity and electric conductivity are simultaneously depending on the lung height.

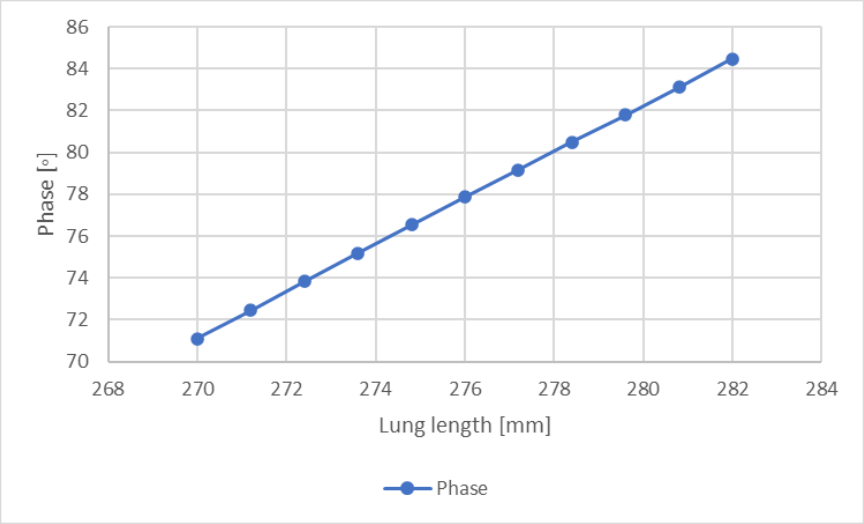

Figure 4.37: Reflection coefficient phase depending of the lung length varying electric conductivity and relative permittivity.

The difference of reflection coefficient phase that takes place in Figure 4.37 is from about 13.374 degrees. Comparing the three axis on the total variation of the lungs, the shifting in phase is greater in the Z axis.

4.4.4 Total variation of the lungs

Since every movement from each axis was analyzed, the total movement of the lungs can now be simulated. Meaning the movements showed in Figure 4.38 of the last three sections will be combined in only one. The properties such as the relative permittivity and the electric conductivity will be changed depending from the total movement of the lungs. This last simulation will only have five points since there are a lot of variables in change.

The results from the total variation from every axle and lung property is displayed in Figure 4.39.

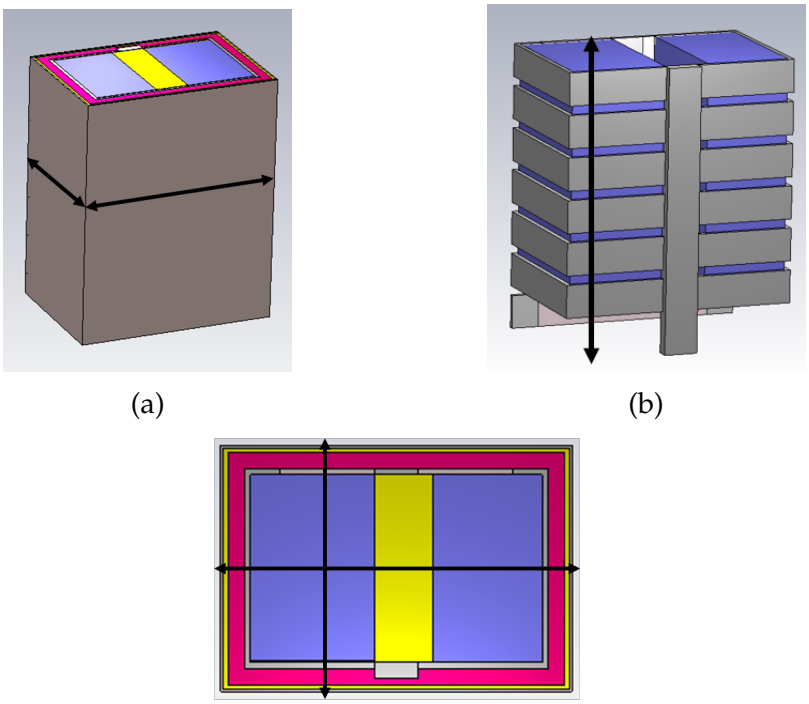

(a) (b)

(c)

Figure 4.38: Illustration of the total movement of the body: a) Width and thickness; b) Height; c) Width and thickness view from above.

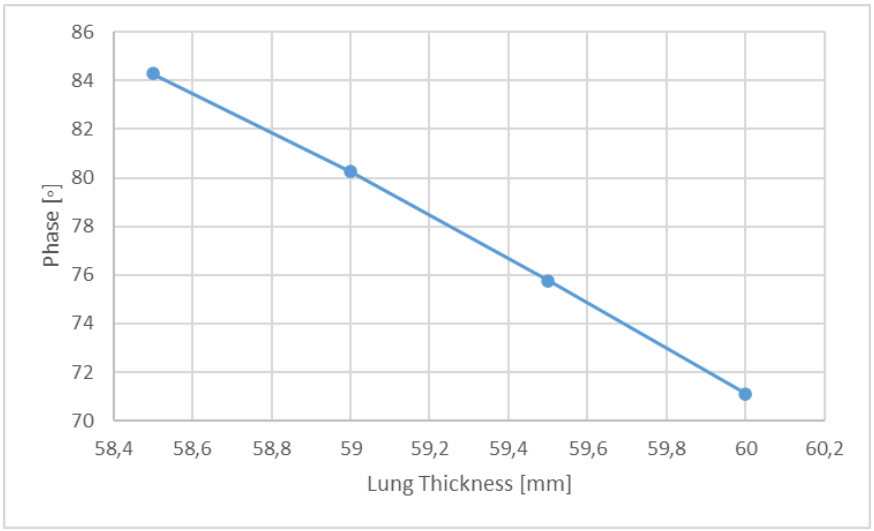

Figure 4.39: Reflection coefficient phase varying permittivity, electric conductivity depending on the lung thickness.

In Figure 4.39, the graphic only shows lung thickness but the length and width of the lungs were also simulated but could not be displayed. The difference in reflection coefficient phase obtained is 13.186 degrees. This result is as comprehensible since the final results from previous sections 4.4.1 4.4.2 and 4.4.3, are close to this precise value.

4.4.5 Variation of the heart

This last subsection is to display how the change in dimensions of the heart will affect the reflection coefficient phase of the antenna. Only the dimensions of the heart will be differed in this simulations. That is due to the fact of the lack of information about the dielectric properties of the heart when the cardiac cycle occurs.

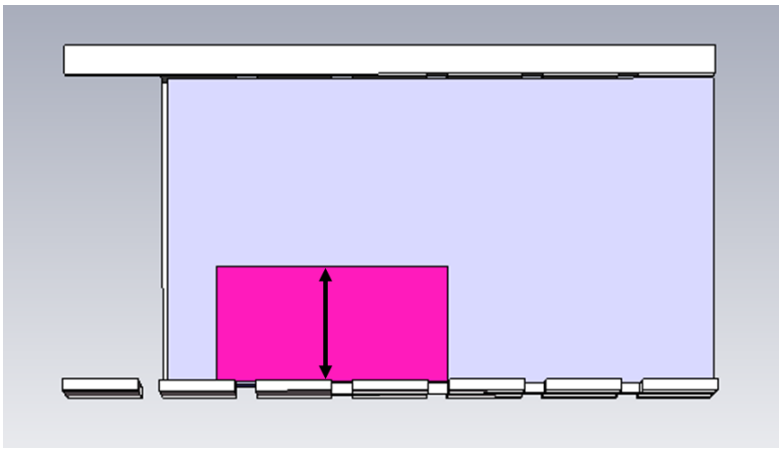

Figure 4.40: Movement of the heart.

Figure 4.40 represents from a side view, how the heart will be moving in this test. The cardiac cycle causes a variation of the heart from about 1.2 mm [6].

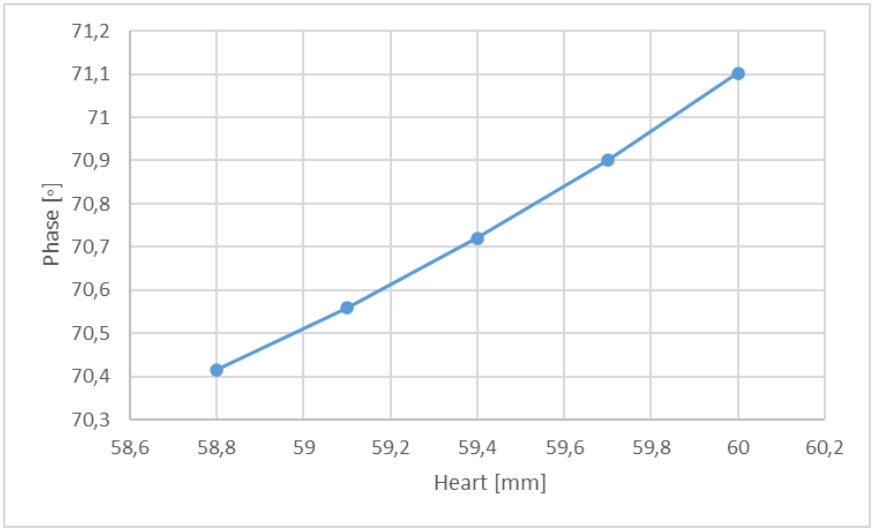

Figure 4.41: Reflection coefficient phase depending on the heart dimensions.

The Figure 4.41 is the representation of the reflection coefficient phase depending on

the heart dimensions which only vary 1.2 mm. And as expected the reflection coefficient phase does not vary as much as the lungs. The difference in the reflection coefficient phase is 0.686 degrees. This might be due to the fact that the heart is much more small comparing to the lungs. In addition to this, the movement is less and in these case the lack of knowledge about the dielectric properties.

5

Experimental Results

The textile patch antenna with slots was built after all the simulations have been done. The antenna was tested on the human body in five different subjects. This chapter will explain how the tests were done and the conclusions taken.

The textile antenna tested is introduced in Figure 5.1.

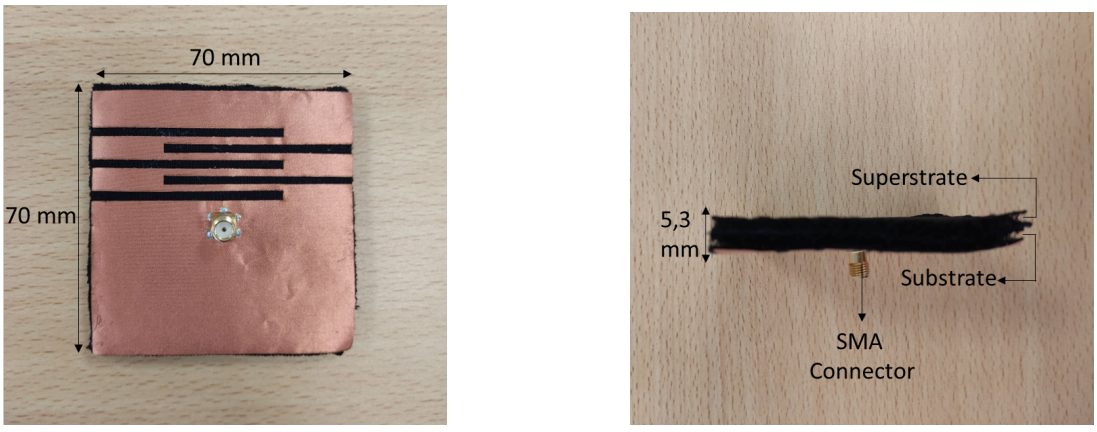

(a) (b)

Figure 5.1: Textile antenna using slots in the patch and ground: a) Back view of the antenna; b) Side view of the antenna.

Figure 5.1a presents the back side of the antenna, showing the ground plane with the slots designed and the SMA connector. The side of the antenna is displayed in Figure 5.1b, where is possible to see the superstrate, substrate and the SMA connector. It was not possible to obtain a representation of the patch since it was behind the superstrate.

5.1 Experimental Setup

In this project was required a device capable of analyzing the reflection coefficient phase of the antenna in which was used a PNA-X (N5242A) from Keysight. The device mentioned is displayed in Figure 5.2, and this device will show the reflection coefficient phase of the antenna in real time in order to be visualized the vital signs.

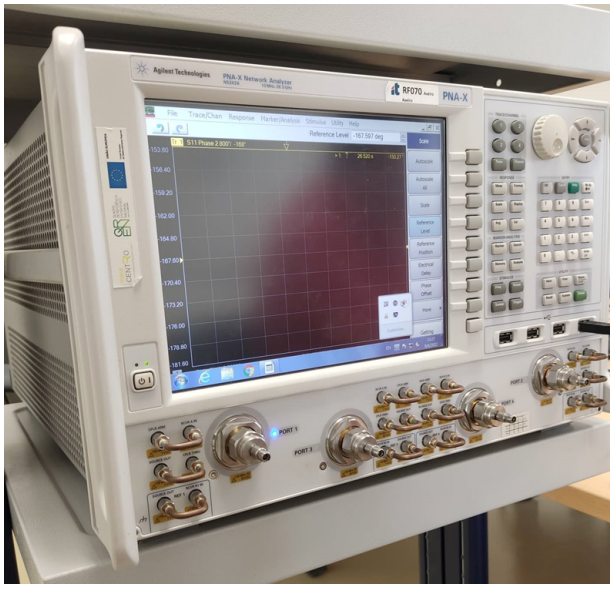

Figure 5.2: Phase Network Analyzer.

The results obtained using this device will then be put on a file that will be transferred to a computer and then will be treated and analyzed. To compare the results obtained from the antenna tested, another device is used. A chest band with a respiration transducer from BIOPAC Systems was used to capture the respiratory cycle of each individual, Figure 5.3a.

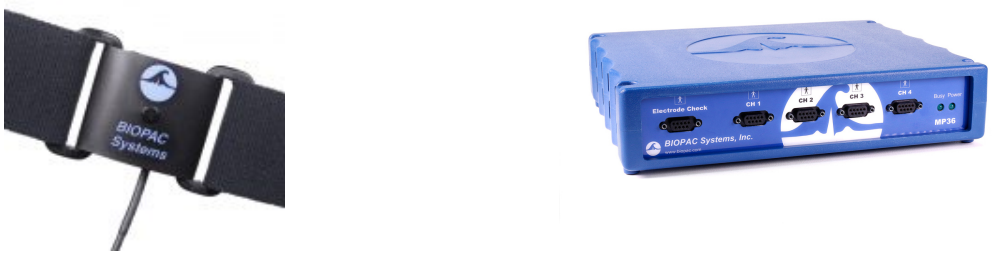

(a) (b)

Figure 5.3: Devices used from BIOPAC [47]: a) Chest band with respiration transducer; b) Data acquisition unit.

This device was then connected to the BIOPAC system shown in Figure 5.3b to record the signal and then the data is processed on the computer. The Figure 5.4 shows the used setup.

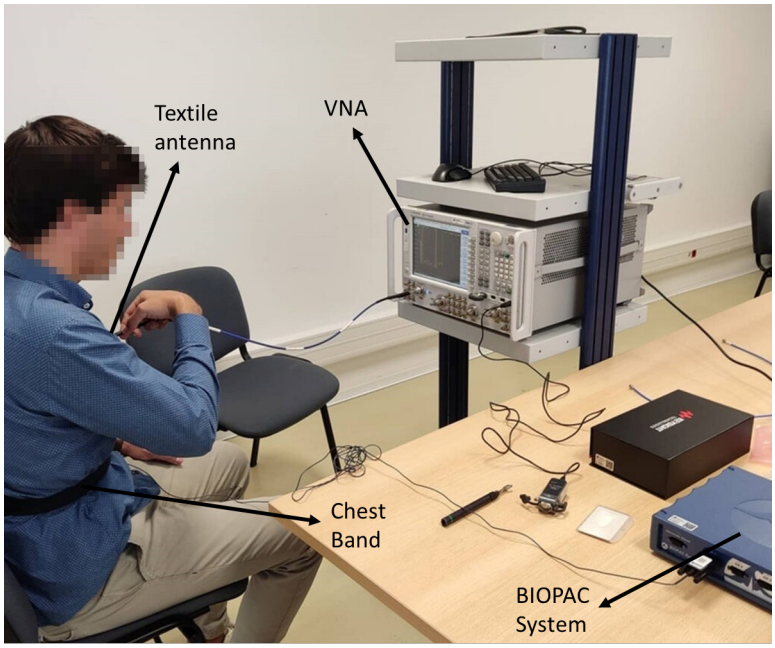

Figure 5.4: Setup for the tests.

5.2 Textile antenna with slots calibration

The first measurement to be done was the S_{11} parameter of the antenna. The coaxial cable is connected between the PNA-X and the automatic gauge, to calibrate the PNA-X. This automatic calibration kit is the Keysight N7555A CalKit showed in Figure 5.5. The calibration was made for a transmitting power of -10 dBm and a range of frequencies from 0 to 800 MHz.

Figure 5.5: Keysight N7555A CalKit [48].

As said before, this antenna was tested on five different subjects with different morphologies. Each subject was subjected to measurement of the perimeter of the thoracic cage and BMI (Body Mass Index). The measurements are pointed out in Table 5.1.

Table 5.1: BMI and perimeter of each subject.

	Subject 1	Subject 2	Subject 3	Subject 4	Subject 5
BMI [kg/m^2]	18.7	22.5	30	22.4	23
Perimeter of Thoracic cage [cm]	78	89	110	94	95

The subjects mentioned in Table 5.1 tested the antenna in contact with the chest area. In order to check the S_{11} parameter resulted from each subject, Figure 5.6 is presented.

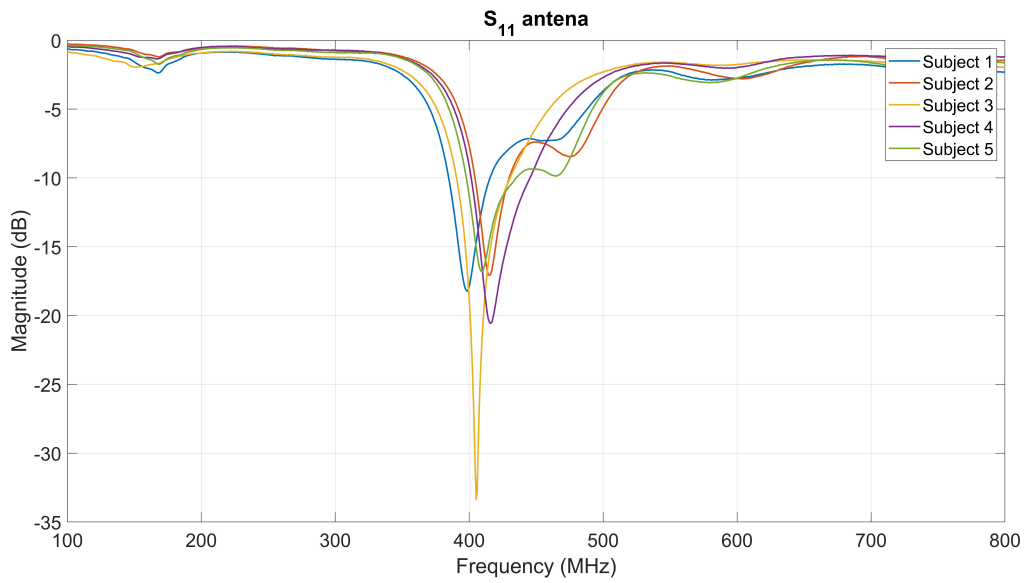

Figure 5.6: S_{11} parameter of the designed antenna for five different subjects.

The resonance frequency tested in simulations was 433.92 MHz but the built textile antenna when tested had a slight shift to about 409 MHz. The position and how the antenna was handled had a major influence in the final results. Since there was no type of structure in order to maintain the antenna in the same position, the subject had to hold the antenna in a stable position. A simple movement or a slight change in strength when holding the antenna could change the result. Observing Figure 5.6, the results for each subject, having in mind the different morphologies, could be considered very good since the resonance frequency for each one does not change a lot. Overall the antenna seems well adapted for a frequency of 409 MHz.

5.3 Acquisition of vital signs

The next tests after checking the S_{11} parameter is the acquisition of vital signs, the main goal of this work. For this test, each subject had to use the chest band with the respiration transducer mentioned before and the antenna at the same time. So that the two devices get the same period of respiration. The respiration of each single subject was monitored for about 40 seconds. After each test the results were collected and the frequency for the respiration was calculated for the antenna and the chest band with the respiration transducer. The Figures 5.7-5.11 ahead represent each result of monitoring each subject respiration, using the blue line for the result obtained from the designed antenna and the red line for the BIOPAC device. The first subject have the results presented in Figure 5.7. The two signals when compared are pretty similar in terms of period of the signal and the peak for each respiration seem to synchronized.

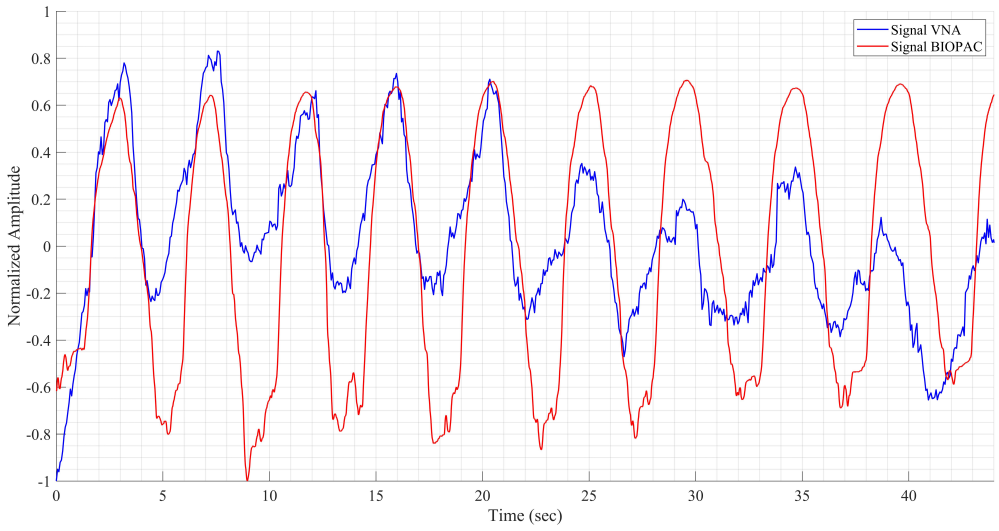

Figure 5.7: Respiration from subject 1.

The synchronization was made using Matlab, both the results from the BIOPAC and the VNA were exported and rearranged in the application. To synchronize both signals each subject started the test by holding the breath for about six seconds and then breathing normally. When the breath is hold it created a high value for six seconds which would be a reference point to synchronize both signals.

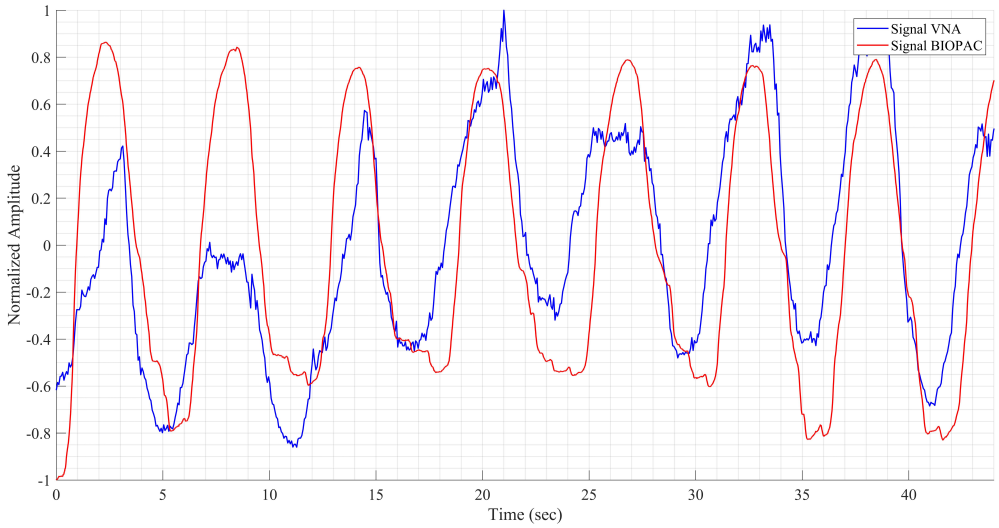

Figure 5.8: Respiration from subject 2.

The BMI from subject 2 is higher when comparing to subject 1, but the two signals does not seem to be that different. The signal in subject 1 presented less noise this might be due to subject 1 has the lowest BMI. Each peaks from each signals seem aligned and the noise is still low.

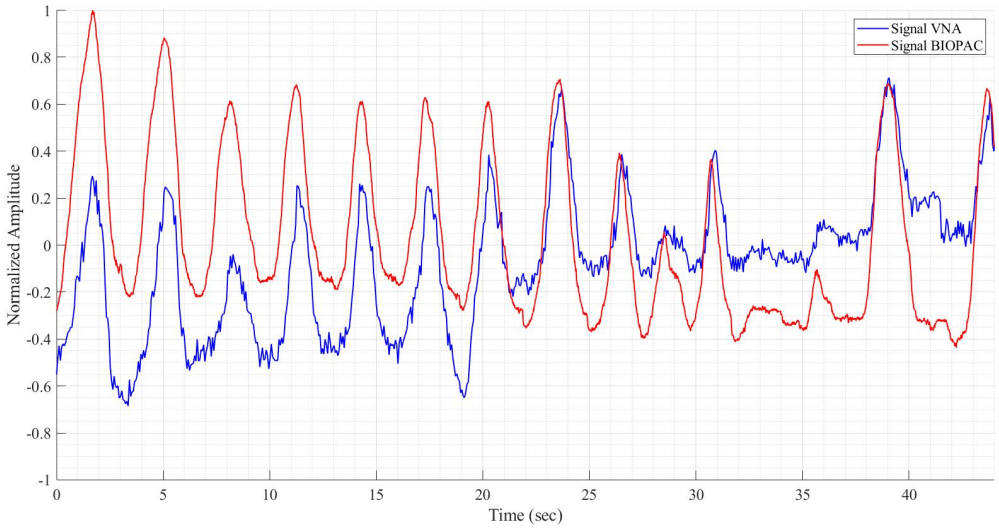

Figure 5.9: Respiration from subject 3.

In this case the signal seem to have more noise then the other ones. The BMI might have an influence in this case since the subject 3 has the highest BMI from the five individuals.

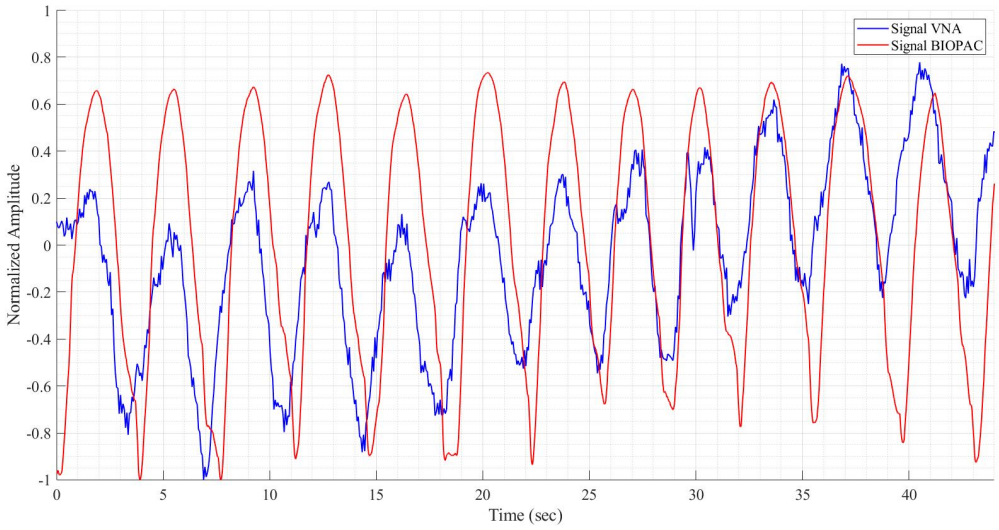

Figure 5.10: Respiration from subject 4.

The BMI of subject 2 and 4 are not that different but in this case the subject 4 might have the antenna well positioned or is not holding the antenna the right way.

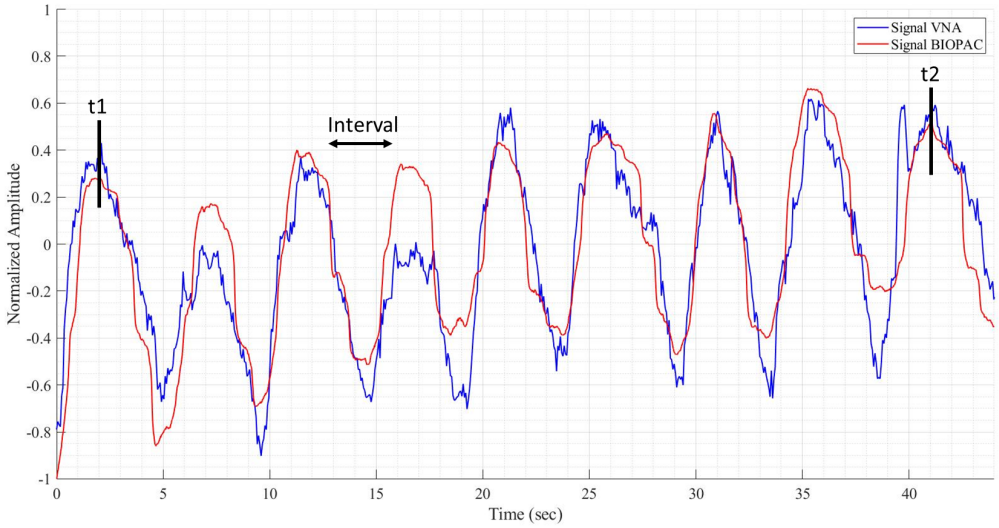

Figure 5.11: Respiration from subject 5.

The last subject had the second highest BMI from the five subjects (only 0.6 more the the subject 4). This last results had some noise comparing to the other subjects. The BMI actually could have a real influence in these values. Not forgetting that the placement of the antenna and the way the individual is holding it has a big importance for this case.

Lastly, each result was then acknowledge to be used in order to calculate the respiratory rate, using Equations 5.1 and 5.2.

$$\Delta t = \frac{t_2 - t_1}{N_i} \tag{5.1}$$

$$F = \frac{1}{\Delta t} \times 60 \tag{5.2}$$

Where:

- t_1 = Instant of first peak value
- t_2 = Instant of last peak value
- N_i = Number of intervals between t_1 and t_2
- F = Respiratory rate

These variables are represented in Figure 5.11. The results obtained from using Equations 5.1 and 5.2 are presented in Table 5.2.

Table 5.2: Respiration frequency from each subject and each device.

	Subject 1	Subject 2	Subject 3	Subject 4	Subject 5
Respiration frequency VNA [bpm]	13.51	10.1	20.87	16.95	16.94
Respiration frequency BIOPAC [bpm]	13.09	9.96	20.93	16.79	16.79

The Mean Absolute Error from the results obtained in Table 5.2 is 0.206. When an adult is at rest the respiration cycle is between 12 and 20 breaths per minute. These values change if the subject at matter has some type of lung disease [6, 49]. The respiration rate observed in Table 5.2 obtained from the designed antenna is valid, since the BIOPAC was used as a ground truth and the values are similar.

6

Conclusions and future work

6.1 Conclusions

This dissertation, had the main objective of designing a textile antenna capable of working close to a human body, capture vital signs of a human body and to be as thin as possible to be integrated in clothes. This type of antenna will help to create another method of measuring vital signs, with the antenna integrated in clothes. Therefore the vital signs would be detected in a less invasive way and being more comfortable and discrete. Fulfilling a hole in the studies for these antennas focused on medicinal applications. For this dissertation, was used the software CST Studio Suite 2018 in order to design and simulate the antennas presented.

The search for the design to be used in the textile antenna began. The materials that were used for the superstrate and the substrate was the 3D Spacer knit, a light material resistant to water and deformations such as stretching. Starting with a simple patch antenna using a resonance frequency of 2.45 GHz. The design was not used since the patch would become thinner as the human body would get closer. A simple triangle patch using inset feed was then used at the same frequency but the conclusions were the same. With the inset feed and the antenna being to thin, would make problems in the manufacture. The final and chosen design, was an antenna where the patch and ground would have horizontal slots. This antenna had a different resonance frequency from the others, working on a resonance frequency of 433.32 MHz. The change in

frequencies was related to prevent the shrinking of the patch, and with a lower frequency, the capacity of penetration in tissues increases. The slots helped to reduce the frequency as well. This design was successful, achieving an antenna that can be close to a human body only using a single layer of the 3D Spacer knit, meaning the patch was separated from the body only using a superstrate with 2.650 mm thickness. For this case the patch would not change its dimensions, only the dimensions of the slots were changed in order to optimize the antenna. Concluding that this design would be able to use even thinner materials to be even closer to the human body. The human body models used in CST then imitated the respiratory and cardiac cycle, so it would be possible to verify how the antenna would behave. For this simulations, the objective was to observe if the reflection coefficient phase of the antenna would change as the organs would change properties and with the movement of the body. The variation in the phase of the antenna was then verified in the simulations. Obtaining good results as the antenna had a noticeable variation of reflection coefficient phase. Simulating the total movement of the body and the properties changing, the reflection coefficient phase had a difference from about 13.186 degrees. Therefore the construction of the textile antenna with slots was proceeded. The antenna was then tested on different subjects to understand how it would affect from each different person. In order to prove that the results achieved from the antenna were viable, it was used a body strap with a respiration transducer from BIOPAC. The product from each device was then collected and treated. For this case the positioning of the antenna, the manner that the subject holds and the person itself, made a big impact in the antenna performance. The results obtained from the design were as expected. The antenna showed variation in the reflection coefficient phase as the subject was respiration. Ending on successfully detecting vital signs for each subject as the respiration transducer from BIOPAC helped to understand if the results were right. Achieving the main goal of the dissertation that were the detection of vital signs.

6.2 Future work

From this dissertation, future work can be done with the study made. Starting with the study of more designs with slots that could be made in order to be close to the human body and having an even smaller antenna. Only one textile material was used for these tests, therefore different materials can be tested. As it was proved that the design presented could perform with even thinner layers of superstrate. Making it even closer to the human body. The deformations were simulated but not tested with the manufactured antenna, such as the application of some kind of humidity in the

antenna. These factors are important to the antenna performance and are tests that can be done in the future. Finally with this textile antenna there is now a possibility to develop a portable system capable of acquiring vital signs with the antenna integrated in a suit.

References

[1] Joel J.P.C. Rodrigues, Dante Borges De Rezende Segundo, Heres Arantes Junqueira, Murilo Henrique Sabino, Rafael Mac Iel Prince, Jalal Al-Muhtadi, and Victor Hugo C. De Albuquerque, "Enabling technologies for the internet of health things", *IEEE Access*, vol. 6, pages 13 129–13 141, Jan. 2018, ISSN: 21693536.

[2] Ankita Priya, Ayush Kumar, and Brajlata Chauhan, "A review of textile and cloth fabric wearable antennas", *International Journal of Computer Applications*, vol. 116, pages 1–5, 17 Apr. 2015.

[3] Kashif Nisar Paracha, Sharul Kamal Abdul Rahim, Ping Jack Soh, and Mohsen Khalily, "Wearable antennas: A review of materials, structures, and innovative features for autonomous communication and sensing", *IEEE Access*, vol. 7, pages 56 694–56 712, 2019.

[4] Craig Lockwood, Tiffany Conroy-Hiller, and Tamara Page, "Vital signs", *JBI Reports*, vol. 2, pages 207–230, 6 Jul. 2004.

[5] *How to read a vital signs monitor*, Nov. 2021. [Online]. Available: https://www.webmd.com/cancer/vital-signs-monitor.

[6] Abubakar Tariq, "Vital signs monitoring using doppler radar and on-body antennas", University of Birmingham, 2013.

[7] Custódio Peixeiro, "Microstrip patch antennas: An historical perspective of the development", 2011, pages 684–688.

[8] John F Fie and Charles M Helms, "Respiratory rate predicts cardiopulmonary arrest for internal medicine lnpatients", *J GEN INTERN MED*, vol. 8, pages 354–360, 1993.

[9] C. P. Subbe, R. G. Davies, E. Williams, P. Rutherford, and L. Gemmell, "Effect of introducing the modified early warning score on clinical outcomes, cardiopulmonary arrests and intensive care utilisation in acute medical admissions", *Anaesthesia*, vol. 58, pages 797–802, 8 Aug. 2003.

[10] Anuradha Singh, Saeed Ur Rehman, Sira Yongchareon, and Peter Han Joo Chong, "Modelling of chest wall motion for cardiorespiratory activity for radar-based ncvs systems", *Sensors 2020, Vol. 20, Page 5094*, vol. 20, page 5094, 18 Sep. 2020.

[11] Fei Han, Zhongquan Wan, Yan Wang, Alec Boksenberg, Wallace L W Sargent, C Gabriel, S Gabriel, and E Corthout, "The dielectric properties of biological tissues: I. literature", *Physics in Medicine and Biology*, vol. 41, pages 2231–2249, 1996.

[12] Tuba Yilmaz, Robert Foster, and Yang Hao, *Detecting vital signs with wearable wireless sensors*, Dec. 2010.

[13] Kevin Bennett, *The simple science of hands-only cpr*, Dec. 2021. [Online]. Available: https://kevin-bennett-health.medium.com/the-simple-science-of-hands-only-cpr-f49f889e3f9e.

[14] Peter J. Zimetbaum and Mark E. Josephson, "The evolving role of ambulatory arrhythmia monitoring in general clinical practice", *Annals of Internal Medicine*, vol. 130, pages 848–856, 10 May 1999.

[15] *Synthetic and natural fibers*, Nov. 2021. [Online]. Available: https://www.geeksforgeeks.org/synthetic-and-natural-fibers/.

[16] V K Singh, Ashok Yadav, Vinod Kumar Singh, Manu Chaudhary, and Himanshu Mohan, "A review on wearable textile antenna", *Journal of Telecommunication, Switching Systems and Networks*, vol. 2, pages 37–41, 3 2015.

[17] V K Singh, Seema Dhupkariya, Vinod Kumar Singh, and Arun Shukla, "A review of textile materials for wearable antenna", *J. Microw. Eng. Technol*, vol. 1, pages 1–8, 2015.

[18] Rita Salvado, Caroline Loss, Ricardo Gonçalves, and Pedro Pinho, "Textile materials for the design of wearable antennas: A survey", *Sensors*, vol. 12, pages 15 841–15 857, 11 2012.

[19] Pranita Manish Potey and Kushal Tuckley, "Design of wearable textile antenna with various substrate and investigation on fabric selection", 2018, pages 1–2.

[20] Adel Y.I. Ashyap, Zuhairiah Zainal Abidin, Samsul Haimi Dahlan, Huda A. Majid, A. M.A. Waddah, Muhammad Ramlee Kamarudin, George Adeyinka Oguntala, Raed A. Abd-Alhameed, and James M. Noras, "Inverted e-shaped wearable textile antenna for medical applications", *IEEE Access*, vol. 6, pages 35 214–35 222, Jun. 2018.

[21] Shaozhen Zhu and Richard Langley, "Dual-band wearable textile antenna on an ebg substrate", *IEEE Transactions on Antennas and Propagation*, vol. 57, pages 926–935, 4 2009.

[22] Carla Hertleer, Hendrik Rogier, Luigi Vallozzi, and Lieva Van Langenhove, "A textile antenna for off-body communication integrated into protective clothing for firefighters", *IEEE Transactions on Antennas and Propagation*, vol. 57, pages 919–925, 4 2009.

[23] M. Catrysse, R. Puers, C. Hertleer, L. Van Langenhove, H. van Egmond, and Matthys D., "Towards the integration of textile sensors in a wireless monitoring suit", *Sensors and Actuators A: Physical*, vol. 114, 2-3 Sep. 2004.

[24] Carla Hertleer, Anneleen Tronquo, Hendrik Rogier, and Lieva Van Langenhove, "The use of textile materials to design wearable microstrip patch antennas", *Textile Research Journal*, vol. 78, pages 651–658, 8 2008.

[25] Alex P J Hum, "Fabric area network – a new wireless communications infrastructure to enable ubiquitous networking and sensing on intelligent clothing", *Computer Networks*, vol. 35, pages 391–399, 4 2001, Pervasive Computing.

[26] I Locher, H Junker, T Kirstein, and G Troster, "Wireless, low-cost interface for body area networks", vol. 1, 2004, pages 170–171.

[27] Johan Coosemans, Bart Hermans, and Robert Puers, "Integrating wireless ecg monitoring in textiles", *Sensors and Actuators A: Physical*, vol. 130-131, pages 48–53, SPEC. ISS. Aug. 2006.

[28] H J Visser and A C F Reniers, "Textile antennas, a practical approach", 2007, pages 1–8.

[29] J C G Matthews and G Pettitt, "Development of flexible, wearable antennas", 2009, pages 273–277.

[30] Jung Sim Roh, Yong Seung Chi, Jae Hee Lee, Youndo Tak, Sangwook Nam, and Tae Jin Kang, "Embroidered wearable multiresonant folded dipole antenna for fm reception", *IEEE Antennas and Wireless Propagation Letters*, vol. 9, pages 803–806, 2010.

[31] G F Studor, Kennedy T.F., Fink P.W., and Chu A.W., "Potential space applications for body-centric wireless and e-textile antennas", *IET Conference Proceedings*, 77–83(6), Jan. 2007.

[32] C. Hertleer and L. Langenhove, "A textile antenna for fire fighter garments", *AUTEX (Association of Universities for Textiles)*, 2007.

[33] Timothy F Kennedy, Patrick W Fink, Andrew W Chu, Nathan J Champagne, Gregory Y Lin, and Michael A Khayat, "Body-worn e-textile antennas: The good, the low-mass, and the conformal", *IEEE Transactions on Antennas and Propagation*, vol. 57, pages 910–918, 4 2009.

[34] Mohamed Mohamed and Mohammad Sharawi, "Ltcc based patch antenna for biomedical applications at ism band", *IEEE 5th Asia-Pacific Conference on Antennas and Propagation (APCAP)*, 2016.

[35] Sarmad Nozad Mahmood, Asnor Juraiza Ishak, Tale Saeidi, Azura Che Soh, Ali Jalal, Muhammad Ali Imran, and Qammer H Abbasi, "Full ground ultra-wideband wearable textile antenna for breast cancer and wireless body area network applications", *Micromachines*, vol. 12, 3 2021.

[36] *Dielectric properties*, Jan. 2022. [Online]. Available: https://itis.swiss/virtual-population/tissue-properties/database/dielectric-properties/.

[37] Yuriy I. Nechayev, Peter S. Hall, Imdad Khan, and Costas C. Constantinou, "Wireless channels and antennas for body-area networks", *WONS 2010 - 7th International Conference on Wireless On-demand Network Systems and Services*, pages 137–144, 2010.

[38] P S Hall and Y Hao, "Antennas and propagation for body centric communications", 2006, pages 1–7.

[39] Adel Y.I. Ashyap, Samsul Haimi Bin Dahlan, Zuhairiah Zainal Abidin, and Muhammad Inam Abbasi, *An overview of electromagnetic band-gap integrated wearable antennas*, 2020.

[40] Luís Ferreira, "Antena para transferência de potência sem fios para alimentação de dispositivos biomédicos", Instituo Politécnico de Lisboa, May 2021.

[41] Gary H. Kramer, Kevin Capello, Brock Bearrs, Aimée Lauzon, and Lysanne Normandeau, "Linear dimensions and volumes of human lungs obtained from ct images", *Health Physics*, vol. 102, pages 378–383, 4 Apr. 2012, ISSN: 00179078.

[42] *Heart anatomy | anatomy and physiology.* Jul. 2022. [Online]. Available: https://www.coursehero.com/study-guides/nemcc-ap/heart-anatomy/.

[43] Constantine A. Balanis, *Antenna Theory: Analysis and Design - Constantine A. Balanis*. 2015.

[44] Murthy S. Chavali and Maria P. Nikolova, "Metal oxide nanoparticles and their applications in nanotechnology", *SN Applied Sciences 2019 1:6*, vol. 1, pages 1–30, 6 May 2019, ISSN: 2523-3971.

[45] Ali Arif, Muhammad Zubair, Mubasher Ali, Muhammad Umar Khan, and Muhammad Qasim Mehmood, "A compact, low-profile fractal antenna for wearable on-body wban applications", *IEEE Antennas and Wireless Propagation Letters*, vol. 18, pages 981–985, 5 May 2019, ISSN: 15485757.

[46] S. Sankaralingam and Bhaskar Gupta, "Determination of dielectric constant of fabric materials and their use as substrates for design and development of antennas for wearable applications", *IEEE Transactions on Instrumentation and Measurement*, vol. 59, pages 3122–3130, 12 Dec. 2010, ISSN: 00189456.

[47] *Body strap for rsp transducers | rxstrap-rsp | consumable, education, research | biopac*, Sep. 2022. [Online]. Available: https://www.biopac.com/product/rsp-strap/.

[48] *N7553a electronic calibration module (ecal), dc-14 ghz, 2-port | keysight*, Sep. 2022. [Online]. Available: https://www.keysight.com/zz/en/product/N7553A/electronic-calibration-module-ecal-dc-14-ghz-2-port.html.

[49] *Vital signs*, Sep. 2022. [Online]. Available: https://my.clevelandclinic.org/health/articles/10881-vital-signs.